Enhancement of Gene Therapy by Exploring Functional Gene Vectors Based on Chitosan Modification

Bingyang Shi

A thesis submitted for the degree of Doctor of Philosophy

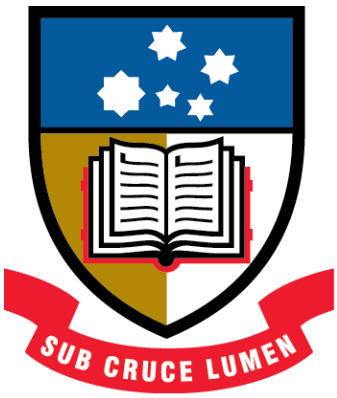

School of Chemical Engineering

Faculty of Engineering, Computer and Mathematic Sciences

The University of Adelaide

August 2013

To my parents

Yufeng and Honglu

Declaration

This work contains no material which has been accepted for the award of any other degree or diploma in any university or other tertiary institution to Bingyang Shi and, to the best of my knowledge and belief, contains no material previously published or written by another person, except where due reference has been made in the text.

I give consent to this copy of my thesis, when deposited in the University Library, being made available for loan and photocopying, subject to the provisions of the Copyright Act 1968.

The author acknowledges that copyright of published works contained within this thesis (as listed below) resides with the copyright holder(s) of those works.

I also give permission for the digital version of my thesis to be made available on the website, via the University's digital research repository, the Library catalogue, and also through web search engines, unless permission has been granted by the University to restrict access for a period of time.

Name: Bingyang Shi

Signed..... Date.....

Acknowledgements

I gratefully acknowledge my supervisors Dr Jingxiu Bi and Associate Prof. Sheng Dai, for their invaluable guidance, encouragement and constructive criticism during my candidature period. The knowledge that I learnt from my supervisors is not only just valuable for my PhD, and will benefit for my whole academic career.

I am so lucky to study under the guide of proferssor Shizhang Qiao. Thanks a lot for his guidance, suggestion and supporting. What I learnt from Prof. Qiao is beyond the science and will support me for my whole academic career and life.

I am particularly grateful to Dr. Hu Zhang for not only giving research supports but also polishing the submitted and published journal papers in the past three years.

Many thanks go to Dr Zheyu Shen and Dr Xin Du for supervision and cooperation on exploring of functional gene delivery system.

Many thanks go to my all lab members and the staff of the School of Chemical Engineering for their individual help and support.

I would like to specially thank the China Scholarship Council (CSC) and The University of Adelaide, who provided me this scholarship to support my PhD.

Finally, I would also like to thank my parents, for their endless love and encouragement throughout my life.

Table of Contents

List of Tables

List of Figures

Abstract

Gene therapy is a broad term that encompasses any strategy to treat a disease by transferring an exogenous gene, gene segments, or oligonucleotides into patient's cells to manipulate the defective genes or encoding the correct proteins. Gene therapy is becoming more efficient and has been successfully used in the treatment of genetic diseases such as cancers, infectious diseases, vascular diseases due to the rapid development of knowledge in elucidating the molecular basis of genetic diseases, as well as the availability of the complete sequence information of the human genome. However, it is difficult to obtain satisfactory efficiency by using naked nucleic acid without carrier/vectors since gene transfer in eukaryotic cells is a multiple-step process, in which naked nucleic acid can easily be digested. Therefore, the development of safe, efficient and specific delivery vectors for transporting appropriate genes to specific cells or tissues, where they can replace or regulate defective genes, is one of the key strategies in gene therapy.

In my phD project, a serial of functional polymers, named chitosan supported imidazole Schiff-base (CISB), N-imidazolyl-O-carboxymethyl chitosan (IOCMCS), folic acid factionalized Schiff-base linked imidazole chitosan (FA-SLICS), have been designed and successfully developed as gene carriers based on the modification of chitosan. Additionally, a new strategy for promoting endoplasmic gene delivery and nucleus uptake has been proposed by developing pH-sensitive Schiff-base linked imidazole biodegradable polymers. This delivery system can efficiently load nucleic acids at a neutral pH, release imidazole-gene complexes from the polymer backbones at intracellular endosmal pH, transport nucleic acids into nucleus through multiple-stage intracellular gene delivery, and thus leads to a high cell transfection efficiency.

These smart polymers display good biocompatibility, multiple-functions, and efficient

gene delivery efficiency as gene carriers. Hence they have promising potential applications in future gene delivery and enhance the development of gene therapy.

Key words: Gene delivery, chitosan, pH sensitive, cancer therapy

Chapter 1 Introduction

1.1 Project structure, objectives and strategy

Gene therapy is a broad term that encompasses any strategy to treat a disease by transferring an exogenous gene, gene segments, or oligonucleotides into patient's cells to manipulate the defective genes or encoding the correct proteins. Although gene therapy protocols have been successfully used in the treatment of cancers, infectious diseases, vascular diseases, and others, it has been currently, limited by safe and efficient gene-delivery vector.

Chitosan has been considered to be a potential nucleic acid carrier since it is known as a biocompatible, biodegradable, and low toxic biomaterial with cationic charges. However, the low specificity and low transfection efficiency of chitosan must be overcome before its end-use in gene delivery. Fortunately, chitosan provides several functional groups along its backbone for further modification, so that the final property of the modified chitosan can be tailored.

In this PhD project, we aim to design and develope a serial of intracellular microenvironment responsive chitosan derivatives through the modification of chitosan with functional groups to improve water solubility, gene loading and protection capability, cell transfection efficiency and targeted specificity of chitosan. These chitosan derivatives expect to show high-performance in gene delivery as gene carriers for gene therapy. Furthermore, the new mechanism of intracellular gene delivery will be systematically investigated based on the developed gene carriers,. The structure of the PhD project is illustrated in Figure 1.1.

Objectives and strategy:

1. To improve the water solubility, gene loading and protection capability, and cell transfection efficiency of chitosan in gene delivery, chiotsan will be modified with imidazole ring via the formation of pH sensitive linkage.
2. To further enhance gene release and biocompatibility of the developed *N*-imidazole chitosan in gene delivery, a carbonyl group will be further grafted onto the backbone of *N*-imidazole chitosan.
3. To endue targeting capability and apply the developed *N*-imidazole chitosan in cancer-targeted gene delivery, folic acid will be further introduced to the backbone of *N*-imidazole chitosan.
4. To guide the exploring of polymeric gene carriers in the future, the gene delivery mechanism of Schiff-base linked *N*-imidazole chitosan will be investigated.

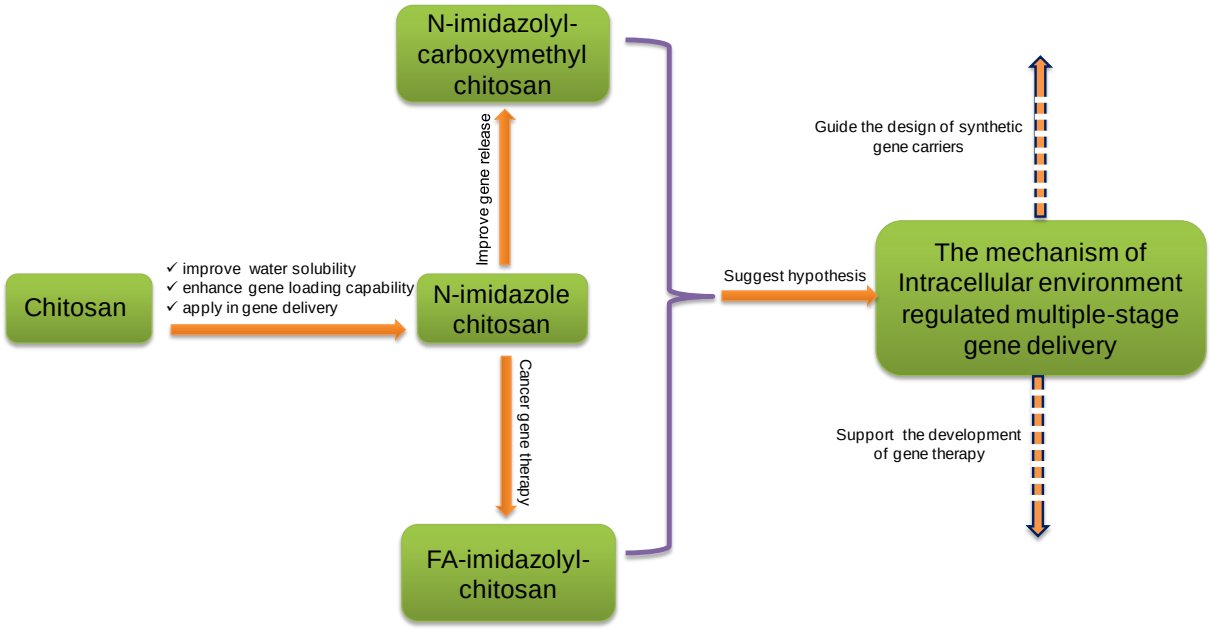

Figure 1.1 The designed and experimental structure of the PhD project.

1.2 Thesis outline

The major research contributions are presented in four journal publications which are composed of the thesis. The titles of Chapters 3 through 6 reflect the titles of the journal papers.

In Chapter 1, the gap, importance, aim, structure, thesis outine of this PhD project are introduced.

In Chapter 2, the challenges in nucleic acid delivery and the recent advances in design and development of chitosan based gene delivery systems are reviewed for better understanding and improving gene therapy.

In Chapter 3, to improve the water solubility and gene delivery capability of chitosan, a chitosan supported imidazole Schiff-base (CISB) has been developed to be used as the gene carrier in gene therapy through coupling imidazole ring to the backbone of chitosan. As expected, the resulted CISB shows higher solubility at physiological pH, stronger gene binding and protection capability comparing to chitosan. In addition, the low cytotoxicity and high efficiency in cell transfection render it a potential gene carrier candidate for gene delivery. However, the gene release, biocompatibility and targeting capability of CISB need to be further improved as a promising gene delivery system.

In Chapter 4, to enhance the gene release and improve the biocompatibility of CISB, a novel ampholytical chitosan derivative, N-imidazolyl-O-carboxymethyl chitosan (IOCMCS), was developed via introducing a carboxyl group to the backbone of CISB. The results display that the IOCMCS is a promising candidate as the DNA delivery vector in gene therapy due to the efficient gene loading/release capability and excellent biocompatibility after carboxyl conjugation.

In Chapter 5, to further improve the targeting capability of CISB and apply it to cancer-targeted gene therapy, a folic acid functionalized Schiff-base linked imidazole chitosan (FA-SLICS) was designed and developed by introducing folic acid to the backbone of CISB. The results demonstrate that FA-SLICS is potentially an efficient nucleic acid carrier for cancer gene therapy due to the targeted and pH sensitivity controlled intracellular gene delivery mechanism.

In Chapter 6, to investigate the intracellular gene delivery mechanism of Schiff-base linked *N*-imidazole polymers developed above and guide the exploring of polymeric gene carriers in the future, a serials of Schiff-base linked *N*-imidazole polymers were designed and systematically studied. The results demonstrate that the Schiff-base linked *N*-imidazole polymers can efficiently load nucleic acids at a neutral pH, release imidazole-gene complexes from the polymer backbones at intracellular endosmal pH, transport nucleic acids into nucleus through multiple-stage intracellular gene delivery, and thus leads to a high cell transfection efficiency. This efficient intracellular gene delivery mechanism could guide the exploring of polymeric gene carrier in the future.

In Chapter 7, the future development and directions of gene delivery are described based on our understanding.

Chapter 2 Literature Review: Challenges and Recent Advances in Gene Carriers based on chitosan modification

2.1 Introduction

Gene therapy is defined as the strategy that entails transporting therapeutic genes into chromosomes of targeted tissues or cells, in order to regulate or replace abnormal genes. This area of medicine has been intensively investigated for the last 20 years and has become one of the most potentially promising treatments of genetic diseases, such as mitochondrial-related diseases,[1] blindness,[2] muscular dystrophy,[3] cystic fibrosis[4] and cancer[5]. Rapid development of knowledge in elucidating the molecular basis of genetic diseases, as well as the availability of the completed sequence information of the human genome, has accelerated research in this area.

Up to 2012, more than 1500 gene therapy clinical trials have been approved since the first successful gene therapy trials for severe combined immunodeficiencies (SCIDs) in the 1990s,[6] which include cancer-related diseases (64.4%), monogenic diseases (8.7%), cardiovascular disease (8.4%), infectious diseases (8%) and others. However, technical and scientific barriers still continue to slow progress in gene therapy.[7] For example, most of the approved clinical trials (95.3%) are still in phase I or II, and only 2 clinical trials (0.1 %) are in the stage of phase IV due to the limitation of ideal gene carriers.[8] In addition, gene delivery of naked plasmid DNA (pDNA) without the aid of gene carriers (18.3%; 345 clinical trials) shows unacceptable transfection efficiency, while the intensive use of viral gene carriers leads to undesirable immune responses.[9]

In meeting the challenges of gene delivery, the synthetic gene delivery model shows promising advantages and has been widely investigated in last 15 years. Nevertheless, the

relatively low transfection efficiency and high cytotoxicity of synthetic gene carriers still cannot fully satisfy the requirements of gene therapy in clinical applications for humans, thus leaving synthetic carrier delivery of therapeutic genes in its infancy. In addition, performance of synthetic gene carriers *in vitro* does not always correlate well *in vivo*, making translation of positive results from the cell to the human even more difficult.[10] Therefore, in order to break these barriers and accelerate the process of allowing synthetic gene carriers to become the mainstream for gene delivery models used in clinical trials, various kinds of functional synthetic gene carriers have been designed and developed for gene therapy. For example, such carriers include polymeric gene carriers,[11] silica-based hybrid gene carriers,[12] gold nanoparticle-based hybrid gene carriers,[13] stimuli-responsive gene carriers[14] and targeted gene carriers.[15] In this review, we focus on the challenges in nucleic acid (pDNA and siRNA) delivery, including recent advances in the design and development of synthetic gene delivery systems based on chitosan modification, in order to enable better understanding and improvements in future gene therapy.

2.2 Understanding the mechanisms and challenges of polymer based gene delivery

Gene delivery in eukaryotic cells is a multi-step process that includes the condensation of pDNA, cellular uptake, endosomal release, nuclear transport, carrier/pDNA complexes unpacking and translation (Figure 2.1). Except translation, all of these steps can be a challenge to carrier-aided gene delivery, where the rate-limiting step can be any of these steps mentioned above, depending upon the structure and properties of the gene carrier (Table 2.1). Therefore, it is a prerequisite to understand these steps thoroughly, in order to improve gene delivery for clinical applications.

Table 2.1. The cellular and extracellular barriers for polymer based gene delivery

Cellular Barriers	Extracellular Barriers
1) Interaction with cell surface	1) Stability in solution with or without the presence of negative charged biomacromolecules
2) Membrane-limited cellular uptake	
3) Cytosolic nuclease degradation	2) Nuclease degradation in surrounding tissue or blood
4) Endosomal escape	3) The specific recognition of polycation by targeted tissues or cells
5) Nuclear entry	4) Accumulation of polycation in cell or tissue
6) Gene release and expression	

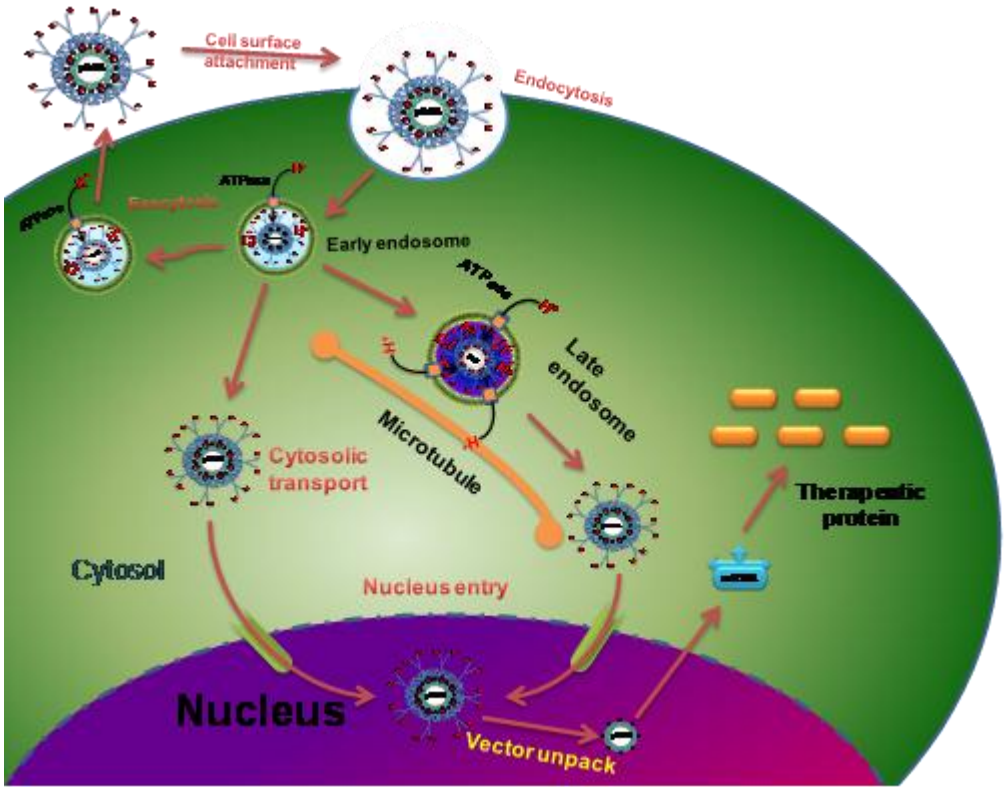

Figure 2.1 Polymer mediated gene delivery.

2.2.1 Condensation of pDNA

To protect pDNA from the digestion of nuclease and aid its cell uptake, the negatively charged pDNA needs to be loaded onto gene carriers and condensed into compacted nanoparticles with desirable size rang less than 150 to 200 nm. The process of pDNA

condensation is a reversible and globule transition, which is associated by the electrostatic interaction between the positively charged binding sites of the gene carrier and the negatively charged pDNA phosphate groups (Figure 2.2). However, the formulation of synthetic gene carriers has been constrained by the compromise between transfection efficiency and cytotoxicity,[16] which is controlled by the surface charge and molecular weight of the gene carrier. In essence, higher surface charges result in stronger gene loading capability and longer polymeric chains lead to more efficient gene condensation ability, which overall favours cell uptake and gene transfection. Still, the use of gene carriers with high charge densities and high molecular weight (HMW) will result in high cytotoxicity. In addition, an excess of positive charge can interact with polyanionic biomolecules situated in the bloodstream, leading to the inhibition of crucial cellular processes *in vivo*.[17] Hence, a major challenge to overcome is the design of gene carriers that not only have high gene binding capability, but also low positive charge density.

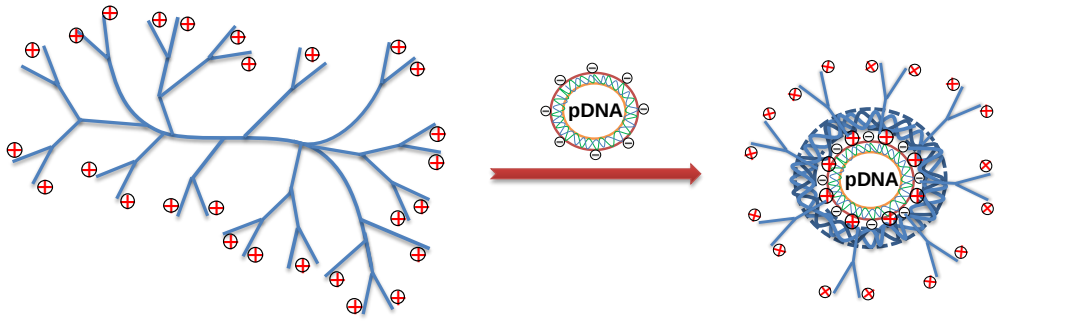

Figure2.2 The self assembled polymer/nucleic acid nano-structure.

2.2.2 Cellular uptake

The condensed nanoparticles or polyplexes are considered as the primary vehicles for gene delivery since they need to pass through biological barriers via energy dependent pathways, in order to transport the therapeutic gene to the nuclei of targeted cells. Classically, the uptake pathways are divided into two groups: endocytic pathways and non-endocytic pathways. The

endocytic pathways include phagocytosis, clathrin-mediated endocytosis (CME), caveolae-mediated endocytosis (CvME), and macropinocytosis.[18] In such endocytic pathways, once the non-viral gene polyplexes pass through the cellular membrane, they tend to be trapped in intracellular vesicles that eventually fuse with lysosomes. Subsequently, they are typically digested by hydrolyase – if they cannot escape. For synthetic gene carrier mediated non-endocytic pathways, such as fusion and penetration, these are non-endosomal mediated, and are therefore more useful in enhanced intracellular availability to non-viral gene polyplexes.[19] To date, studies show that the cellular uptake of non-viral polyplexes is affected by many factors including the size[20] and shape of polyplexes,[21] the surface charge,[22] the ligands on the polyplex surface,[23] the hydrophobic effect,[24] concentration of pDNA at the surface[25] and the cell cycle.[26] These factors not only affect the cellular uptake efficiency, but also what pathways that the non-viral gene polyplexes will follow, which is essential in improving the design and development of synthetic gene carriers.[27]

2.2.3 Endosomal escape

As previously discussed, it is known that the endocytic pathway is the main uptake mechanism in non-viral gene carrier-based gene delivery systems, where cellular trafficking of endocytic pathways typically involves directly transmitting endocytosed polyplexes to lysosomes after cell uptake. Specifically in this process, endosomes grow from the “early” to “late” stage and endosomal pH drops from 7 to 5 respectively, before fusing with lysosomes that possess a lower pH and accompanying hydrolytic enzymes for pDNA degradation.[28] Hence, this is considered to be a limiting step for intracellular gene transport.[29] Good gene carriers that possess endosomolytic components should aid the therapeutics’ escape from the endosomal/lysosomal stage before degradation, which could result in higher transfection efficiency. Up to now, the exact mechanism of polyplex escape from the endosomal/lysosomal pathway after internalization is still elusive. Although, several

mechanisms of endosomal escape have been proposed, including the "proton sponge" effect,[30] pore formation in the endosomal membrane,[31] fusion in the endosomal membrane[32] and photochemical disruption.[33] Out of these mechanistic hypothesises, the "proton sponge" concept remains the most accepted mechanism, but it is still controversial. For example, Davis' group found that the buffering capability of non-viral gene carriers did not always correlate with gene expression when combined with cell uptake and luciferase expression data,[34] which disagrees with the hypothesis of "proton sponge" effect. In addition, Andresen's group reported that polyethylenimine (PEI) does not induce change in lysosomal pH as previously suggested, and current quantification of PEI concentrations in lysosomes makes it uncertain that the "proton sponge" effect is the dominant mechanism of polyplex escape.[35] This is in light of quantitative measurements carried out of lysosomal pH as a function of PEI content. Therefore, the mechanism of cell uptake should be more intensively investigated, which would benefit the design and development of non-viral gene carriers.

2.2.4 Cytosolic transport and nuclear import

After release from the endosome into the cytosol, the polyplexes must then enter the nucleus to transfect the genome. The transport of polyplexes through the cytoplasm to the nucleus is still not thoroughly understood; however, it is accepted that whilst cellular uptake and endosomal escape present barriers to achieving satisfactory transfection rates for clinical applications, transport of nucleic acid from the cytoplasm to the nucleus might be a more prominent bottleneck.[36] Specifically, the movement of pDNA in the cytosol after release from endocytic vesicles is a crucial step that is unclear.[37] It is reported that cytoskeleton components might be involved in the cytoplasmic motion of therapeutics – either free or complexed with carriers. [36b] Given this uncertainty, the cytosolic travel of polyplexes could be greatly improved if these particles bear a signal molecule that allows their binding to microtubules, thus facilitating migration directly towards the nucleus envelope. Despite this

concept being proposed years ago, achieving signal-guidance of polyplexes remains challenging and little data has yet been published. Although, Reineke's group reported that the intracellular trafficking pathways of therapeutics are dependent on the chemical structure of carriers.[38] Nonetheless, the synthetic gene carrier-based delivery system might transport therapeutics through the Golgi apparatus and endoplasmic reticulum (ER) to the nucleus for uptake in certain situations, which would ultimately aid or even lead to efficient delivery similar to that of viruses. Therefore, understanding how the chemical structure of synthetic gene carrier impact on trafficking pathways will benefit the design and development of non-viral gene carriers.

A major biophysical limiting step at the latter stage of gene delivery occurs at the nuclear membrane, where mechanisms of nuclear entry are still not fully understood. In non-dividing cells, the general consensus is that nuclear trafficking occurs through nuclear membrane embedded nuclear pore complexes (NPCs), which regulate the passage in and out of the nucleus. [39] Molecules that are smaller than roughly 40 kDa or 10 nm diffuse passively, while larger molecules must display specific nuclear localization signals (NLS) or molecules, in order to overcome the limitation of NPC for active transport. For dividing cells, it is much easier for polyplexes – even naked genes – to enter the nucleus during this cell mitosis (M) phase.[26] Unfortunately, most cells are in the non-dividing (quiescent) situation *in vivo;* therefore, nuclear entry as a limiting step in gene therapy is an imperative consideration for gene carrier design. Studies estimate that only 0.1% of pDNA microinjected into the cytosol can access the cell nucleus,[37] and the ratio is only higher than approximately 1% with the aid of gene carriers[40]. Furthermore, it was also reported that cationic polymers (polycations) might be capable of disrupting the nuclear envelope, like for the plasma membrane, which could be another mechanism of how therapeutics are transported into the nucleus, other than just nuclear envelope breakdown during mitosis.[41] For these reasons, better understanding of

how nuclear uptake mechanisms work and how the chemical structure of gene carriers impact on nuclear importation would improve the development of synthetic gene carriers.[42]

2.2.5 Carrier unpacking

Disassembly of the polyplex is the final prerequisite for the transcription apparatus of the cell to access the pDNA efficiently in the final stage of gene expression. This leads to the insertion of pDNA into the nuclear genome, thereby inducing a therapeutical effect. The main issue at present is where the pDNA exactly is unpacked. For instance, such unpacking could occur at various locations in and around the nucleus depending on the properties of gene carriers, the stage of the cell cycle and the type of the cell.[43]

The most desirable feature of carrier unpacking that will result in higher transfection efficiency is the ability to judicially release the pDNA, which is dependent on the design of the carrier that encapsulates it. The design parameters that enable this must incorporate conditions that pertain to the area of the nucleus. An analogous example is that a series of pH-sensitive polycations are stable at neutral pH but disassemble in acidic conditions of the lysosome due to full protonation of the tertiary amine groups.[44] Once carrier unpacking occurs, the consequential expression or desirable therapeutical effect may occur slowly or suddenly, depending on the pDNA itself.[45] More importantly, is the potential oversight of any remaining polycation and/or its fragments to affect the nuclear genome, like the pDNA itself.

Gene expression studies have shown that carriers amenable for transfection can affect the nuclear genome, changing metabolic, house-keeping and cell cycle genes.[46] This level of change also depends on the cell and polycation type, where branched PEI (bPEI) is a prime example for inducing severe changes. Nevertheless, not much is known about whether these induced gene changes are directly related to bPEI entering the nucleus and displacing histones, or if it arises from upstream signalling events that are induced by bPEI conjugates affecting organelles beforehand. Therefore, the situation of signalling between the nucleus

and its intracellular environment has to be observed when polyplexes are travelling through the cell. Conversely, even though multiple gene changes may be a concern, they might also be of advantage for selected therapeutic purposes, which is an area required to be intensively investigated further.[47]

2.3. Gene carrier design considerations

Given the processes and barriers of gene delivery mentioned previously, several issues need to be considered when gene carriers are designed and prepared (Table 2.2). Firstly, safety is the most important consideration since the final aim of the designed gene carrier is for application to human gene therapy. Therefore, the cytotoxicity of the designed carriers should be considered and determined *in vitro* and *vivo*. In addition, they should also be biodegradable, in order to avoid the accumulation *in vivo* during long term therapy in clinical cases. As commonly known, the biggest problem of highly efficient viral gene carriers is immunogenicity, which poses a high risk of rejection responses or even disease for the clinical subject. Therefore, the immunogenicity of the polymeric designed carriers should be controlled likewise.[48] Furthermore, the stability of these gene carriers needs to be considered since gene delivery is a relatively long process.

The gene loading and consequent protection capability are other important factors for gene carriers, which are decided by the interaction between the carrier and nucleic acid cargos in application. In general, hydrophobic-hydrophilic and anionic-cationic interactions are two main types of interaction that drive the formation of the carrier/nucleic acid polyplex.[49] Particularly, as these interactions increase in strength, the gene loading capability of these gene carriers will also increase. Accordingly, for denser polyplexes, higher protection ability is exhibited. However, getting the right balance between gene loading and release is an important consideration, in order to develop highly efficient gene delivery systems.[50] The endocytic machinery and cell membrane have well defined geometries and flexibility that

restrict the entry of incompatible particles. Particularly, small particles can be up-taken via endosome-mediated endocytosis and large particles may be preferentially trafficked through a slow, non-degradative, caveolae-mediated route.[51] Therefore, size control of the carrier/nucleic acid nanoparticle is also a vital design consideration.

As covered earlier, endosome escape and nuclear entry are considered to be the two biggest potential bottlenecks for polymer-based gene delivery. For endosomal escape, non-viral gene carriers usually overcome this barrier through two proposed ways: the "proton sponge effect" and membrane fusion. Therefore, the ideal gene carrier should have strong buffering capability for the proton sponge effect and also strong membrane fusion ability.[29] For the latter particularly, special ligands or functional peptides are popularly utilized to enhance access across the nuclear envelope.[52] Separately, the highly efficient release of loaded pDNA is also necessary for a good gene delivery system. As a result, methods of unpacking the polyplex after they reach the nucleus of the targeted cells is another issue that should be considered when design gene carriers. For instance, biodegradable and stimuli-responsive polymer-based gene carriers have been designed to improve controlled pDNA release.[53]

Overall, a promising carrier for gene delivery should be one that efficiently conveys pDNA to a specific targeted cell or tissue. Internalization of the gene carrier can be enhanced by simple coupling of extracellular and intracellular targeting moieties that take advantage of natural endocytosis pathways.[54] Using this strategy, a variety of ligands,[55] peptides,[56] sugars,[57] antibodies[58] and aptamers[59] have been used to facilitate the uptake of carriers inside target cells. During this process, the targeting moiety-bound receptors are sequestered in caveolae, internalized into postcaveolar plasma vesicles, released from the receptor via an intravesicular reduction in pH, and then subsequently transported into the cytoplasm. The free receptor is then recycled to the cell surface by the re-opening of the caveolae. Another method of improving the targeting capability could be obtained by the design of stimuli-

responsive chemical structures, such as pH and thermo-mediated targeting structures for special cells like cancer cells.[60]

Table 2.2 Design consideration of synthetic gene carriers

Gene carrier design consideration
1) The biocompatibility a. The cytotoxicity of the materials b. The biodegradability of the materials c. The immunogenicity of the materials d. The solubility of the materials
2) The gene loading and protection capability a. Hydrophobic/hydrophilic interaction b. Anionic/cationic interaction c. The stability of the carriers/nucleic acid polyplexes d. The size of the carriers/nucleic acid polyplexes
3) Endosome escape and nucleus uptake capability a. The buffering capability of the materisals b. The membrane fusion ability c. The nucleus entry pathway and ability
4) The gene release capability a. The biodegradability of the gene carriers b. The stimuli-responsive ability of the gene carriers (such as enzyme, pH, thermo triggered gene release) c. The application of click chemistry
5) The targeted delivery ability a. The specific receptor-ligand mediated pathway b. The polypeptide mediated specific uptake pathway c. The stimuli-responsive targeting ability (such as thermo, pH, magnetic)

2.4. Recent advances in chitosan based gene carriers

To date, the biggest barrier in gene therapy is the lack of a satisfying gene delivery system for humans that is fully biocompatible and highly efficient.[61] In regards to safety, non-viral gene carriers are more popular and represent the future of gene delivery, as previously discussed.[62]

Accordingly, to overcome the challenges and accelerate the development of gene therapy, researchers have explored multitudes of synthetic gene carriers based on better understanding of transfection efficiency in the last five years.[63] Chitosan is typically obtained by deacetylation of chitin, which is an abundant organic material that exists as a major component in exoskeletons of crustaceans and in the cell walls of fungi. Chitosan is a copolymer composed of glucosamine and *N*-acetyl glucosamine units linked by 1, 4– glycosidic bonds, with the latter unit usually exceeding 80% depending on the alkaline treatment. The proportion of glucosamine is known the degree of deacetylation (DD) and becomes soluble in an aqueous acidic medium. When the DD of chitin is higher than 50%, then the structure is usually known as chitosan.[67]

Chitosan has been considered to be a potential gene carrier since it is known as a biocompatible,[53] biodegradable,[68] and low toxic biomaterial with high cationic charges. However, the poor specificity and low transfection efficiency of chitosan must be overcome before its end-use in clinical trials.[55] Fortunately, chitosan provides several functional groups along its backbone for further surface modification, so that the final property of the modified chitosan derivatives can be tailored.[69]

2.4.1 Chitosan modification with small functional groups

The chemical and physical properties of chitosan, such as solubility and surface charge, can be improved by the conjugation of small functional groups to the backbone of chitosan. For example, phosphorylated chitosan (P-chitosan) was prepared by using the $H_3PO_4/P_2O_5/Et_3PO_4$/hexanol method resulting in a high yield and degree of substitution (DS) and improved solubility (Figure 2.3). In addition, P-chitosan also showed less thermal stability and crystallinity than chitosan due to the phosphorylation,[70] therefore resulting in significantly higher cell transfection efficiency. In another case, *N*-succinyl-chitosan (NSC), which was synthesized via the introduction of succinyl groups at the *N*-position of the

glucosamine units of chitosan, resulted in water solubility, low cytotoxicity and partial biodegradability *in vivo*.[71]

A quaternized derivative, such as *N*,*N*,*N*-trimethyl chitosan chloride (TMC) was also developed and found to have much higher aqueous solubility than chitosan in a broader pH and concentration range, overcoming the problem of the poor solubility.[72] TMC with low-molecular-weight chitosan was also synthesized and the cytotoxicity was evaluated in epithelial cell lines with respect to increasing degree of trimethylation using the 3-(4, 5-dimethylthiazol-2-yl)-2, 5-diphenyl tetrazolium bromide (MTT) assay. [73] Cytotoxicity results showed that both oligomeric chitosan and polymeric chitosan derivatives were significantly less toxic than linear polyethylenimine (lPEI). However, higher cytotoxicity was seen in the former over the latter at similar degrees of trimethylation, whilst showing a general trend of increasing cytotoxicity with increasing degree of trimethylation overall. Separately, N-Trimethylated chitosan (NMC) was cross-linked with glutaraldehyde and formed microspheres exhibiting a very smooth and hollow structure. The emulsion droplets covered with cross-linked NMC in an oil-in-water system aggregated together to form a precipitate of microspheres by coagulating with acetone. Moreover, the cross-linked NMC on the surface of the microspheres continuously curled to form a tight shell, whereas the inner area became a cavity over time, leading to hollow microspheres, which can be used in gene and drug delivery due to their unique structure.[74] Such quaternized chitosans also showed better hydroxyl radical scavenging activity in comparison to other chitosans, making them more suitable for gene delivery.[75] Li et al. reported the development of *N*, *N*-dialkyl chitosan, where its monolayer properties were particularly investigated. [76] It was found that with increasing molecular weight of backbone and length of alkyl chain, the rigidities of *N*, *N*-dialkyl chitosan monolayers were also enhanced, making this a suitable carrier in gene/drug delivery. Furthermore, the longer the alkyl chain and/or the larger the molecular weight of

chitosan backbone, the slower the gene/drug release rate of chitosan-based vesicles was found to be, as well as the equilibrium drug-release ratio.

6-amino-6-deoxy-chitosan (6-ACT) was successfully developed by introducing 6-deoxy-6-halo derivatives to the *N*-phthaloyl-chitosan backbone by reaction of N-halosuccinimides and triphenylphosphine in N-methyl-2-pyrrolidone. In contrast to chitosan, 6-ACT was found to be soluble in water at neutral pH. In addition, the transfection efficiency and cytotoxicity of the synthesized 6-ACT were shown to be superior to chitosan when it was evaluated as a gene carrier against COS-1 cells.[77] To increase the targeted capability of 6-ACT, galactosylated 6-amino-6-deoxy-chitosan (Gal-6-ACT) was designed and investigated as a gene carrier against HepG2 cell lines. It was found that Gal-6-ACT was 5–10 times more efficient than both 25 kDa PEI (PEI 25k) and unmodified 6-ACT at its optimum N/P ratio when the HepG2 cells were transfected, due to the aid of the receptor mediated cell uptake pathway. Moreover, Gal-6-ACT also could efficiently transfer genes in both A549 and HeLa cells without the galactose receptor.[78]

In another study, deoxycholic acid conjugated chitosan (COSD) was synthesized by grafting deoxycholic acid (DOCA) to chitosan, which was found to form self-aggregated nanoparticles with nucleic acid in aqueous milieu, owing to the amphiphilic characters. The COSD nanoparticles showed superior pDNA loading and protection capability from endonuclease attack than unmodified chitosan.[79] Separately, amphiphilic linoleic acid (LA) and poly (beta-malic acid) (PMLA) double grafted chitosan (LMC) was synthesized via hydrophobic and hydrophilic modification. Compared to chitosan, LMC polymers show stronger gene binding ability in a broader pH range and could form nanosized polyplexes (<300 nm) with encoding enhanced green fluorescence protein (pEGFP) pDNA in narrow distribution. An *in vitro* transfection assay suggested that the optimal LMC/pEGFP polyplexes mediated an eight-fold improved transfection efficiency in comparison to

chitosan/pEGFP polyplexes. As well, *in vivo* experimental results showed that 4.2-fold and 2.2-fold higher intramuscular gene expressions occurred in mice compared to chitosan/pEGFP and PEI/pEGFP polyplexes, respectively, demonstrating the superiority of LMC/pDNA polyplexes.[80] In another study that aimed to improve the gene binding capability of chitosan, a primary amine of glycol chitosan was modified with 5-beta-cholanic acid to prepare a hydrophobically modified glycol chitosan (HGC). The HGC could spontaneously form polymer/pDNA nanoparticles through a hydrophobic interaction with hydrophobized pDNA. As the HGC content increased, the encapsulation efficiencies of pDNA increased, resulting in smaller HGC/DNA nanoparticles. Interestingly, upon increasing HGC content, the HGC nanoparticles became less cytotoxic and could facilitate endocytic uptakes of HGC nanoparticles by COS-1 cells. As for delivery capability, the HGC nanoparticles showed increasing *in vitro* transfection efficiencies in the presence of serum. *In vivo* results also showed that the HGC polymers had superior transfection efficiencies to commercial transfection agents such as lipo.[81] In another study, *N*-carboxyethyl chitosan (*N*-CECS) was synthesized by coupling 3-halopropionic acid to the 2-*N* site of chitosan under mild alkaline media (pH 8–9).[82] From the results, *N*-CECS displays a number of advantages including water solubility in a wide pH range, antioxidant characteristics and biodegradability in comparison to chitosan.[83] In addition, *N*-CECS was found to be a suitable mediator for transport of hydrophilic drugs and nucleic acid through the skin, or as a substrate for the introduction of nitrogen oxide for medical purposes.[84]

A functional and biodegradable chitosan supported imidazole Schiff-base (CISB) was developed in our group for gene delivery applications, through the introduction of a imidazole ring to the backbone of chitosan via the formation of a Schiff-base.[25] From this introduction of Schiff-bases and imidazole functional groups to the chitosan backbone, water solubility, gene binding, protection capacity and gene delivery abilities were significantly

improved. The enhancement in water solubility and pDNA binding capability is attributed to the presence of more nitrogen atoms with different protonation capability, with the resulting polymers retaining the basic characteristics of chitosan. CISB also shows higher transfection efficiency against HEK293 cells than commercial transfection carriers such as lPEI and lipofectamine 2000. The transfection efficiency was found to reach up to 69.47% after systematical optimization, indicating its great potential application in future gene therapy. To further investigate the application of imidazole chitosan in gene delivery, an amphiprotic imidazolyl-*O*-carboxymethyl chitosan (IOCMCS) was also developed by step-introduction of carboxyl and imidazolyl groups onto chitosan backbones.[85] Water solubility was improved due to the presence of functional carboxymethyl and imidazole groups. The gene binding capacity was also dramatically increased due to the introduction of the imidazole ring. In addition, the presence of carboxymethyl groups could enhance the gene release process, which would result in higher cell transfection efficiency against HEK293 cells than commercial transfection reagents, such as PEI and lipofectamine 2000. Overall, the IOCMCS polymer demonstrated its potential as a safe and efficient gene carrier.

In another experiment, graphene oxide (GO) was introduced to chitosan (CS) via EDC chemistry and formed CS-grafted GO (GO–CS) sheets, which resulted in good aqueous solubility and biocompatibility.[86] Characterization shows that GO–CS condenses pDNA into stable, nanosized complexes (<200 nm), and the resulting GO–CS/pDNA nanoparticles exhibit higher transfection efficiency than that of chitosan in HeLa cells at certain nitrogen/phosphate ratios. Thus, GO–CS nanocarriers could have potential as a gene carrier in future gene therapy.

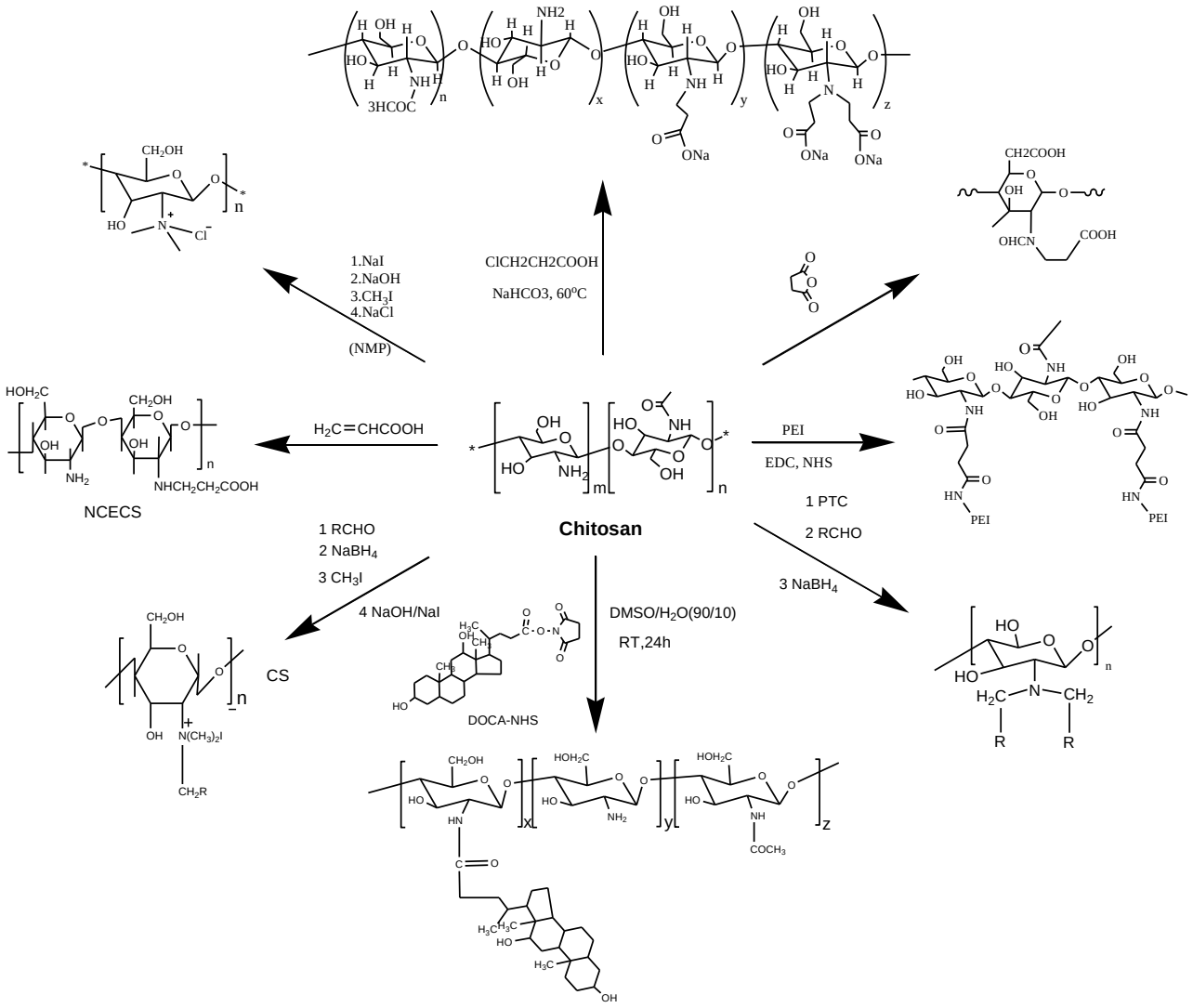

Figure 2.3 Modifications of chitosan.

2.4.2 Chitosan modification with ligands

Ligand conjugation is another important way of modifying carriers in the development for targeted delivery systems. A desirable aspect of this modification is that this conjugation is less heavily dependent on the sophisticated forethought of structure–activity relationships (SAR) during operational design. In addition, the chemical modification process of ligand conjugation is simple since biological properties of the ligand are easily accessible from public databases, which would also avoid potential problems in the systematic design for

intricate chemical conversions.

Proteins and peptides are an important family of ligands for polycation carrier conjugation. Mao's group grafted knob protein and transferrin to chitosan, where conjugation of these proteins to chitosan boosted the transfection efficacy of the carrier when compared to unmodified chitosan. [87] Particularly, pDNA delivery mediated by knob protein and transferrin conjugated chitosan nanoparticles lead to approximately 130-fold and four-fold higher gene expression levels in HeLa, respectively. This is due to related receptors on the membrane of the HeLa cell which can enhance the uptake of polymer/pDNA nanoparticles. Alternatively, OX26 monoclonal antibody was conjugated to poly (ethylene glycol) (PEG) grafted chitosan using avidin (SA)-biotin (BIO) technology to result in the functionalized CS-PEG-BIO-SA/OX26 polymer. [88] This polymer has affinity for the transferrin receptor (TfR) and could improve the transport of therapeutic materials into the brain by triggering receptor-mediated transport across the the blood-brain barrier (BBB).

Apart from proteins and peptides, non-protein ligands have also been widely employed for development of targeted delivery systems. As an example, Cho et al. designed and prepared mannosylated chitosan (MC), which can induce mannose receptor-mediated endocytosis of the IL-12 gene directly into dendritic cells which reside within the tumour of study. [89] Upon characterization, MC was proven to be suitable for IL-12 gene delivery, attributed to good physicochemical properties and low cytotoxicity. Moreover, MC exhibited much enhanced IL-12 gene transfer efficiency to dendritic cells in comparison to chitosan itself, in terms of the induction of murine IL-12 p70 and murine IFN-gamma.

Hyaluronic acid (HA) was conjugated to chitosan using an ionotropic gelation technique and found to enhance the transfection efficacy of chitosan in both HCE cells and normal human conjunctive IOBA-NHC cells. Furthermore, the HA and CD44 receptors enhanced complex internalization, confirmed by using fluorescence confocal microscopy.[90] Similarly,

folic acid (FA), a special ligand for cancer cells, allows endocytosis of nanoparticles with the aid of folate receptors (FR). [91] The FR is over-expressed on most human cancer cell surfaces, which has high affinity to folate. Therefore, higher transfection efficiency can be obtained by using folic acid-conjugated polymer as a gene carrier. For example, Mansouri et al. synthesized FA-chitosan by introducing FA to chitosan through amide linkages between amino groups of chitosan and the carboxylic group of FA for folate-mediated endocytosis, although the transfection efficiency of the FA chitosan/pDNA complexes *in vitro* was not reported.[92] Furthermore, Lee conjugated FA as a targeting ligand to chitosan, in order to specifically deliver pDNA to over-expressed FR on cancer cells. [93] It was concluded that FA-conjugated chitosan exhibited significantly enhanced gene transfer potential in FR over expressed cancer cells, as compared to unmodified chitosan.

2.4.3 Chitosan modification with grafting copolymerization

Copolymerization is a popular method in macromolecular chemistry to modify polymeric properties of macromolecules. Among the different polymeric modifiers used, PEG, an amphiphilic polyether diol, is one of the popular choices in chitosan carrier modification. As evidenced by the literature, chitosan grafted with PEG (MW = 5 kDa, grafting degree = 9.6%) can prevent aggregation of polyplex, even in the presence of serum and bile.[94, 95]

PEI is another modifier that is commonly used in chitosan derivatives as gene carriers. Wong et al. grafted PEI on chitosan and developed PEI-g-chitosan, where *in vivo* studies suggested that the transfection ability of PEI-g-chitosan graft copolymer was approximately three-fold, 58-fold and 141-fold higher than that of chitosan, PEI, and naked pDNA, respectively. However, the cytotoxicity assay showed that approximately 50% of HeLa cells were killed after incubation with PEI-g-chitosan at incubation concentrations of approximately 100 mg/L *in vitro*.[96] As an alternative to Wong's cationic polymerization method, Wing’s group conjugated low molecular weight (LMW) PEI (600 Da and 1.2 kDa)

with chitosan by using a coupling reagent and this polymer showed low cytotoxicity and high transfection efficacy (1000 fold higher than chitosan) in 293A kidney cells.[97] Therefore, the conjugation mechanism and grafting ratios of PEI appear to be two important factors in determining the properties of CHI-g-PEI produced. Recently, other CHI-g-PEI have been synthesized and published. For example, Lou et al. synthesized PEI-g-CHI that contains an EX-810 spacer, which displayed lower cytotoxicity than chitosan in 293T cells.[98] Jiang et al. synthesized galactosylated CHI-g-PEI (Gal-CHI-g-PEI), which exhibited high transfection efficacy after galactosylation in $HepG_2$, even though the cytotoxicity was a little high;[99] nevertheless, the cytotoxicity problem in Gal-CHI-g-PEI can be alleviated via PEGylation.[95b]

To further improve the transfection ability of the chitosan derivative, a number of secondary derivative carriers have been made, including trimethyl chitosan-g-poly(*N*-isopropyl-acrylamide) and PEG-graft-trimethyl chitosan.[100] The former is a thermoresponsive copolymer synthesized by coupling PNIPAAm-COOH to trimethyl chitosan which has zeta potential and pDNA affinity adjustable by controlling the solution temperature below or above the lower critical solution temperature (LCST) of 32ºC. For the latter, it was reported that this carrier showed improved colloidal stability, decreased cytotoxicity and 10-fold more effectiveness than non-PEGylated quaternized chitosan in transfecting L929 and NIH/3T3 cells.[101]

Besides the aforementioned examples, there are also other chitosan graft copolymers that have been developed with promising results. For example, PLL was introduced onto the 2-*N* site in chitosan and generated PLL-graft-chitosan (PLL-g-CHI), whereby showing significant improvement in solubility and gene binding ability.[102] Sun et al. synthesized a chitosan-NIPAAm/vinyl laurate copolymer, and the solubility and gene binding ability were found to be also improved; however, the transfection efficiency obtained with this polymer was only 50% to that of lipofectamine 2000.[103] Another biodegradable polycation, (PDMAEMA-

Chitosan, PDCS) was developed as a highly efficient gene carrier through coupling poly ((2-dimethylamino) ethylmethacrylate) (P(DMAEMA)) side chains of different length to chitosan backbones via ATRP in a well-controlled manner. [104] These PDCS carriers exhibited good ability to condense pDNA and protect it from enzymatic degradation by DNase I. In addition, the PDCS carriers showed a higher level of gene transfer capability and lower cytotoxicity in COS7, HEK293 and HepG2 cell lines in comparison with HMW P(DMAEMA) and 'gold-standard' PEI 25k. These well-defined PDCS polymers demonstrate great potential as efficient gene carriers in future gene therapy.

2.5 Conclusion

Gene therapy can theoretically cure a variety of genetic diseases; however, the lack of ideal gene carriers hinders its further application. Particularly, polymer-based gene carriers hold great potential in gene therapy, but their effectiveness, biocompatibility and targeting capabilioty remain weak as gene carriers and need to be improved, therefore being generally considered unacceptable in clinical applications. In this review, we focus on the mechanism and challenges in polycation mediated nucleic acid delivery, in order to better understand and improve gene therapy. Furthermore, design considerations of polymeric carriers were analysed and concluded according to the processes and barriers of gene delivery for development of new polymer-based gene carriers. Finally, the recent advances in design and development of synthetic gene delivery systems based on chitosan conjugation were reviewed. On the basis of studies of "off-the-shelf" gene carriers, much knowledge about structure-function relationship of polymeric gene carriers including the interaction between gene carriers and its cargo, surface characteristics, and the regulation of gene transport journey via the design of carriers can be learned. Inspired by these knowledges, chitosan is chosen as a mother polymer and modified with various small functional moleculars to develope smart chitosan based polymers as gene carrier in gene theray, which will be

introduced with details in the following charpers.

References

1.Tachibana M; Amato P; Sparman M; Woodward J; Sanchis DM; Ma H; Gutierrez NM; Tippner-Hedges R; Kang E; Lee HS; Ramsey C; Masterson K; Battaglia D; Lee D; Wu D; Jensen J; Patton P; Gokhale S; Stouffer R; S., M., Towards germline gene therapy of inherited mitochondrial diseases. *Nature* **2013,** *493* (7434), 627-631.

2. Mancuso, K.; Hauswirth, W. W.; Li, Q. H.; Connor, T. B.; Kuchenbecker, J. A.; Mauck, M. C.; Neitz, J.; Neitz, M., Gene therapy for red-green colour blindness in adult primates. *Nature* **2009,** *461* (7265), 784-U34.

3. Mendell, J. R.; Campbell, K.; Rodino-Klapac, L.; Sahenk, Z.; Shilling, C.; Lewis, S.; Bowles, D.; Gray, S.; Li, C. W.; Galloway, G.; Malik, V.; Coley, B.; Clark, K. R.; Li, J. A.; Xiao, X. A.; Samulski, J.; McPhee, S. W.; Samulski, R. J.; Walker, C. M., Brief Report: Dystrophin Immunity in Duchenne's Muscular Dystrophy. *New England Journal of Medicine* **2010,** *363* (15), 1429-1437.

4. London Gene Therapy Trial for Cystic Fibrosis Saved. *Science* **2012,** *335* (6075), 1423-1423.

5. (a) Harris, T., Gene and drug matrix for personalized cancer therapy. *Nature Reviews Drug Discovery* **2010,** *9* (8), 660-U100; (b) Gustafson, J. A.; Ghandehari, H., Silk-elastinlike protein polymers for matrix-mediated cancer gene therapy. *Adv Drug Deliver Rev* **2010,** *62* (15), 1509-1523.

6. (a) Fischer, A.; Hacein-Bey-Abina, S.; Cavazzana-Calvo, M., 20 years of gene therapy for SCID. *Nature Immunology* **2010,** *11* (6), 457-460; (b) Mavilio, F., Gene therapies need new development models. *Nature* **2012,** *490* (7418), 7-7.

7. High, K. A., Gene therapy - The moving finger. *Nature* **2005,** *435* (7042), 577-578.

8. *http://www.wiley.com/legacy/wileychi/genmed/clinical/* **2012**.

9. Check, E., Gene-therapy trials to restart following cancer risk review. *Nature* **2005,** *434* (7030), 127-127.

10. Luo, D.; Saltzman, W. M., Synthetic DNA delivery systems. *Nat Biotechnol* **2000,** *18* (1), 33-37.

11. Kost, J.; Langer, R., Responsive polymeric delivery systems. *Adv Drug Deliver Rev* **2012,** *64*, 327-341.

12. Vallet-Regi, M.; Colilla, M.; Gonzalez, B., Medical applications of organic-inorganic hybrid materials within the field of silica-based bioceramics. *Chemical Society Reviews* **2011,** *40* (2), 596-607.

13. Dreaden, E. C.; Alkilany, A. M.; Huang, X. H.; Murphy, C. J.; El-Sayed, M. A., The golden age: gold nanoparticles for biomedicine. *Chemical Society Reviews* **2012,** *41* (7), 2740-2779.

14. Shim, M. S.; Kwon, Y. J., Stimuli-responsive polymers and nanomaterials for gene delivery and imaging applications. *Adv Drug Deliver Rev* **2012,** *64* (11), 1046-1058.

15. Lu, Y. J.; Low, P. S., Folate-mediated delivery of macromolecular anticancer therapeutic agents. *Adv Drug Deliver Rev* **2012,** *64*, 342-352.

16. Breunig, M.; Lungwitz, U.; Liebl, R.; Goepferich, A., Breaking up the correlation between efficacy and toxicity for nonviral gene delivery. *P Natl Acad Sci USA* **2007,** *104* (36), 14454-14459.

17. Mastrobattista, E.; Hennink, W. E., Polymers for Gene Delivery Charged for Success. *Nat Mater* **2012,** *11* (1), 10-12.

18. Bae, Y. U.; Kim, B. K.; Park, J. W.; Seu, Y. B.; Doh, K. O., Endocytic Pathway and Resistance to Cholesterol Depletion of Cholesterol Derived Cationic Lipids for Gene Delivery. *Mol Pharmaceut* **2012,** *9* (12), 3579-3585.

19. Xiang, S. N.; Tong, H. J.; Shi, Q.; Fernandes, J. C.; Jin, T.; Dai, K. R.; Zhang, X. L.,

Uptake mechanisms of non-viral gene delivery. *J Control Release* **2012,** *158* (3), 371-378.

20. Jiang, W.; Kim, B. Y. S.; Rutka, J. T.; Chan, W. C. W., Nanoparticle-mediated cellular response is size-dependent. *Nature Nanotechnology* **2008,** *3* (3), 145-150.

21. Cho, E. C.; Au, L.; Zhang, Q.; Xia, Y. N., The Effects of Size, Shape, and Surface Functional Group of Gold Nanostructures on Their Adsorption and Internalization by Cells. *Small* **2010,** *6* (4), 517-522.

22. LaManna, C. M.; Lusic, H.; Camplo, M.; McIntosh, T. J.; Barthelemy, P.; Grinstaff, M. W., Charge-Reversal Lipids, Peptide-Based Lipids, and Nucleoside-Based Lipids for Gene Delivery. *Accounts of Chemical Research* **2012,** *45* (7), 1026-1038.

23. Kamaly, N.; Xiao, Z. Y.; Valencia, P. M.; Radovic-Moreno, A. F.; Farokhzad, O. C., Targeted polymeric therapeutic nanoparticles: design, development and clinical translation. *Chemical Society Reviews* **2012,** *41* (7), 2971-3010.

24. Liu, Z. H.; Zhang, Z. Y.; Zhou, C. R.; Jiao, Y. P., Hydrophobic modifications of cationic polymers for gene delivery. *Prog Polym Sci* **2010,** *35* (9), 1144-1162.

25. Shi, B. Y.; Zhang, H.; Shen, Z. Y.; Bi, J. X.; Dai, S., Developing a chitosan supported imidazole Schiff-base for high-efficiency gene delivery. *Polym Chem-Uk* **2013,** *4* (3), 840-850.

26. Kim, J. A.; Aberg, C.; Salvati, A.; Dawson, K. A., Role of cell cycle on the cellular uptake and dilution of nanoparticles in a cell population. *Nature Nanotechnology* **2012,** *7* (1), 62-68.

27. Gratton, S. E. A.; Ropp, P. A.; Pohlhaus, P. D.; Luft, J. C.; Madden, V. J.; Napier, M. E.; DeSimone, J. M., The effect of particle design on cellular internalization pathways. *P Natl Acad Sci USA* **2008,** *105* (33), 11613-11618.

28. Gruenberg, J.; van der Goot, F. G., Mechanisms of pathogen entry through the endosomal compartments. *Nature Reviews Molecular Cell Biology* **2006,** *7* (7), 495-504.

29. Varkouhi, A. K.; Scholte, M.; Storm, G.; Haisma, H. J., Endosomal escape pathways for

delivery of biologicals. *J Control Release* **2011,** *151* (3), 220-228.

30. Akinc, A.; Thomas, M.; Klibanov, A. M.; Langer, R., Exploring polyethylenimine-mediated DNA transfection and the proton sponge hypothesis. *J Gene Med* **2005,** *7* (5), 657-663.

31. Thiery, J.; Keefe, D.; Boulant, S.; Boucrot, E.; Walch, M.; Martinvalet, D.; Goping, I. S.; Bleackley, R. C.; Kirchhausen, T.; Lieberman, J., Perforin pores in the endosomal membrane trigger the release of endocytosed granzyme B into the cytosol of target cells. *Nature Immunology* **2011,** *12* (8), 770-U146.

32. Ohya, T.; Miaczynska, M.; Coskun, U.; Lommer, B.; Runge, A.; Drechsel, D.; Kalaidzidis, Y.; Zerial, M., Reconstitution of Rab- and SNARE-dependent membrane fusion by synthetic endosomes. *Nature* **2009,** *459* (7250), 1091-U77.

33. Mellert, K.; Lamla, M.; Scheffzek, K.; Wittig, R.; Kaufmann, D., Enhancing Endosomal Escape of Transduced Proteins by Photochemical Internalisation. *Plos One* **2012,** *7* (12).

34. Kulkarni, R. P.; Mishra, S.; Fraser, S. E.; Davis, M. E., Single cell kinetics of intracellular, nonviral, nucleic acid delivery vehicle acidification and trafficking. *Bioconjugate Chem* **2005,** *16* (4), 986-994.

35. Benjaminsen, R. V.; Mattebjerg, M. A.; Henriksen, J. R.; Moghimi, S. M.; Andresen, T. L., The Possible "Proton Sponge" Effect of Polyethylenimine (PEI) Does Not Include Change in Lysosomal pH. *Mol Ther* **2013,** *21* (1), 149-157.

36. (a) Srinivas, R.; Samanta, S.; Chaudhuri, A., Cationic amphiphiles: promising carriers of genetic materials in gene therapy. *Chemical Society Reviews* **2009,** *38* (12), 3326-3338; (b) Pichon, C.; Billiet, L.; Midoux, P., Chemical vectors for gene delivery: uptake and intracellular trafficking. *Curr Opin Biotech* **2010,** *21* (5), 640-645.

37. Pouton, C. W.; Wagstaff, K. M.; Roth, D. M.; Moseley, G. W.; Jans, D. A., Targeted delivery to the nucleus. *Adv Drug Deliver Rev* **2007,** *59* (8), 698-717.

38. K.M. Fichter; N.P. Ingle; P.M. McLendon; Reineke, T. M., Polymeric Nucleic Acid Vehicles Exploit Active Interorganelle Trafficking Mechanisms. *Acs Nano* **2013,** *7* (1), 347-364.

39. Stewart, M., Molecular mechanism of the nuclear protein import cycle. *Nature Reviews Molecular Cell Biology* **2007,** *8* (3), 195-208.

40. Glover, D. J.; Leyton, D. L.; Moseley, G. W.; Jans, D. A., The efficiency of nuclear plasmid DNA delivery is a critical determinant of transgene expression at the single cell level. *J Gene Med* **2010,** *12* (1), 77-85.

41. Grandinetti, G.; Smith, A. E.; Reineke, T. M., Membrane and Nuclear Permeabilization by Polymeric pDNA Vehicles: Efficient Method for Gene Delivery or Mechanism of Cytotoxicity? *Mol Pharmaceut* **2012,** *9* (3), 523-538.

42. Grandinetti, G.; Reineke, T. M., Exploring the Mechanism of Plasmid DNA Nuclear Internalization with Polymer-Based Vehicles. *Mol Pharmaceut* **2012,** *9* (8), 2256-2267.

43. Ruponen, M.; Arkko, S.; Reinisalo, M.; Urtti, A.; Ranta, V. P., Intracellular elimination and unpacking kinetics of DNA mediated with various non-viral gene delivery systems. *Hum Gene Ther* **2008,** *19* (10), 1094-1095.

44. Guo, C. P.; Chen, W. C.; Lin, S. D.; Li, H.; Cheng, D.; Wang, X. Y.; Shuai, X. T., Synthesis and characterization of polycation block copolymer Poly(L-lysine)-b-poly N-(N ',N '-diisopropyl-aminoethyl)aspartamide as potential pH responsive gene delivery system. *Polymer* **2012,** *53* (2), 342-349.

45. Jiang, X. A.; Zheng, Y. R.; Chen, H. H.; Leong, K. W.; Wang, T. H.; Mao, H. Q., Dual-Sensitive Micellar Nanoparticles Regulate DNA Unpacking and Enhance Gene-Delivery Efficiency. *Adv Mater* **2010,** *22* (23), 2556-2560.

46. (a) Omidi, Y.; Hollins, A. J.; Benboubetra, M.; Drayton, R.; Benter, I. F.; Akhtar, S., Toxicogenomics of non-viral vectors for gene therapy: A microarray study of lipofectin- and

oligofectamine-induced gene expression changes in human epithelial cells. *J. Drug Target.* **2003,** *11* (6), 311-323; (b) Omidi, Y.; Hollins, A. J.; Drayton, R. M.; Akhtar, S., Polypropylenimine dendrimer-induced gene expression changes: The effect of complexation with DNA, dendrimer generation and cell type. *J. Drug Target.* **2005,** *13* (7), 431-443.

47. Parhamifar, L.; Larsen, A. K.; Hunter, A. C.; Andresen, T. L.; Moghimi, S. M., Polycation cytotoxicity: a delicate matter for nucleic acid therapy-focus on polyethylenimine. *Soft Matter* **2010,** *6* (17), 4001-4009.

48. Guo, Y.; Chen, W. J.; Wang, W. W.; Shen, J.; Guo, R. M.; Gong, F. M.; Lin, S. D.; Cheng, D.; Chen, G. H.; Shuai, X. T., Simultaneous Diagnosis and Gene Therapy of Immuno-Rejection in Rat Allogeneic Heart Transplantation Model Using a T-Cell-Targeted Theranostic Nanosystem. *Acs Nano* **2012,** *6* (12), 10646-10657.

49. Piest, M.; Engbersen, J. F. J., Effects of charge density and hydrophobicity of poly(amido amine)s for non-viral gene delivery. *J Control Release* **2010,** *148* (1), 83-90.

50. Grigsby, C. L.; Leong, K. W., Balancing protection and release of DNA: tools to address a bottleneck of non-viral gene delivery. *J R Soc Interface* **2010,** *7*, S67-S82.

51. Ahmed, M.; Jawanda, M.; Ishihara, K.; Narain, R., Impact of the nature, size and chain topologies of carbohydrate-phosphorylcholine polymeric gene delivery systems. *Biomaterials* **2012,** *33* (31), 7858-7870.

52. Lam, A. P.; Dean, D. A., Progress and prospects: nuclear import of nonviral vectors. *Gene Ther* **2010,** *17* (4), 439-447.

53. Hynes, A. P.; Mercer, R. G.; Watton, D. E.; Buckley, C. B.; Lang, A. S., DNA packaging bias and differential expression of gene transfer agent genes within a population during production and release of the Rhodobacter capsulatus gene transfer agent, RcGTA. *Mol Microbiol* **2012,** *85* (2), 314-325.

54. Dai, M.; Liu, J.; Chen, D. E.; Rao, Y.; Tang, Z. J.; Ho, W. Z.; Dong, C. Y., Tumor-targeted

gene therapy using Adv-AFP-HRPC/IAA prodrug system suppresses growth of hepatoma xenografted in mice. *Cancer Gene Ther* **2012,** *19* (2), 77-83.

55. Zhao, Y.; Lam, D. H.; Yang, J.; Lin, J.; Tham, C. K.; Ng, W. H.; Wang, S., Targeted suicide gene therapy for glioma using human embryonic stem cell-derived neural stem cells genetically modified by baculoviral vectors. *Gene Ther* **2012,** *19* (2), 189-200.

56. Liu, M.; Li, Z. H.; Xu, F. J.; Lai, L. H.; Wang, Q. Q.; Tang, G. P.; Yang, W. T., An oligopeptide ligand-mediated therapeutic gene nanocomplex for liver cancer-targeted therapy. *Biomaterials* **2012,** *33* (7), 2240-2250.

57. Wasungu, L.; Scarzello, M.; van Dam, G.; Molema, G.; Wagenaar, A.; Engberts, J. B. F. N.; Hoekstra, D., Transfection mediated by pH-sensitive sugar-based gemini surfactants; potential for in vivo gene therapy applications. *J Mol Med-Jmm* **2006,** *84* (9), 774-784.

58. Wang, J. L.; Tang, G. P.; Shen, J.; Hu, Q. L.; Xu, F. J.; Wang, Q. Q.; Li, Z. H.; Yang, W. T., A gene nanocomplex conjugated with monoclonal antibodies for targeted therapy of hepatocellular carcinoma. *Biomaterials* **2012,** *33* (18), 4597-4607.

59. McNamara, J. O.; Andrechek, E. R.; Wang, Y.; D Viles, K.; Rempel, R. E.; Gilboa, E.; Sullenger, B. A.; Giangrande, P. H., Cell type-specific delivery of siRNAs with aptamer-siRNA chimeras. *Nat Biotechnol* **2006,** *24* (8), 1005-1015.

60. Stuart, M. A. C.; Huck, W. T. S.; Genzer, J.; Muller, M.; Ober, C.; Stamm, M.; Sukhorukov, G. B.; Szleifer, I.; Tsukruk, V. V.; Urban, M.; Winnik, F.; Zauscher, S.; Luzinov, I.; Minko, S., Emerging applications of stimuli-responsive polymer materials. *Nat Mater* **2010,** *9* (2), 101-113.

61. Seymour, L. W., The future of gene therapy in the UK. *Trends in Biotechnology* **2006,** *24* (8), 347-349.

62. Galy, A.; Charrier, S.; Merten, O. W.; Caizergues, D., Vector Safety Data Leading to a Clinical Trial for the Gene Therapy of Wiskott Aldrich Syndrome: A Perspective on Future

Developments. *Hum Gene Ther* **2010,** *21* (9), 1178-1178.

63. Behr, J. P., Synthetic Gene Transfer Vectors II: Back to the Future. *Accounts of Chemical Research* **2012,** *45* (7), 980-984.

64. Holmes, C. A.; Tabrizian, M., Substrate-Mediated Gene Delivery from Glycol-Chitosan/Hyaluronic Acid Polyelectrolyte Multilayer Films. *Acs Appl Mater Inter* **2013,** *5* (3), 524-531.

65. Sun, J.; Zeng, F.; Jian, H. L.; Wu, S. Z., Conjugation with Betaine: A Facile and Effective Approach to Significant Improvement of Gene Delivery Properties of PEI. *Biomacromolecules* **2013,** *14* (3), 728-736.

66. Zhai, X. Y.; Wang, W.; Wang, C. D.; Wang, Q.; Liu, W. G., PDMAEMA-b-polysulfobetaine brushes-modified epsilon-polylysine as a serum-resistant vector for highly efficient gene delivery. *J Mater Chem* **2012,** *22* (44), 23576-23586.

67. Cho, Y. W.; Cho, Y. N.; Chung, S. H.; Yoo, G.; Ko, S. W., Water-soluble chitin as a wound healing accelerator. *Biomaterials* **1999,** *20* (22), 2139-2145.

68. (a) Kumar, T. R.; Shanmugasundaram, N.; Babu, M., Biocompatible collagen scaffolds from a human amniotic membrane: physicochemical and in vitro culture characteristics. *J Biomat Sci-Polym E* **2003,** *14* (7), 689-706; (b) Sashiwa, H.; Yajima, H.; Aiba, S., Synthesis of a chitosan-dendrimer hybrid and its biodegradation. *Biomacromolecules* **2003,** *4* (5), 1244-1249.

69. (a) Berscht, P. C.; Nies, B.; Liebendorfer, A.; Kreuter, J., In-Vitro Evaluation of Biocompatibility of Different Wound Dressing Materials. *Journal of Materials Science-Materials in Medicine* **1995,** *6* (4), 201-205; (b) Muzzarelli, R. A. A., Human enzymatic activities related to the therapeutic administration of chitin derivatives. *Cellular and Molecular Life Sciences* **1997,** *53* (2), 131-140.

70. Jayakumar, R.; Nagahama, H.; Furuike, T.; Tamura, H., Synthesis of phosphorylated

chitosan by novel method and its characterization. *International Journal of Biological Macromolecules* **2008,** *42* (4), 335-339.

71. (a) Sun, S. L.; Wang, A. Q., Adsorption properties of N-succinyl-chitosan and cross-linked N-succinyl-chitosan resin with Pb(II) as template ions. *Separation and Purification Technology* **2006,** *51* (3), 409-415; (b) Lu, B.; Sun, Y. X.; Li, Y. Q.; Zhang, X. Z.; Zhuo, R. X., N-Succinyl-chitosan grafted with low molecular weight polyethylenimine as a serum-resistant gene vector. *Molecular Biosystems* **2009,** *5* (6), 629-637; (c) Zhu, A. P.; Yuan, L. H.; Dai, S., Preparation of well-dispersed superparamagnetic iron oxide nanoparticles in aqueous solution with biocompatible N-succinyl-O-carboxymethylchitosan. *Journal of Physical Chemistry C* **2008,** *112* (14), 5432-5438.

72. Zhang, C.; Ding, Y.; Yu, L. L.; Ping, Q. N., Polymeric micelle systems of hydroxycamptothecin based on amphiphilic N-alkyl-N-trimethyl chitosan derivatives. *Colloids and Surfaces B-Biointerfaces* **2007,** *55* (2), 192-199.

73. Kean, T.; Roth, S.; Thanou, M., Trimethylated chitosans as non-viral gene delivery vectors: Cytotoxicity and transfection efficiency. *Journal of Controlled Release* **2005,** *103* (3), 643-653.

74. Peng, X. H.; Zhang, L., Surface fabrication of hollow microspheres from N-methylated chitosan cross-linked with gultaraldehyde. *Langmuir* **2005,** *21* (3), 1091-1095.

75. Guo, Z. Y.; Liu, H. Y.; Chen, X. L.; Ji, X.; Li, P. C., Hydroxyl radicals scavenging activity of N-substituted chitosan and quaternized chitosan. *Bioorganic & Medicinal Chemistry Letters* **2006,** *16* (24), 6348-6350.

76. Li, M. C.; Su, S.; Xin, M. H.; Liao, Y. Z., Relationship between N,N-dialkyl chitosan monolayer and corresponding vesicle. *Journal of Colloid and Interface Science* **2007,** *311* (1), 285-288.

77. Satoh, T.; Kano, H.; Nakatani, M.; Sakairi, N.; Shinkai, S.; Nagasaki, T., 6-Amino-6-

deoxy-chitosan. Sequential chemical modifications at the C-6 positions of N-phthaloyl-chitosan and evaluation as a gene carrier. *Carbohyd Res* **2006,** *341* (14), 2406-2413.

78. Satoh, T.; Kakimoto, S.; Kano, H.; Nakatani, M.; Shinkai, S.; Nagasaki, T., In vitro gene delivery to HepG2 cells using galactosylated 6-amino-6-deoxychitosan as a DNA carrier. *Carbohyd Res* **2007,** *342* (11), 1427-1433.

79. Nah, J. W.; Chae, S. Y.; Son, S.; Lee, M.; Jang, M. K., Deoxycholic acid-conjugated chitosan oligosaccharide nanoparticles for efficient gene carrier. *J Control Release* **2005,** *109* (1-3), 330-344.

80. Yin, C. H.; Wang, B. Q.; He, C. B.; Tang, C., Effects of hydrophobic and hydrophilic modifications on gene delivery of amphiphilic chitosan based nanocarriers. *Biomaterials* **2011,** *32* (20), 4630-4638.

81. Jeong, S. Y.; Yoo, H. S.; Lee, J. E.; Chung, H.; Kwon, I. C., Self-assembled nanoparticles containing hydrophobically modified glycol chitosan for gene delivery. *J Control Release* **2005,** *103* (1), 235-243.

82. Skorik, Y. A.; Gomes, C. A. R.; Vasconcelos, M. T. S. D.; Yatluk, Y. G., N-(2-carboxyethyl)chitosans: regioselective synthesis, characterisation and protolytic equilibria. *Carbohyd Res* **2003,** *338* (3), 271-276.

83. Pan, Y. N.; Luo, X. D.; Zhu, A. P.; Dai, S., Synthesis and Physicochemical Properties of Biocompatible N-carboxyethylchitosan. *J Biomat Sci-Polym E* **2009,** *20* (7-8), 981-992.

84. Song, Q. P.; Zhang, Z.; Gao, J. G.; Ding, C. M., Synthesis and Property Studies of N-Carboxymethyl Chitosan. *J Appl Polym Sci* **2011,** *119* (6), 3282-3285.

85. Shi, B. Y.; Shen, Z. Y.; Zhang, H.; Bi, J. X.; Dai, S., Exploring N-Imidazolyl-O-Carboxymethyl Chitosan for High Performance Gene Delivery. *Biomacromolecules* **2012,** *13* (1), 146-153.

86. Bao, H. Q.; Pan, Y. Z.; Ping, Y.; Sahoo, N. G.; Wu, T. F.; Li, L.; Li, J.; Gan, L. H.,

Chitosan-Functionalized Graphene Oxide as a Nanocarrier for Drug and Gene Delivery. *Small* **2011,** *7* (11), 1569-1578.

87. Mao, H. Q.; Roy, K.; Troung-Le, V. L.; Janes, K. A.; Lin, K. Y.; Wang, Y.; August, J. T.; Leong, K. W., Chitosan-DNA nanoparticles as gene carriers: synthesis, characterization and transfection efficiency. *Journal of Controlled Release* **2001,** *70* (3), 399-421.

88. Couvreur, P.; Aktas, Y.; Yemisci, M.; Andrieux, K.; Gursoy, R. N.; Alonso, M. J.; Fernandez-Megia, E.; Novoa-Carballal, R.; Quinoa, E.; Riguera, R.; Sargon, M. F.; Celik, H. H.; Demir, A. S.; Hincal, A. A.; Dalkara, T.; Capan, Y., Development and brain delivery of chitosan-PEG nanoparticles functionalized with the monoclonal antibody OX26. *Bioconjugate Chem* **2005,** *16* (6), 1503-1511.

89. Cho, M. H.; Kim, T. H.; Jin, H.; Kim, H. W.; Cho, C. S., Mannosylated chitosan nanoparticle-based cytokine gene therapy suppressed cancer growth in BALB/c mice bearing CT-26 carcinoma cells. *Mol Cancer Ther* **2006,** *5* (7), 1723-1732.

90. Alonso, M. J.; de la Fuente, M.; Seijo, B., Novel hyaluronic acid-chitosan nanoparticles for ocular gene therapy. *Invest Ophth Vis Sci* **2008,** *49* (5), 2016-2024.

91. Lee, R. J.; Sudimack, J., Targeted drug delivery via the folate receptor. *Adv Drug Deliver Rev* **2000,** *41* (2), 147-162.

92. Mansouri, S.; Cuie, Y.; Winnik, F.; Shi, Q.; Lavigne, P.; Benderdour, M.; Beaumont, E.; Fernandes, J. C., Characterization of folate-chitosan-DNA nanoparticles for gene therapy. *Biomaterials* **2006,** *27* (9), 2060-2065.

93. Mohapatra, S.; Lee, D.; Lockey, R., Folate receptor-mediated cancer cell specific gene delivery using folic acid-conjugated oligochitosans. *J Nanosci Nanotechno* **2006,** *6* (9-10), 2860-2866.

94. Jiang, X.; Dai, H.; Leong, K. W.; Goh, S. H.; Mao, H. Q.; Yang, Y. Y., Chitosan-g-PEG/DNA complexes deliver gene to the rat liver via intrabiliary and intraportal infusions.

Journal of Gene Medicine **2006,** *8* (4), 477-487.

95. (a) Zhang, Y. Q.; Chen, J. J.; Zhang, Y. D.; Pan, Y. F.; Zhao, J. F.; Ren, L. F.; Liao, M. M.; Hu, Z. Y.; Kong, L.; Wang, J. W., A novel PEGylation of chitosan nanoparticles for gene delivery. *Biotechnology and Applied Biochemistry* **2007,** *46*, 197-204; (b) Jiang, H. L.; Kwon, J. T.; Kim, E. M.; Kim, Y. K.; Arote, R.; Jere, D.; Jeong, H. J.; Jang, M. K.; Nah, J. W.; Xu, C. X.; Park, I. K.; Cho, M. H.; Cho, C. S., Galactosylated poly(ethylene glycol)-chitosan-graft-polyethylenimine as a gene carrier for hepatocyte-targeting. *Journal of Controlled Release* **2008,** *131* (2), 150-157.

96. Wong, K.; Sun, G. B.; Zhang, X. Q.; Dai, H.; Liu, Y.; He, C. B.; Leong, K. W., PEI-g-chitosan, a novel gene delivery system with transfection efficiency comparable to polyethylenimine in vitro and after liver administration in vivo. *Bioconjugate Chem* **2006,** *17* (1), 152-158.

97. Lai, W. F.; Lin, M. C. M., Nucleic acid delivery with chitosan and its derivatives. *J Control Release* **2009,** *134* (3), 158-168.

98. Lou, Y. L.; Peng, Y. S.; Chen, B. H.; Wang, L. F.; Leong, K. W., Poly(ethylene imine)-g-chitosan using EX-810 as a spacer for nonviral gene delivery vectors. *Journal of Biomedical Materials Research Part A* **2009,** *88A* (4), 1058-1068.

99. Jiang, H. L.; Kwon, J. T.; Kim, Y. K.; Kim, E. M.; Arote, R.; Jeong, H. J.; Nah, J. W.; Choi, Y. J.; Akaike, T.; Cho, M. H.; Cho, C. S., Galactosylated chitosan-graft-polyethylenimine as a gene carrier for hepatocyte targeting. *Gene Therapy* **2007,** *14* (19), 1389-1398.

100. Ma, L.; Mao, Z. W.; Yan, J.; Yan, M.; Gao, C. Y.; Shen, J. C., The gene transfection efficiency of thermoresponsive N,N,N-trimethyl chitosan chloride-g-poly(N-isopropylacrylamide) copolymer. *Biomaterials* **2007,** *28* (30), 4488-4500.

101. Germershaus, O.; Mao, S. R.; Sitterberg, J.; Bakowsky, U.; Kissel, T., Gene delivery

using chitosan, trimethyl chitosan or polyethylenglycol-graft-trimethyl chitosan block copolymers: Establishment of structure-activity relationships in vitro. *Journal of Controlled Release* **2008,** *125* (2), 145-154.

102. Xiang, Y.; Yu, Q. S.; Qi, Z.; Du, Z. A.; Xu, S. Q.; Zhang, H. F., Enhancement of immunological activity of CpG ODN by chitosan gene carrier. *Journal of Huazhong University of Science and Technology-Medical Sciences* **2007,** *27* (2), 128-130.

103. Sun, S. J.; Liu, W. G.; Cheng, N.; Zhang, B. Q.; Cao, Z. Q.; Yao, K. D.; Liang, D. C.; Zuo, A. J.; Guo, G.; Zhang, J. Y., A thermoresponsive chitosan-NIPAAm/vinyl laurate copolymer vector for gene transfection. *Bioconjugate Chemistry* **2005,** *16* (4), 972-980.

104. Ping, Y. A.; Liu, C. D.; Tang, G. P.; Li, J. S.; Li, J.; Yang, W. T.; Xu, F. J., Functionalization of Chitosan via Atom Transfer Radical Polymerization for Gene Delivery. *Adv Funct Mater* **2010,** *20* (18), 3106-3116.

Chapter 3 Developing a chitosan supported imidazole Schiff-base for high-efficiency gene delivery

Bingyang Shi, Hu Zhang, Zheyu Shen, Sheng Dai*, Jingxiu Bi*

School of Chemical Engineering, The University of Adelaide, Adelaide, SA 5005, Australia

Polym. Chem., 2013, 4, 840 / doi:10.1039/C2PY20494K

STATEMENT OF AUTHORSHIP

Developing a chitosan supported imidazole Schiff-base for high-efficiency gene delivery

Bingyang Shi, Hu Zhang, Zheyu Shen, Jingxiu Bi*, Sheng Dai*

School of Chemical Engineering, The University of Adelaide, Adelaide, SA 5005, Australia

Polym. Chem., 2013, 4, 840 / doi:10.1039/C2PY20494K

By signing the Statement of Authorship, each author certifies that their stated contribution to the publication is accurate and that permission is granted for the publication to be included in the candidate's thesis.

Bingyang Shi (Candidate)

Performed experiments, analysed results and wrote the manuscript.

I hereby certify that the statement of contribution is accurate.

*Signed.....Date...*15/08/2013
.....

Hu Zhang

Assisted in writing the manuscript.

I hereby certify that the statement of contribution is accurate.

*Signed.....Date...*15/08/2013
.....

Zheyu Shen

Assisted in writing the manuscript.

I hereby certify that the statement of contribution is accurate.

*Signed..... .....Date..*15/08/2013
.....

Jingxiu Bi

Supervised development of work and assisted in writing the manuscript.

I hereby certify that the statement of contribution is accurate.

*Signed.....Date..*15/08/2013
.....

Sheng Dai

Supervised development of work and assisted in writing the manuscript.

I hereby certify that the statement of contribution is accurate and I give permission for inclusion of the paper in the thesis.

*Signed.....Date...*15/08/2013
.....

Developing a Chitosan Supported Imidazole Schiff-base for High-Efficiency Gene Delivery

Bingyang Shi, Hu Zhang, Zheyu Shen, Jingxiu Bi*, Sheng Dai*

Abstract

A chitosan supported imidazole Schiff-base (CISB) has been developed to be used as the vector for high efficient gene delivery. Introduction of the imidazole Schiff-base to the branch of chitosan should improve its water solubility and gene binding ability significantly, and enhance gene delivery of chitosan due to the formation of Schiff-bases and substitution of imidazole functional groups along chitosan backbones without altering its biocompatibility and biodegradability. Gel electrophoresis and light scattering results show the formation of CISB/pDNA polyplexes in solution can effectively bind and protect pDNA from DNase I digestion. The CISB does not induce remarkable cytotoxicity against HEK 293 cells and can enhance delivery of plasmid DNA into both cytoplasm and nucleus efficiently. A cell transfection efficiency of 69.47 % can be reached after systematically optimizing cell transfection conditions. The CISB is a promising gene delivery vector due to its high solubility in physiological pH, strong gene binding and protection capability, low cytotoxicity, good biodegradability, and high efficiency in gene delivery and cell transfection.

3.1 Introduction

Gene therapy can be defined as treatment of human diseases by delivering therapeutic genes into patients' abnormal cells or tissues, and it has been intensively investigated over the last 15 years [1]. Gene delivery systems mainly employ viral and non-viral vectors. Viral vectors, such as adenoviruses and retroviruses, have been widely used due to their higher transfection efficiency than non-viral vectors.[2,3] However, viral vectors are not ideal candidates due to their various limitations, such as, random insertion into host genome, toxic immunological and inflammatory reactions.[4] The non-viral vector based gene delivery system has attracted great attention because of the potential for limited immunogenicity, the ability to accommodate and deliver large-size genetic materials, and the capability of its chemical structure modification.[5] The most attractive non-viral vectors are cationic lipids and cationic polymers, which are safer and more amenable to large-scale production. In comparison, the application of cationic lipids is limited due to its toxicity and relatively low transfection efficiency.[6] On the other hand, cationic polymer carriers are widely accepted because of their higher ability to complex DNA and interact with cells. Additionally, the polyplex formation between cationic polymers and DNA molecules is able to effectively prevent DNA from nuclease degradation.[7] To date, a variety of cationic polymers for gene delivery purpose, such as poly(2-dimethylaminoethyl methacrylate) (PDMAEMA),[8] gelatin,[9] polybrene,[10] tetraminofullerene [11] and poly(l-lysine) (PLL),[12] have been broadly studied. The high charge density gives rise to an increase not only on gene transfection efficiency, but also the cytotoxicity. Moreover, the non-biodegradability of cationic polymers might result in polymer accumulation in cells or body after repeated administrations.

The Schiff-base is a compound with a functional group that a carbon-nitrogen double bond with the nitrogen atom connected to an aromatic or alkyl group, but not hydrogen. Schiff-bases are widely investigated as one of imine type compounds because of their structural

variety and specific molecular properties such as intramolecular hydrogen bonding. Compounds containing Schiff–base functional groups have been contains in many biochemical processes, drug development and functional biomaterials.[13, 14] The pK_a of a Schiff base (-N=C-) is between 10.6 and 16.0 at 25 ^oC, and it can be fully protonated at physiological pH[15]. In addition, it has been reported that Schiff-base can enhance gene binding ability[16,17]. Since one polymer has many repeat units, the polymer supported Schiff-bases should be a good candidate as the gene carrier in gene delivery. However, to our knowledge, almost no relevant study has been reported.

Chitosan is a popular biomaterial due to its biocompatibility, biodegradability, low cytotoxicity, and high cationic charge density.[18] The poor water solubility and low transfection efficiency of chitosan make it not suitable to be used as a potential non-viral gene delivery carrier. However, chitosan involves both hydroxyl and amino functional groups along its backbone, which allows further chemical modification to tailor the physicochemical properties of chitosan so as to satisfy various end-used applications.[19] In gene delivery application, proton-sponge ability is crucial for exploring off-the-shelf materials as the gene carriers. It would be desirable for efficient gene carriers to mimic the proton-sponge mechanism, which requires the buffering capacity between physiological and lysosomal pH range. Imidazole exhibits the required proton-sponge property and is the functional moiety of many biomolecules (such as histidine).[20] Therefore, the conjugation of imidazole to the backbone of chitosan should increase its gene transfection efficiency without scarifying the biocompatibility and biodegradability. In literature, new gene delivery vector based on the imidazolyl modified chitosan has been developed recently[21] where the *N*-imidazolyl-chitosan molecules are synthesized by coupling the amino groups of chitosan and urocanic acid via the EDC (N-(3-Dimethylaminopropyl)-N-ethylcarbodiimide) chemistry. The synthesized *N*-imidazolyl-chitosan has been used in small interfering RNA (si-RNA) delivery for the

potential treatment of lung diseases[22] and targeted gene delivery in nervous system[23]. For those *N*-imidazolyl-chitosans, the imidazolyl groups are linked to the chitosan backbone by the formation of amide bonds. However, the amide linkage might be easily digested by enzymes *in vivo* [24, 25]. In addition, the solubility of *N*-imidazolyl-chitosan is poor in the physiological pH.[21, 23]

Based on previous studies, we hypothesize that the Schiff-base linked imidazole and chitosans will have obvious advantages (such as high solubility in neutral pH, satisfying gene binding and protection ability, and good gene delivery capability), and should be a more efficient gene delivery vector (Figure 3.1). We here synthesized various chitosan supported imidazole Schiff-bases (CISB) and systematically examined their gene binding and protection capability, nucleic acid deliver ability and transfection efficiency. It was found that the CISB is a potential safe and efficient vector in gene therapy.

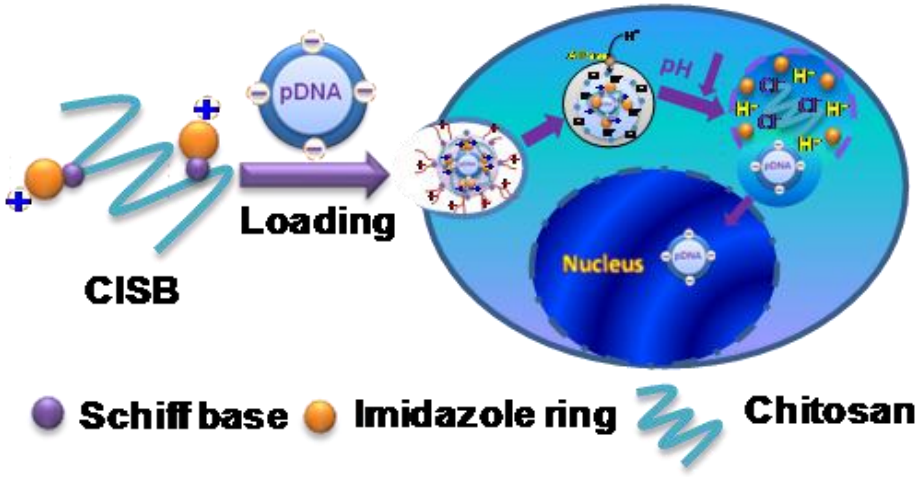

Figure 3.1 Intracellular gene delivery using CISB polymers as gene carrier.

3.2 Experimental section

3.2.1 Materials

Chitosan (molecular weight ~ 200 kDa, degree of acetylation: 90%) was purchased from

Acros (New Jersey, USA). The plasmid DNA pEGFP-N1 (4.7 kb) encoding green fluorescent protein gene with a cytomegalovirus (CMV) promoter was kindly supplied by Dr Julian Adams (Flinders University, Australia). QIAGEN Maxi kit was obtained from Qiagen (Boncaster, Australia). Fetal bovine serum (FBS), trypsin-EDTA, penicillin-streptomycin (PS) mixture, RPMI 1640 cell culture medium, phosphate buffered saline (PBS), TAE (tris-acetate), agarose and Lipofectamin^{TM} 2000 reagent were purchased from Gibco-BRL (Grand Island, USA). Dimeric cyanine nucleic acid stains, live plasma membrane and nuclear labeling kit were purchased from Molecular Probes (Grand Island, USA). Sucrose, gel red, *3*-(*4*, *5*-dimethylthiazol-*2*-yl)-*2*, *5*-diphenyltetr-azolium bromide (MTT), kanamycin, *4*-imidazolecarboxaldehyde (ICD) and other chemicals or solvents were purchased from Sigma-Aldrich.

3.2.2 Plasmid DNA preparation

The pEGFP-N1 plasmid was prepared in *E. coli* DH5 α strain and extracted using the QIAGEN Maxi kit. The integrity and purity of the prepared plasmid DNA (pDNA) were analyzed using 0.8 % agarose gel electrophoresis, and the DNA concentrations is determined by using a Jasco UV-vis spectrophotometer (Japan) at the fixed wavelengthes at 260 and 280 nm.[26] Plasmid DNA was fluorescently labelled with the intercalating nucleic acid stain YOYO-1 with a molar ratio of 1 dye molecule per 100 base pairs for 60 min at RT in the dark for the cellular uptake study.

3.2.3 Synthesis of chitosan supported imidazole Schiff-base (CISB)

Chitosan (0.5 g, 2 mmol glucosamine repeat unit) was dissolved in 15 mL deionized water, adjusted pH to 4 using 0.1 M HCl and incubated at 65 ^{o}C overnight. In a typical experiment for the CISB-1 synthesis, *4*-imidazolecarboxaldehyde (0.0192 g or 0.2 mmol) was dissolved in 15 mL deionized water, and dropwisely charged to the chitosan solution over a 20 min period. The reaction mixture was stirred at room temperature for 4 h and then condensed

using a rotary evaporator. The concentrated polymer solution was precipitated in excess amount of anhydrous acetone. The products were filtered, rinsed thrice with anhydrous acetone, and vacuum-dried at room temperature. Different CISB samples were prepared by charging various amounts of *4*-imidazolecarboxaldehyde. The resulting polymers are noted as the CISB-1 (feed ratio of *4*-imidazolecarboxaldehyde to amine ~ 1:5), CISB-2 (1:1) and CISB-3 (2:1). The obtained CISB samples were subjected to FTIR and ^{1}H-NMR analysis.

3.2.4 Imidazole Schiff-base substitution

UV-visible spectrophotometer (UV-1601, SHIMADZU) was used to determine the percentage of imidazole Schiff-base along the chitosan backbone. The imidazolyl moiety has a maximal absorption at the wavelength of 257 nm. The standard absorption calibration curve was set up, and the percentages of the imidazole Schiff-base substitution in the above synthesized CISB polymers were determined using the UV absorbance at 257 nm through the Beer-Lambert's law.[27] The UV path length was 1 cm, and the details on the UV absorption curves together with the calibration curve are included in the Supporting Information.

3.2.5 FTIR and ^{1}H-NMR

The IR spectra of chitosan and the CISB were examined using a Thermo NICOLET6700 Fourier Transform Infrared Spectrometer (FTIR) at room temperature. The ^{1}H-NMR experiments were recorded using a 600 MHz Bruker NMR in D_2O.

3.2.6 Polymer solubility

The solubility of chitosan and its derivatives was evaluated at different pH, where 1 mg/mL chitosan or CISB samples was first dissolved in 0.2 wt% acetic acid aqueous solution. The pH of various polymer solutions was adjusted by the addition of NaOH. The transmittances of the polymer solutions were monitored as functions of pH using a UV/vis spectrophotometer equipped with a 1 cm quartz cell at a fixed wavelength of 600 nm.[28]

3.2.7 Nucleic acid binding assay

The binding interaction of pDNA to the CISB was examined using agarose gel electrophoresis. The polyplexes contain CISB and 0.2 μg plasmid DNA at various mixing weight ratios (W/W of CISB to plasmid DNA). The weight ratio of 1 for CISB-1/pDNA, CISB-2/pDNA and CISB-3/pDNA corresponds to their N/P molar ratios of 2.02, 1.61, and 1.48. The polymer/pDNA polyplexes were prepared at pH 7.2, incubated at room temperature for 20 min before loading onto the 0.8 wt% agarose gel in a Tris–acetate (TAE) running buffer and electrophoresed at 80 V for 60 min. The resulting pDNA migration patterns were read under UV irradiation (G-BOX, SYNGENE).

3.2.8 Resistance of CISB/pDNA polyplexes against DNase I degradation

CISB/pDNA polyplexes were separately incubated with DNase I (4 units) in DNase/Mg^{2+} digestion buffer (50 mM, Tris-Cl, pH 7.6, and 10 mM $MgCl_2$) at 37 ^{o}C for 30 min using the free pDNA (0.2 μg) as the negative control. The degradation of pDNA was investigated by 0.8 wt% agarose gel in a Tris–acetate (TAE) running buffer and electrophoresed at 80 V for 60 min. The resulting pDNA migration patterns were read under UV irradiation.

3.2.9 Particle sizes and zeta-potentials of the CISB/pDNA polyplexes

The particle sizes and zeta potentials of the polyplexes prepared by mixing CISB and pDNA at different weight ratios and pH 7.2 was measured using a Malvern Zetasizer (Malvern Inst. Ltd. UK), equipped with either a four-side clear cuvette for particle size analysis or ZET 5104 cell [29] for zeta-potential measurement at room temperature. The concentration of plasmid pDNA was kept at 5 μg/mL. For particle size analysis, cumulant method was used to convert intensity-intensity autocorrelation functions to apparent particle sizes via the Stokes-Einstein relation.[30] As for electrokinetics, Smuloschowski model was used to convert electrophoresis mobility to zeta-potential.[31] 10 parallel runs were carried out for each measurement and the final data were obtained based on statistical analysis.

3.2.10 Evaluation of cytotoxicity

HEK 293 cells, kindly supplied by Dr Michael Brown at the Hanson Institute, Adelaide Royal Hospital, were cultured in RPMI 1640 medium supplied with 10 % FBS in 96-well plates (200 μL medium/well) at a cell density of 1.0×10^5 cells/mL. After inoculation, the cells were allowed to adhere overnight at 37 ^oC in a humidified 5 % CO_2-containing atmosphere. The growth medium was replaced with 200 μL fresh medium containing CISB polymers at final concentrations of 0.5, 1, 3, 5, 10, 20, 30, 50 μg/mL. Cells were then incubated for 24 h before 10 μL of MTT (5.0 mg/mL in PBS) was added to each well. After further incubating for additional 4.0 h at 37 ^oC, the growth medium was removed and 150 μL of dimethyl sulfoxide (DMSO) was charged to each well to ensure complete solubilization of the formed formazan crystals. Finally, the absorbance was determined using the Biotek Microplate Reader (Biotek, USA) at a wavelength of 570 nm.[32]

3.2.11 Assessment of cellular uptake by confocal laser scanning microscopy

The ability of vectors to transport plasmid DNA into the cytoplasm and nucleus in HEK 293 cells was evaluated using a confocal laser scanning microscope. The HEK 293 cells were seeded at a concentration of 2×10^5 cells/well into 6-well plates loaded with cover-glass slides in 25 mm diameter and cultured for 24 h. 4 μg YOYO-1- labeled pDNA was loaded on the polymers (chitosan, L-PEI and CISB) at different weight ratios of 5.0, 1.0 and 10.0 to form polymer/DNA complex. And then, HEK 293 cells were incubated with the polymer/pDNA complexes for 4 h. The complexes were removed and the cells were washed with PBS three times after transfection. Then the cell membrane and nucleus were stained with 100 μL of Alexa Fluor 594 (5.0 μg/mL) and Hoechst 33258 (2 μM) for 15 min at 37 °C, the cells were further washed with PBS three times and incubated with 200 μl DMEM. The fluorescence was observed with a confocal laser scanning microscope (Leica Confocal 1P/FCS) equipped with a 405 nm diode for Hoechst33258, a 488 nm argon laser for YOYO-1 and a 561 argon

laser for Alexa Fluor 594 in Adelaide Microscopy. High-magnification images were obtained with a 100 objective. Optical sections were averaged 4 times to reduce noise. Images were processed using Leica Confocal software.

3.2.12 Cell culture and gene transfection

HEK 293 cells were incubated in RPMI 1640 supplemented with 10 % fetal bovine serum (FBS), streptomycine at 100 μg/mL, and penicillin at 100 U/mL. The cells seeded in 24-well plates were incubated at 37 ^{o}C in a humidified incubator in the presence of 5 % CO_2. After 24 h culturing, the medium was replaced with 200 μL of culture medium in the absence of FBS. In the meantime, polymer/pDNA polyplexes, prepared by incubating the CISB polymers and plasmid DNA at various weight ratios at room temperature for 30 min, were added to each well. After 6 h incubation, the medium was replaced by 1 mL fresh complete culture medium with 10 % FBS and the cells were further incubated for another 66 h.

3.2.13 GFP expression analysis by fluorescence microscopy and flow cytometry

For the fluorescence microscopic analysis of GFP (green fluorescence proteins) expression, living cells were rinsed in 1× PBS and visualized by *in situ* detection with an epi-fluorescence microscope (Multi-photon Microscope, Nikon) connected to a CCD camera (RS Photometrics). A band pass filter (BP 485/20) for excitation and a 520 nm long pass filter were used as barrier filter in viewing emission. Digitalized photographs were stored and analyzed by using the Bio-Rad Radiance 2000MP Visualising System. On the other hand, the green fluorescence intensity was detected directly by a FACSCalibur flow cytometry (Becton Dickinson), and the transfection efficiency was calculated by percentage of positive cells using non-transfection cell as the negative control. Briefly, cells were harvested by the digestion of trypsin after post transfection culture. 1×10^{6} cells were washed with 2 % FCS/PBS buffer, and centrifuged at 1000 rpm for 5 min. The cells were stained by 400 μL 0.5

μg /mL propidium iodide in 1× PBS. Approximately 1-2×10^4 cells were analyzed at the rate of 200 – 600 cells per second. Cell Quest 3.3 software was used for data analysis.[26]

3.2.14 Statistical analysis

Data obtained from our experiments are represented as mean ± SE (standard error). Statistical analysis of the numerical variables was performed using a two-sample, two-tailed t-test. A value of $p < 0.05$ is considered to be significant.

3.3 Results and discussion

3.3.1 Synthesis and characterization of Schiff-base linked imidazole chitosan supported Schiff-bases (CISB)

In this study, the imidazole rings are introduced to the 2-*N* position of chitosan via the reaction of the amino group of chitosan and the aldehyde group of *4*-imidazolecarboxaldehyde at room temperature, where the Schiff-base functional groups are formed (Figure 3.2). Both the Schiff-bases and imidazole rings can be protonated in aqueous medium and gives the ternary and secondary nitrogen atoms.[25] The presence of Schiff-bases and imidazole groups along chitosan backbones makes the resulting CISB polymers possess higher solubility in a wide pH range and stronger gene binding capability than the unmodified chitosan.

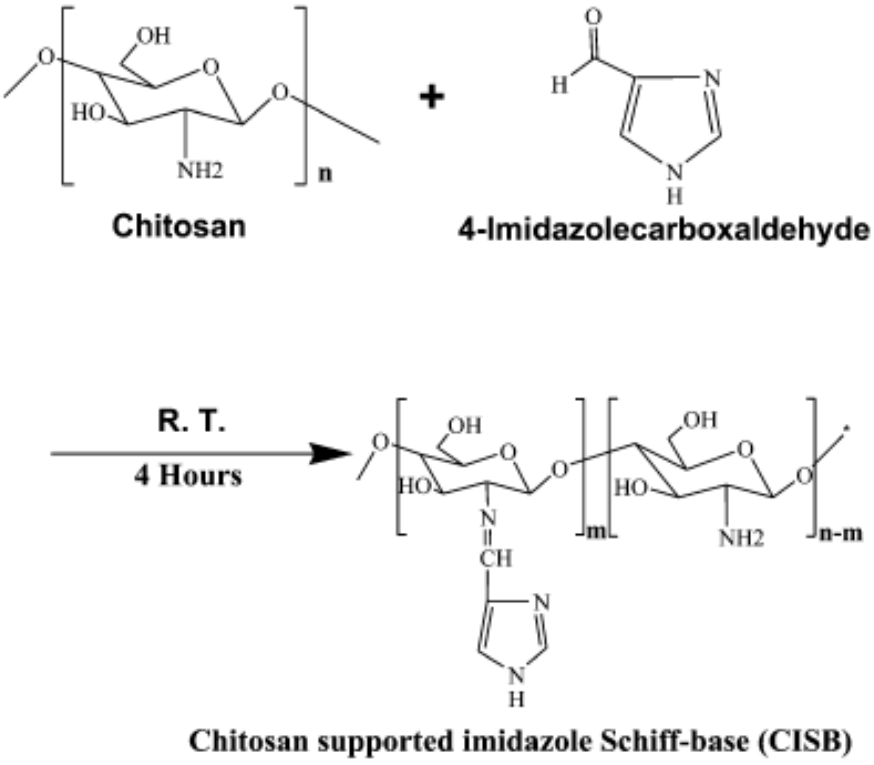

Figure 3.2 The synthesis of chitosan supported imidazole Schiff-bases (CISB).

Different amounts of *4*-imidazolecarboxaldehyde were reacted with chitosan at room temperature with the feed molar ratios of *4*-imidazolecarboxaldehyde to the amino groups of chitosan ranging from 1:5 to 2:1. The degrees of imidazole Schiff-base substitution on chitosan were determined by UV-vis. measurements based on the imidazolyl absorption at 257 nm (water, pH 7) (Figure 3.3). According to the Lambert-Beer's law, the imidazole Schiff-base substitutions are found to be 3.35 %, 55.06 % and 79.20 % for the above synthesized CISB polymers: CISB-1, CISB-2, and CISB-3 (Figure 3.4), respsectively.

The conjugation of imidazole ring to chitosan via the Schiff-base functional group is further confirmed by the FTIR. The comparison on the IR spectra of chitosan and the synthesized CISB polymer is shown in Figure 3.1. For chitosan, the characteristic peaks at 1598 cm^{-1} (N-H bending) and 1080 cm^{-1} (C-O- stretching) are evident.[33] The weak peak at 1655 cm^{-1} is attributed to the stretching of C=O associated with the non-fully deacetatyl residuals. Taking CISB-2 as an example, a strong absorption band at 1634 cm^{-1} is presented, which is attributed to the vibration of -C=N- in the Schiff-base.[34, 35] Such a characteristic peak cannot be observed in the IR spectra of chitosan as control. The peaks at 1577 cm^{-1} and 1405 cm^{-1} can be assigned to the in-plane C–C and C–N, and N-H stretching vibration of the imidazole ring.[36] Additionally, the ^{1}H-NMR was used to further elucidate the chemical structure of the CISB. From the ^{1}H-NMR analysis, the chemical shifts for the H atoms of chitosan are located within the δ range of 2.00 to 4.80 ppm. The chemical shifts of the H atoms of the imidazole ring are located within the δ of 7.60 ~ 8.20 ppm. The successful conjugation of the imidazolyl to chitosan is evident from the chemical shift δ at 9.72 ppm (-**H**C=N-) (Figure 3.5 and 3.6).

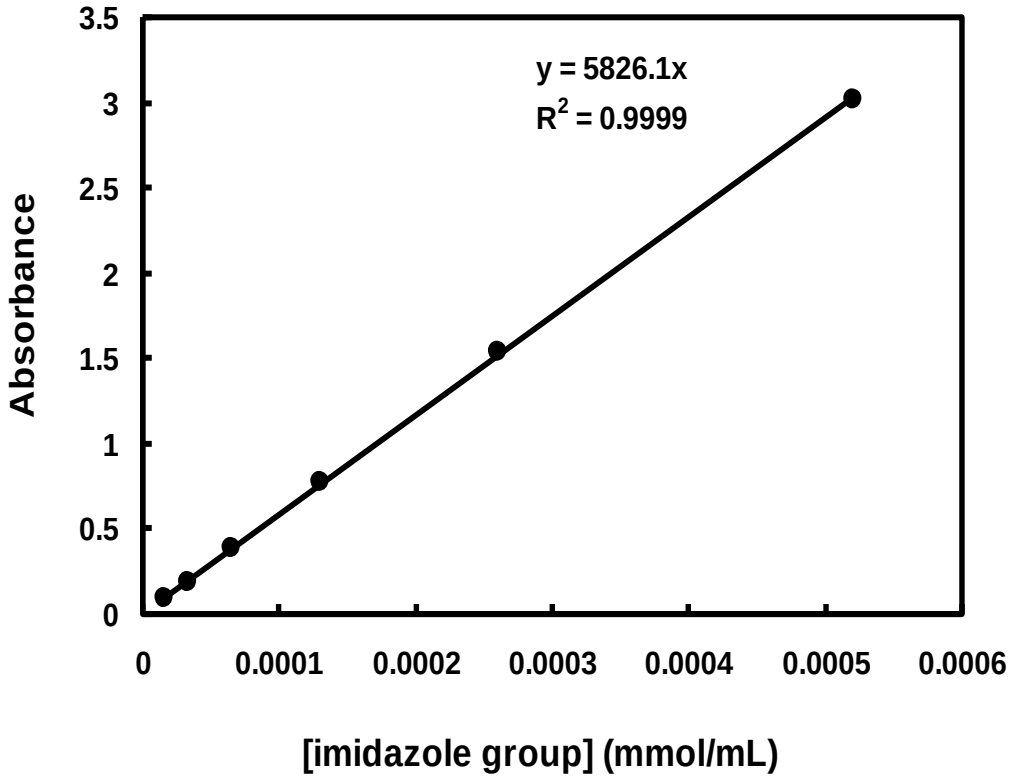

Figure 3.3 Calibration curve of imidazole groups at the wavelength of 257 nm.

The solubility of the chitosan supported imidazole Schiff-bases in aqueous media was examined by light transmittance as shown in Figure 3.7. Chitosan is soluble in water at pH lower than 6, beyond that, it becomes water-insoluble. However, the CISB samples are soluble in a broader pH range (5 to 10). The transmittance of the CISB polymers slightly decreases in the pH range of 6 to 9, and keeps constant beyond that with an average transmittance of more than 60 %. Obviously, the solubility of the CISB samples is much higher than that of chitosan, where the transmittance in the range of pH 6 to 10 is less than 20 %. On the other hand, it is noticed that the trends of transmittance vs. pH are not much different for those three CISB samples although they have different degrees of imidazole Schiff-base substitutions. The result indicates that the both the formed Schiff-base and the substituted imidazole functional groups are able to influence the solubility of chitosan. The increase of the solubility is ascibled to different pK_a values of various ammonium functional

groups. The pK_a value of the imidazole ring is 14.2 and the pK_a for Schiff-base is between 10.6 and 16.0 at 25 ^oC[22], comparing to the pK_a of 6.2 for the amino group of chitosan.[37, 38] The higher pK_a indicates the presence of more protonated positive charges in solution, and thus enhances the solubility of the CISB in a broad pH range. Due to the increase of water solubility in a biological and physiological condition, the applications of CISB in gene delivery can be improved dramatically, such as the resulting polymers make it possible to prepare the polymer and pDNA polyplexes at neutral pH. However, when the *N*-imidazolyl-chitosan is used as a gene carrier, such polyplexes can only be prepared around pH 5 due to its relatively poor water solubility at a neutral pH.[21, 22] The structure of the polyplexes prepared at pH 5 might be changed when they are used in a physiological condition. Therefore, the CISB should be more suitable as a gene delivery carrier than *N*-imidazolyl chitosan.

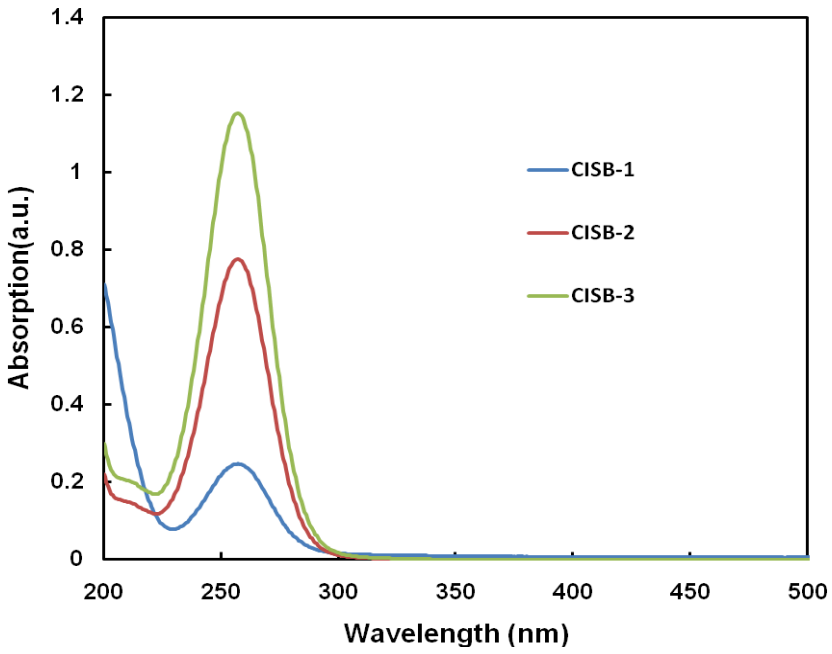

Figure 3.4 UV absorption of the synthesized CISB polymers.

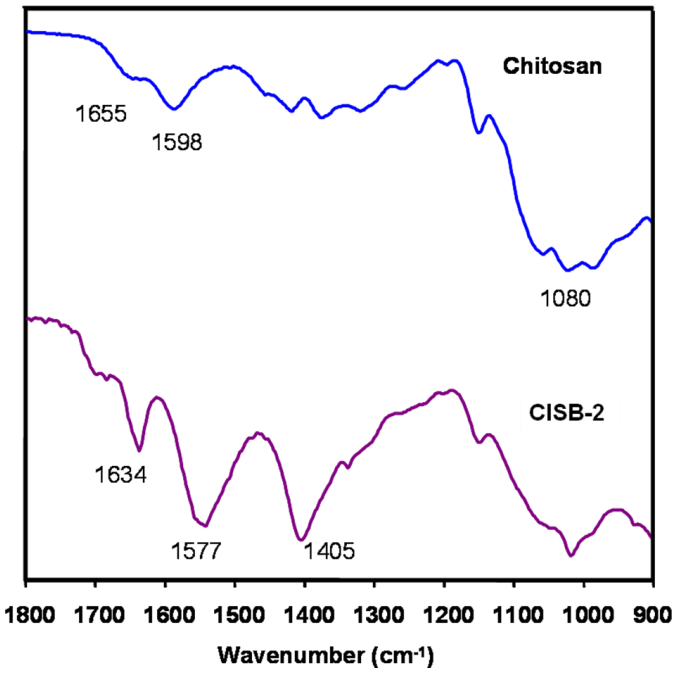

Figure 3.5 Comparison on the FTIR spectra of chitosan and CISB.

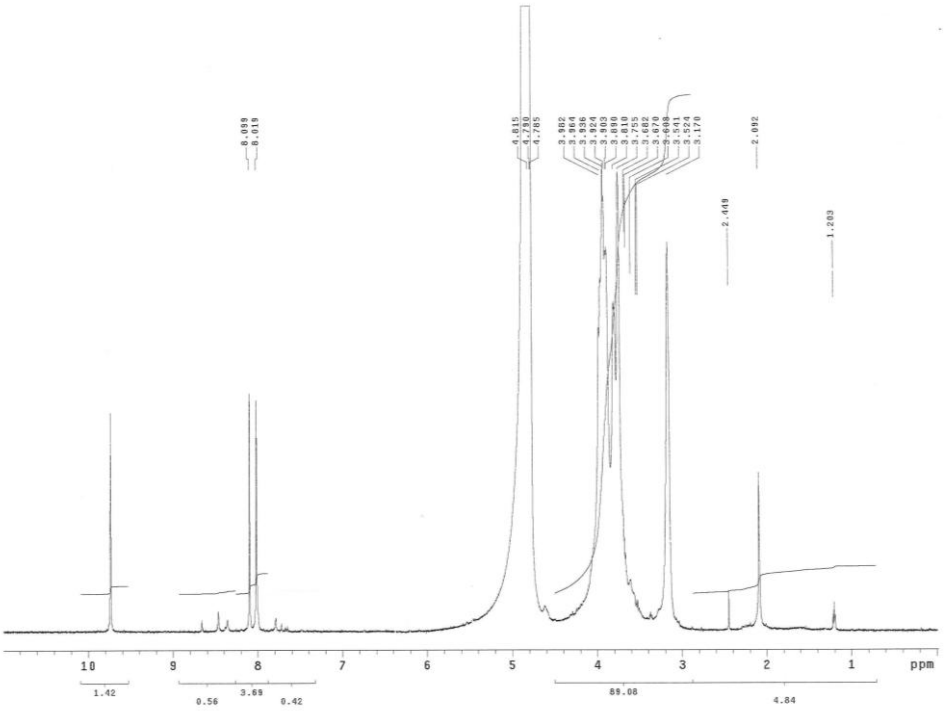

Figure 3.6 The ^{1}H-NMR of the CISB-2 in D_2O.

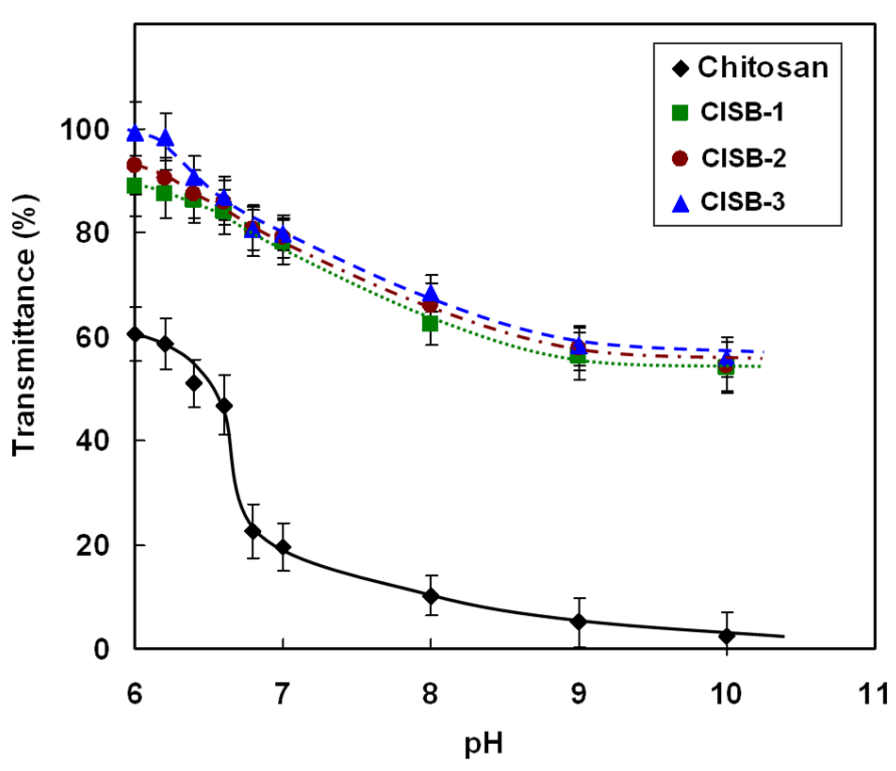

Figure 3.7 Comparison on the solubility of chitosan and various CISB polymers at different pH.

3.3.2 Nucleic acid binding and DNase I digestion assays

The gene binding capabilities of various CISB samples were examined by gel retardation assays using a naked plasmid DNA as control. Figure 3.8A shows the electrophoresis mobility of pDNA in the presence of different amounts of various CISB polymers. The experimental results clearly show that the electrophoretic mobilities of pDNA are retarded by increasing the dose of CISB polymers, especially at a weight ratio of the polymer to pDNA above 3 (The weight ratio of 1 equals to the N/P molar ratios of 2.02, 1.61 and 1.48 for CISB-1, CISB-2 and CISB-3, respectively) (Figure 3.8A) . Comparing with electrophoretic mobility of reference pDNA shown in the first lane of Figure 3A, the retaining of pDNAs at the top of the gel in the presence of CISB polymers suggests all pDNAs have been complexed with CISB polymers in the mixing weight ratio range of 3 to 80. On the other

hand, the pDNA gel retardation for those three CISB polymers are different when the mixing weight ratios are smaller than 3. For CISB-1 with a low degree (3.35%) of imidazole substitution, the free plasmid DNA can be observed within the weight ratios of 0.5 to 1 (equal to the N/P of 1.01 to 2.01). Beyond that, free pDNA bands are not visible. Kim and Ghosn have examined the *N*-imidazolyl-chitosan for gene delivery, where the imidazole rings are conjugated to the chitosan using an amide linkage via the EDC chemistry [21, 23]. The gene binding ability of the CISB-1 is similar to that of *N*-imidazolyl-chitosan with a higher degree of imidazolyl substitution (27.7%). Obviously, it can be concluded that the protonated Schiff-base moieties in the CISB can enhance gene binding/loading capability [21]. For the CISB samples (CISB-2 and CISB-3) with higher degrees (55.06% and 79.20%) of imidazole substitution, free pDNA bands cannot be observed even at a weight ratio of 0.5. Therefore, the polymer/pDNA polyplex formation strongly depends on the extent of imidazole Schiff-base substitution along chitosan backbones. Preliminary studies have proved a low binding capability of chitosan to genes due to its low solubility and the weak intermolecular interaction between the primary amino groups of chitosan and the phosphates of DNA.[39] However, the biocompatibility and biodegradability of chitosan are attractive in biological applications. To improve the performance of chitosan in gene delivery, various chemical modifications have been developed. Lu et al synthesized oligoamine polymers based on chitosan, with which free DNA could be fully retarded at a weight ratio of 4.5.[40] Chae et al synthesized the deoxycholic acid-conjugated chitosan oligosaccharide, which was able to bind all free DNA (0.2μg) and form their stable polyplexes at a weight ratio of 1.0.[41] From our study, the gene binding ability of the CISB polymers with higher substitution of imidazole Schiff-base (CISB-2 and CISB-3) is stronger than those *N*-imidazolyl-chitosan, deoxycholic acid-conjugated chitosan oligosaccharide, and oligoamine chitosan, and similar to that of linear PEI which can eliminate free DNA beyond a N/P molar ratio of 3.[42] For the

CISBs, it can be explained that both the formed Schiff-bases and the substituted imidazole rings have a stronger binding affinity with pDNA after protonation. The more the amino groups along chitosan backbones are substituted by the imidazole Schiff-base, the stronger the polymer/pDNA polyplexes are formed in a solution dominated by electrostatic attraction. Additionally, the presence of the Schiff-bases in CISB polymers is crucial to not only enhance gene binding ability, but also to increase the water solubility. Therefore, the imidazole Schiff-base chitosan has obvious advantages over the *N*-imidazolyl-chitosan.

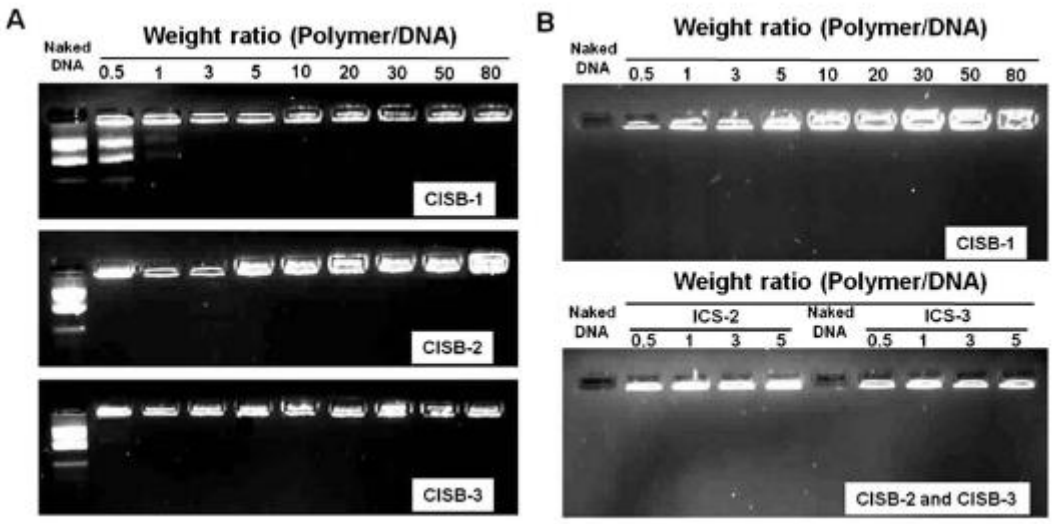

Figure 3.8 Nucleic acid binding and protection ability assays of CISB polymers by agarose gel electrophoresis using 0.8 % agarose in Tris-acetate running buffer. (A): Nucleic acid binding ability assays; (B): Nucleic acid protection capability assays against DNase I.

The representative effect of the CISB polymers on protecting plasmid DNA from DNase degradation was further examined using DNase I as a model enzyme and the results are shown in Figure 3.8 B. When 0.2 μg naked pDNA was incubated with 200 U/mL of excessive DNase I (4 U) at 37 ^{o}C, naked pDNA are completely degraded within 30 min as evident from a significant drop in DNA gel intensity. At the same digestion condition, only approximately half of the pDNA is degraded for the CISB-1/pDNA polyplex at a mixing weight ratio (polymer to DNA) of 0.5, whereas no DNA digestion can be observed at the weight ratios of

1 to 80. The formation of CISB/pDNA polyplexes can effectively protect DNA from DNase I digestion. The polyplexes formed at higher mixing weight ratios have a higher DNA protection ability against DNase I since more pDNAs have been bound to CISB polymers. In addition, plasmid DNA can be fully protected from DNase I digestion using the CISB-2 or CISB-3 at the weight ratios higher than 0.5. It means that CISB-2 or CISB-3 has a stronger pDNA protection capability than CISB-1 due to their higher gene binding capability. As such, all CISB samples are able to protect DNA from digestion at a physiological condition where the nuclease concentration is much lower than our experimental DNase concentration.[29]

3.3.3 Particle sizes and zeta potentials of CISB/pDNA polyplexes

The polyplexes were prepared by mixing plasmid DNA with various CISB-1, 2, 3, respectively at different mixing weight ratios (from 0.5 to 100) in pH 7. The sizes of the CISB/pDNA polyplexes were measured by dynamic light scattering (DLS) and the cumulant approach was used to analyze the intensity-intensity autocorrelation functions of scattered light. As shown in Fig 4A, for all CISB samples, the apparent Z-average particle size of the polyplexes decreases near to half with the increment of the mixing weight ratios of CISB and pDNA from 0.5 to 100 and the range of the polyplexes diameter is between 100 to 200 nm when the weight ratio is above 1. On the other hand, the apparent Z-average polyplex size reduces with an increase of the degree of imidazole Schiff-base substitution, which indicates more compact polyplexes are formed in solution due to the presence of stronger polymer and pDNA electrostatic attraction (Figure 3.9A and 3.10). After protonation, both the formed Schiff-base and the substituted imidazolyl can interact with negative charged pDNAs. The enhanced intermolecular binding interaction results in a decrease in the size of the polyplexes.

Zeta-potential is relevant to the overall net charge density of the CISB/pDNA polyplexes and it is one of the major factors influencing polyplex biodistribution and transfection efficiency in gene delivery. [43] Figure 3.9B compares the zeta-potentials of the polyplexes at

different mixing weight ratios. Due to the presence of phosphate ions, the plasmid DNA is negatively charged. After protonation, the CISB is positively charged. Electrostatic interaction dominates the formation of CISB/pDNA polyplexes in solution. At a lower mixing ratio of CISB to pDNA, the polyplexes are negatively charged since the positive charges of the CISB are not enough to balance all negative charges of pDNA. With an increase in CISB concentrations, the zeta-potentials of the polyplexes trend to be less negative at the mixing weight ratio of 1. With further increase in CISB concentrations, the zeta-potential turns into positive and keeps stable at the mixing weight ratios beyond 20. The change of the zeta-potentials with the CISB concentration is attributed to the electrostatic attraction between CISB and pDNA in various CISB/pDNA polyplexes. Moreover, the zeta-potentials are also influenced by the degree of imidazole Schiff-base substitution in CISB. At a fixed mixing ratio, with the increment of substitution degree, more negative charges along pDNA backbones can be neutralized as evident from their higher zeta-potential values.

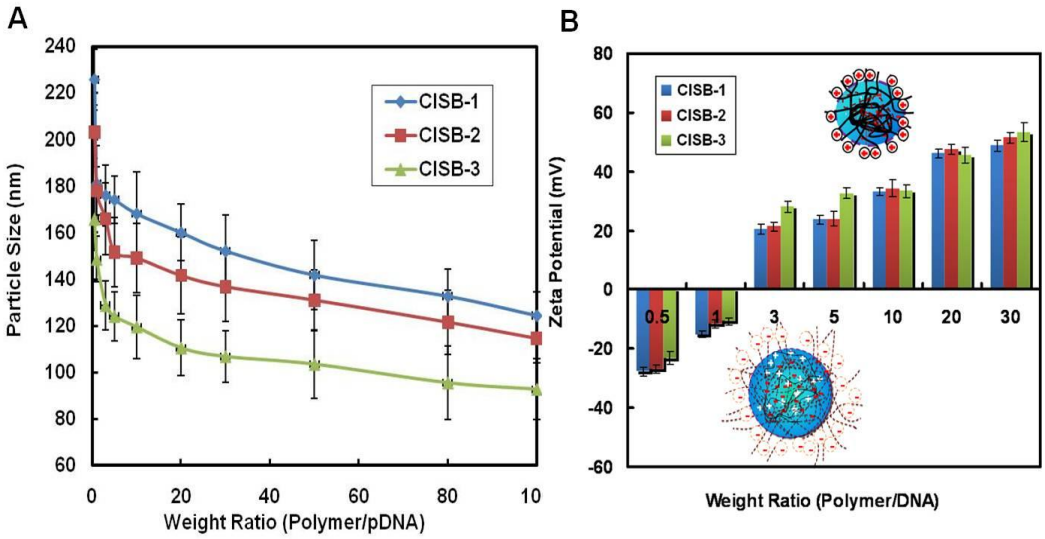

Figure 3.9 Particle size and Zeta-potentials of the CISB/pDNA polyplexes prepared at different mixing weight ratios of CISB to pDNA at pH 7.2, 25 ^{o}C. (A): Sizes the CISB/pDNA polyplexes; B: Zeta-potentials the CISB/pDNA polyplexes, For all measurements, the DNA concentration was fixed at 5 μg/mL. The insets are the representative microstructures of the polyplexes at low and high mixing ratios.

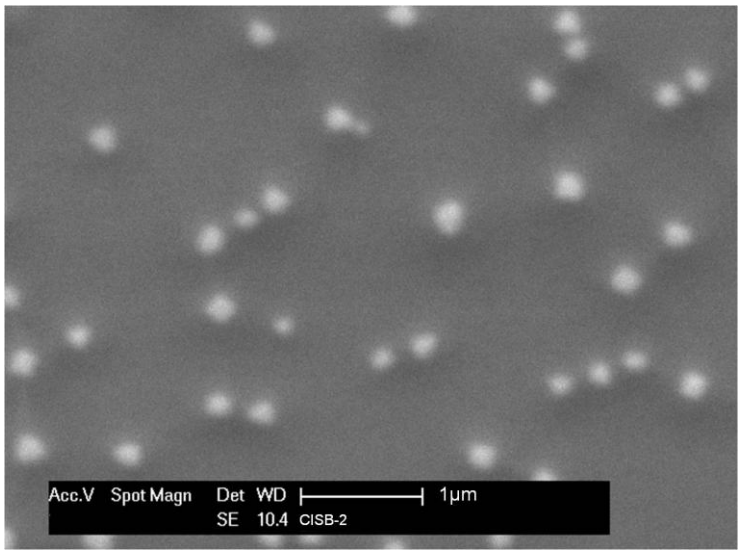

Figure 3.10 SEM image of CISB-2/pDNA polyplexes at the mixing weigh ratios of 10 (polymer to pDNA)

The zeta-potentials of the polyplexes increase with an increase in the mixing ratios of CISB to pDNA and the degrees of imidazole Schiff-base substitution. This is due to the formation of different structured polyplexes. At a small mixing ratio or degree of substitution, the amounts of the positive charges in CISB are not enough to neutralize all negative charges of pDNA resulting in a core-shell structure of the polymer/DNA polyplexes where the neutralized polymer/pDNA core are surrounded with a corona layer composed of negatively-charged plasmid DNA residuals which can be digested by DNase. With an increase in the mixing ratio of polymer to plasmid DNA or the degree of substitution, the zeta-potential of the polyplexes turns into positive. The positive zeta-potential indicates the CISB is excessive for pDNA binding interaction and the formation of CISB/pDNA polyplexes with a core-shell structure whose corona layer is made up of the residual positive charges from the excess CISB which leads to previous gel retardation and DNase resistance. The formation of core-shell structures significantly enhances the stability of the polyplexes and avoids agglomeration. At the same time, slightly positive charges on polyplex surface are helpful for gene delivery since relatively low positive charges can facilitate an easy entry into cells via

the endocytosis but cause negligible or minor damage to cells.[44] Therefore, the synthesized CISB can be expected to have great potential applications for gene transfection.

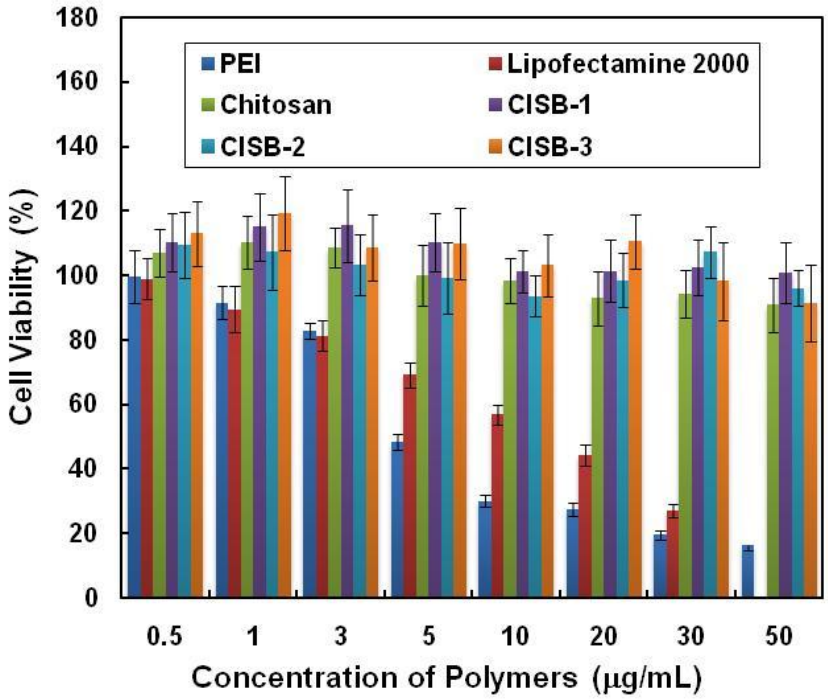

Figure 3.11 Comparison on the cytotoxicity of PEI, lipofectamine 2000, chitosan and various CISB polymers against HEK 293 cells. The absorbance was read at 570 nm using a microplate reader (n = 3).

3.3.4 Cell cytotoxicity

Cell toxicity of the CISB polymers has to be examined before exploring their biomedical applications. Figure 3.11 compares the cytotoxicities of chitosan, CISB, linear PEI (L-PEI) and lipofectamine 2000 against HEK 293 cells at a broad concentration range typically used in transfection experiments by MTT assays. Negligible effect of chitosan and different CISB polymers on cell viability can be observed with an average cell viability of over 90 % at polymer concentrations ranging from 1.0 to 50 μg/mL. For comparison purpose, the cytotoxicity of linear PEI with a molecular weight of 25 kDa and lipofectamine 2000 was included. From the figure 5, 30-50% of cells remain viable with an increase of PEI

concentration from 5.0 to 20 μg/mL, and beyond a PEI concentration of 30 μg/mL, the cell viability is reduced to below 20 %. Lipofectamine 2000 at a concentration of 10 μg/mL decreases the cell viability below 60 %. The cell cytotoxicity of both chitosan and CISBs are lower than those commercial gene delivery vectors. The low cell toxicity of the chitosan derivatives mainly results from the biocompatible characteristics of chitosan. Since the imidazole ring is an important biological building-block for many biomolecules (such as histidine), the introduction of imidazole Schiff-base functional groups does not bring significant cytotoxicity to the CISB.

3.3.5 Cellular uptake of DNA/polymer polyplexes

To analyze the cell uptake of nucleic acid delivered using functional polymers as gene vectors, pEGFP-N1 plasmid DNA was used as a model gene, which was labeled with YOYO-1 with green flourescence. In order to the show the location of DNA, the cell membrane and nucleus were labeled by Alexa Fluor 594 (red flourescence) and Hoechst 33258 (blue flourescence), respectively. The labeled DNA was delivered by CISB-2 into HEK 293 cells at the weight ratio of 10 and analyzed with a confocal microscopy at 4 hr post transfection using chitosan and L-PEI as positive controls. As Figure 3.12 shows, the green fluorescence of labeled plasmid DNA could be found in both cytoplasm and nucleus after 4 h DNA delivery with CISB-2 and L-PEI as well, which indicates that both CISB and L-PEI can deliver gene only not to cytoplasm but also to cell nucleus. However, but the fluorescence intensity of labeled plasmid DNA in cells delivered by L-PEI is slightly lower than that of CISB-2, which might demonstrate that the gene delivery capability of CISB is higher than that of L-PEI. The images of pDNA intracellular distribution also agree with the transfection efficiencies of both gene carriers which are shown in Figure 3.12. However, much weaker green fluorescence of labeled plasmid DNA can be found in cells after 4 h delivery with chitosan comparing with that delivered by CISB. Therefore, the gene delivery ability of chitosan has been improved

significantly by introduction of imidazole Schiff-base onto the backbone of chitosan.

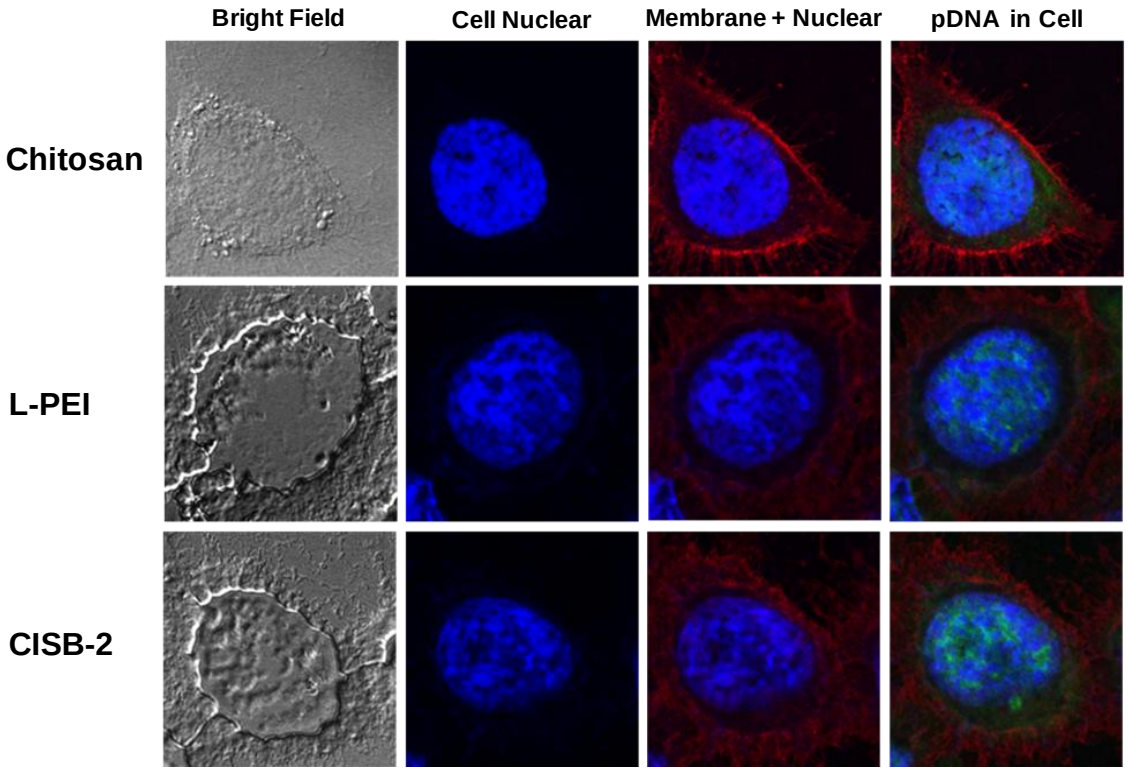

Figure 3.12 Cellular uptake of YOYO-1-labeled pDNA in HEK 293 with the delivery of gene vectors: chitosan, L-PEI and CISB-2. Cells were incubated with ploymer/pDNA complexes for 4 hrs in 6-well plate at the DNA concentration of 4 μg/well. Cells were visualized using a confocal 1P/FCS inverted microscope after cell membrane and nucleus were stained with 100 μL of Alexa Fluor 594 (5.0 μg/mL) and Hoechst 33258 (2 μM).

3.3.6 Cell transfection of CISB *in vitro*

To successfully transfect cells, the pDNA must overcome a series of biological barriers. It should pass surface membrane at first, then go through the endocytic pathway before entering into the nucleus of the target cells, so as to get translated into functional proteins. pDNA can only be translated after overcoming all these barriers with the aids (nucleic acid protection and release) of gene delivery vectors, which are reflected in the transfection efficiency. The optimization of a non-viral gene carrier involves the adjustment on the mixing ratios of polymer vectors and pDNA aiming to balance the competing effects on cellular binding and uptake, DNA protection and release, and size and stability of DNA/vector polyplexes which

decide the final transfection efficiency.[45] The DNA delivery efficiency was evaluated and optimized by transferring plasmid DNA into mammalian cells *in vitro*.

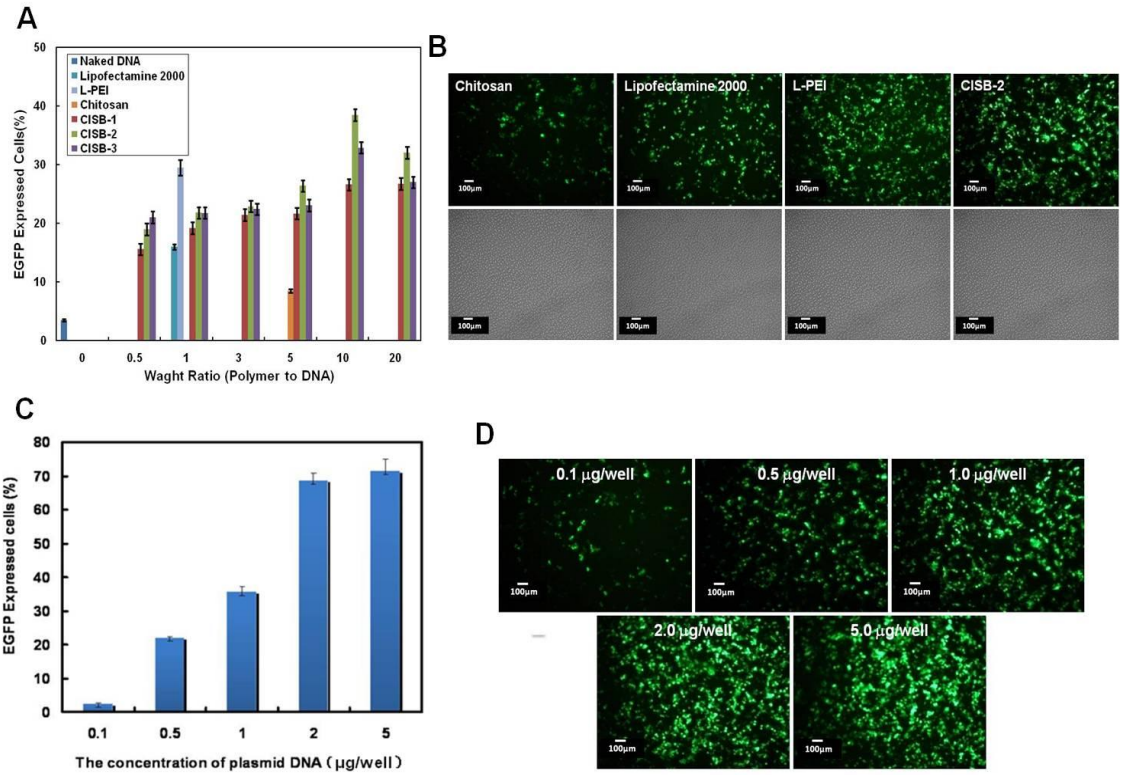

Figure 3.13 (A): Transfection efficiencies of CISB/pEGFP polyplexes determined by flow cytometry against HEK 293 cells at various mixing ratios with positive (L-PEI and lipofectamine 2000) and negative (naked pEGFP) controls. Data shown as mean ± SE (n = 3). (B): Fluorescent micrographs and light inverted micrograph of HEK 239 cells transfected with chitosan; lipofectamine 2000; L-PEI and CISB-2 at the weight ratio of polymer to DNA: 5.0; 1.0; 1.0 and 10.0. Transfection was performed at a plasmid DNA dose of 1 μg/well in 24-well plates, and all transfection efficiencies were determined at 72 hrs post-transfection. (C): Transfection efficiencies of CISB-2/pEGFP polyplexes determined by flow cytometry in HEK 293 cells with different plasmid DNA concentrations at the fixed mixing polymer to plasmid DNA weight ratios of 10. Data shown as mean ± SE (n = 3). (D): Fluorescence micrographs of the HEK 239 cells transfected with CISB-2/pEGFP polyplexes at the fixed polymer to plasmid DNA weight ratios of 10 and varying plasmid DNA concentrations from 0.1 to 5.0 μg pDNA/well in 24-well plate. (All the transfection efficiencies were determined at 72 hrs post-transfection.)

Transfection experiments were carried out using HEK 293 as the host cell line. The CISB/pDNA (pEGFP-N1) polyplexes at different mixing weight ratios of 0.5 to 20 (keeping pDNA constant at 1 μg) were prepared and added to each well in a 24-well plate with RPMI1640 culture medium without fetal bovine serum (FBS). The cell transfection

efficiencies of CISB polymers were assessed by flow cytometry at 72 hrs after transfection. The positive controls are chitosan, linear PEI and lipofectamine 2000, and the negative control is naked pDNA without vector (Figure 3.13A). The transfection efficiency is determined by the actual percentage of cells expressing green fluorescence protein by comparing to the mock transfection.

As shown in Figure 3.13A, the transfection efficiency is dependent on the degree of substitution and the weight ratio of polymer to pDNA. The cell transfection efficiency of the CISB-1/DNA polyplexes increases slowly with the increment of the mixing weight ratio of CISB-1 to plasmid DNA (0.5 to 20). The highest achievable transfection efficiency is 27% at a mixing weight ratio of 20. The cell transfection efficiency of the CISB-3/DNA polyplexes is around 19%, nearly identical at the mixing weight ratios from 0.5 to 5.0, but transfection efficiency sharply increases to 33 % as the weight ratio changes from 5.0 to 10. For the CISB-2 vector, a transfection efficiency of 19% is obtained at a mixing weight ratio of 0.5, similar to that of CISB-3 at the mixing ratios of 1.0 to 3.0. The highest transfection efficiency of 39% is obtained at a weight ratio of 10. The general trend for CIBS vectors is that the transfection efficiency increases with the increment of the mixing ratio (CISB to pDNA) from 0.5 to 10 for all CISB polymers because the increase in the amount of positive charges in CISB facilitates the CISB/pDNA polyplex formation, which makes pDNA more stable and also enhances the binding to the negatively charged proteoglycans on cell surface. As such, the improvement on the uptake of pDNA leads to an increase in gene transfection efficiency. On the other hand, the transfection efficiency decreases for CISB-2 and CISB-3 at high mixing weight ratios (10 and 20), but the decrease is not evident for CISB-1 due to its low degree of imidazole Schiff-base substitution (Fig.3.13A). An ideal gene vector should balance the abilities between protecting DNA from degradation and releasing DNA near or within the nucleus of the target cell. Since the polyplexes are formed based on electrostatic interaction,

the final structure and properties of the CISB/pDNA polyplexes can be tailored by varying the amount of charge groups of gene carriers. High amounts of charged group can effectively prevent pDNA from degradation due to the formation of compact polyplex structure, but they can also inhibit pDNA release in nucleus.[46] A higher mixing ratio of CISB-2 or CISB-3 to plasmid DNA results in formation of tighter CISB/pDNA polylexes, and thus inhibits and decreases gene transfection efficiency. The similar inhibiting results have been observed while using PEI as a gene carrier.[47, 48]

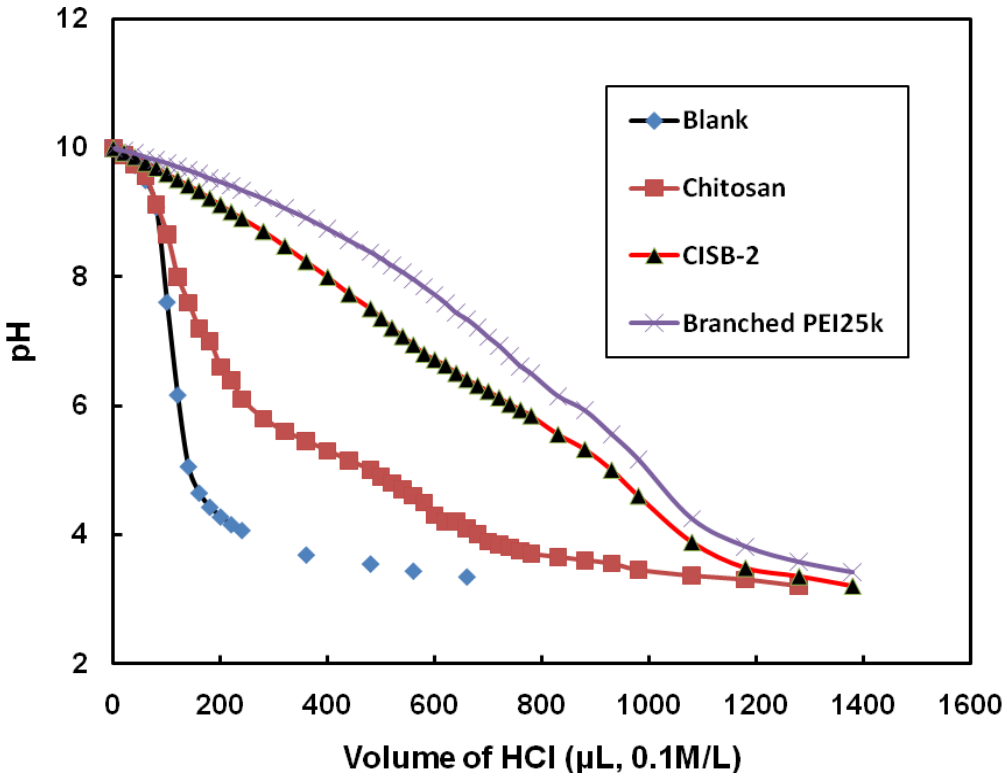

Figure 3.14 Comparison on the buffer capacity of various polymers.

Figure 3.13B compares the fluorescence images of the transfected HEK 239 cells using different gene delivery carriers (chitosan, Lipofectamine 2000 and L-PEI). In the positive controls of chitosan, lipofectamine 2000 and L-PEI, the cell transfection efficiencies of 9%, 16% and 30% are obtained, and the similar efficiency was also reported by Mao et al using lipofectamine 2000 complexes to transfect HEK 293. [29] The transfection efficiency is lower than that of CISB-2 at a weight ratio of 10 (36%) as confirmed by the fluorescence image

analysis (Figure 3.15). Almost non naked DNA can be taken into cells and expressed in cells without help and protection of gene carriers due to its negative charges and digestion of DNases.[46] The transfection efficiency of polymer/pDNA polyplexes depends on the mixing ratios of polyplexes at the balance making polymer/pDNA polyplexes escape from the endo-/lysosomal compartment and pDNA release from polymer/pDNA polyplexes. It has been reported that high transfection efficiency of linear PEI is attributed to its ability of destabilizing the endosome and its high proton sponge effect.[48, 49] CISB contains primary, secondary and tertiary nitrogen atoms, which results in a broad buffering range (Figure 3.14). Therefore, the CISB polymers have a similar proton sponge effect as PEI and thus can improve the polyplex release to the cytoplasm after endocytosis. [50]

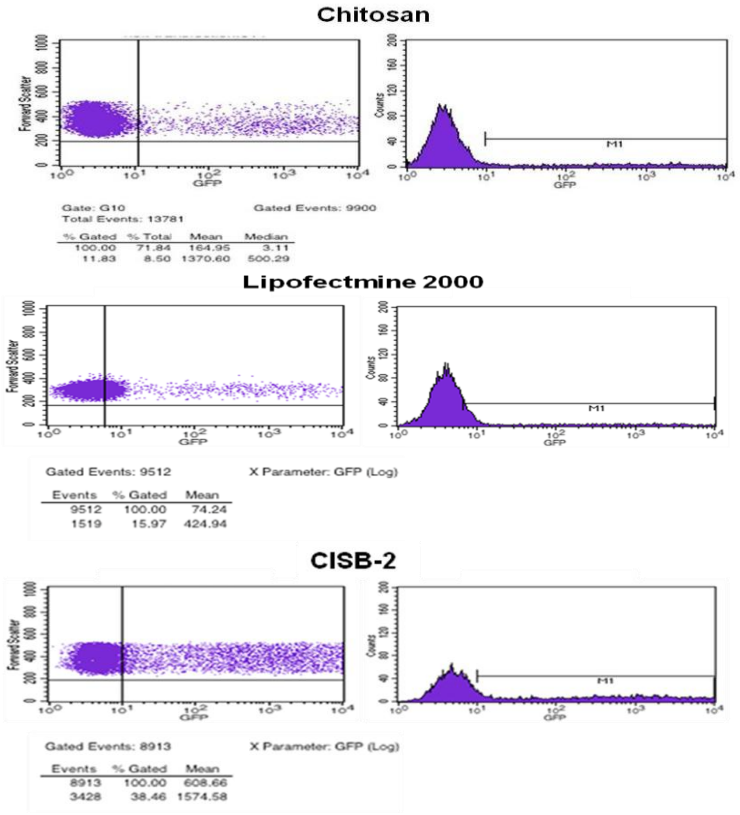

Figure 3.15 Gene transfection efficiency of the CISB-2 against the 293 cells measured by flow cytometer at the pDNA concentration of 1 μg/well in a 24-well plate using naked DNA as negative control, Chitosan and lipofectamine2000 as the positive control.

The concentration of pDNA at cell surface has been suggested to be an important factor in

non-viral gene delivery.[51] In order to optimize the concentration of plasmid DNA at HEK 293 cell surface in the presence of a CISB deliver vector, CISB-2 is chosen as a model polymer (Fig.3.13C). Different amounts of pEGFP-N1 plasmid DNA from 0.1 to 5.0 μg was mixed with CISB-2 at a fixed weight ratio of 10 (polymer to pDNA) and added to the wells of a 24-well culture plate with 1 mL culture medium. The transfection efficiency is determined at 72 h post transfection. As shown in Figure 3.13C, the transfection efficiency is measured up to 70% from 2.5% as the pEGFP-N1 plasmid DNA increases from 0.1 to 2.0 μg per well in the 24-well plate (Figure 3.16), which is also confirmed from the fluorescence images of the transfected cells (Figure 3.13D). With the further increase in the dose of pEGFP-N1 plasmid DNA from 2.0 to 5.0 μg per well in the 24-well plate, the increment in the transfection efficiency is minor. The results suggest 2 μg/mL may be closed to the maximum amount of plasmid DNA complexed with CISB-2 which can be taken in by endocytosis and expressed in HEK 293 cells. Similar results have also been reported from other investigators, for example, Ishii et al. reported the optimal pDNA amount in SOJ cells transfection using chitosan carrier is 2 μg/mL[52] and Lavertu et al obtained the optimal pDNA dose of 2.5 μg/mL in HEK 293 cell transfection using chitosan as vectors [53] Actually, gene transfection is dominated by both forward and reverse transfection. For the forward transfection, the delivery of polyplexes to cell surface is a diffusion-limited process, whereas the reverse transfection can pre-load polyplexes at high levels onto the cell-substrate interface through electrostatic or hydrophobic interaction. The optimal dose of pDNA at cell surface for cell transfection may be between 2 and 2.5 μg/mL which depends on the types of cell and vector.[54]

Recently, various gene delivery vectors have been developed and achieved gene transfection efficiency is from 36% to 59%. Trimethyl chitosan-cysteine conjugate (TMC-Cys) has been evaluated as a non-viral gene carrier with HEK 293 cells, which displayed the highest transfection efficiency of 36%.[55] Comb-shaped copolymers composed of nonionic

hydrophilic dextran and cationic PDMAEMA (poly(2-dimethylaminoethyl methacrylate)) side chains were used for non-viral gene delivery, and a transfection efficiency of 37% was acquired for HEK 293 cells.[56] Cationic polymers composed of chitosan backbones and PDMAEMA side chains resulted in a transfection efficiency of 52% to HEK 293 cells.[57] The ternary copolymer composed by grafting linear PEI onto the block copolymer of poly (L-lysine) and poly (ethylene glycol) gave a transfection efficiency of 59% to HEK 293 cells.[58] In this investigation, a transfection efficiency of 70% can be reached for the HEK 293 cell using the CISB-2 as the gene carrier, which is higher than that of *N*-imidazolyl-chitosan.[59, 60]

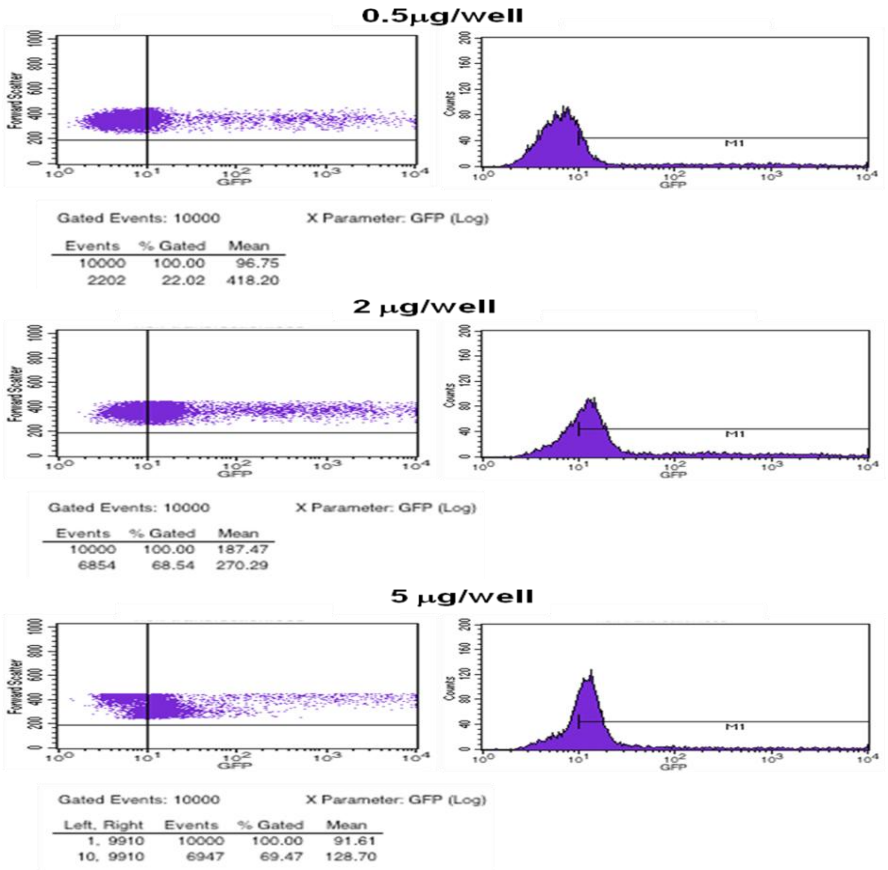

Figure 3.16 Gene transfection efficiency of the CISB-2 against the 293T cells measured by flow cytometer at the pDNA concentration of 0.5, 2.0 and 5.0 μg/well in 24-well plate.

3.4 Conclusion

In this paper, functional biodegradable polymer supported imidazole Schiff-bases have been developed for gene delivery applications. Due to the introduction of Schiff-base and

imidazole functional groups to chitosan backbones, water solubility, gene binding and protection capacity, and gene delivery are significantly improved. The enhancement in water solubility and pDNA binding capability is attributed to the presence of more nitrogen atoms with different protonation capabilities. The resulting polymers retain the basic characteristics of chitosan (non-cytotoxics and biodegrability). The CISB-2 shows higher transfection efficiency against HEK293 cells than commercial transfection carriers such as linear PEI and lipofectamine 2000. The transfection efficiency can reach up to 70% after systematical optimization. The results from this study demonstrates chitosan-supported imidazole Schiff-bases have great potential application in future gene therapy.

References

1. Westphal, E.M. and H. von Melchner, Gene therapy approaches for the selective killing of cancer cells. Current Pharmaceutical Design, **2002**. *8(19)*: p. 1683-1694.

2. Wadhwa, P.D., et al., Cancer gene therapy: Scientific basis. Annual Review of Medicine, **2002**. *53*: p. 437-452.

3.Clark, K.R. and P.R. Johnson, Gene delivery of vaccines for infectious disease. Current Opinion in Molecular Therapeutics, **2001**. *3(4):* p. 375-384.

4.Blomberg, P. and C.I.E. Smith, Gene therapy of monogenic and cardiovascular disorders. Expert Opinion on Biological Therapy, **2003**. *3(6):* p. 941-949.

5.Wu, G.Y. and C.H. Wu, Receptor-Mediated Gene Delivery and Expression Invivo. Journal of Biological Chemistry, **1988**. *263(29)*: p. 14621-14624.

6.Mhashilkar, A., et al., Gene therapy - Therapeutic approaches and implications. Biotechnology Advances, **2001**. *19(4)*: p. 279-297.

7.Deshpande, D., et al., Target specific optimization of cationic lipid-based systems for pulmonary gene therapy. Pharmaceutical Research, **1998**. *15(9)*: p. 1340-1347.

8.Gao, X. and L. Huang, Potentiation of cationic liposome-mediated gene delivery by polycations . Biochemistry, **1996**. *35(28)*: p. 9286-9286.

9.Demeneix, B. and J.P. Behr, Polyethylenimine (PEI). Non-Viral Vectors for Gene Therapy, 2nd Edition: Part 1, **2005**. *53*: p. 217-230.

10.Dai, F.Y., et al., Redox-cleavable star cationic PDMAEMA by arm-first approach of ATRP as a nonviral vector for gene delivery. Biomaterials, **2010**. *31(3)*: p. 559-569.

11.Truong-Le, V.L., J.T. August, and K.W. Leong, Controlled gene delivery by DNA-gelatin nanospheres. Human Gene Therapy, **1998**. *9(12)*: p. 1709-1717.

12.Mumper, R.J., et al., Polyvinyl derivatives as novel interactive polymers for controlled gene delivery to muscle. Pharmaceutical Research, **1996**. *13(5)*: p. 701-709.

13.Isobe, H., et al., Atomic force microscope studies on condensation of plasmid DNA with functionalized fullerenes. Angewandte Chemie-International Edition, **2001**. *40(18)*: p. 3364-+.

14.Zauner, W., M. Ogris, and E. Wagner, Polylysine-based transfection systems utilizing receptor-mediated delivery. Advanced Drug Delivery Reviews, **1998**. *30(1-3)*: p. 97-113.

15.Lee, K.Y., et al., Preparation of chitosan self-aggregates as a gene delivery system. Journal of Controlled Release, **1998**. *51(2-3)*: p. 213-220.

16.Dang, J.M. and K.W. Leong, Natural polymers for gene delivery and tissue engineering. Advanced Drug Delivery Reviews, **2006**. *58(4)*: p. 487-499.

17.Mansouri, S., et al., Characterization of folate-chitosan-DNA nanoparticles for gene therapy. Biomaterials, **2006**. *27(9)*: p. 2060-2065.

18.Kim, T.H., et al., Chemical modification of chitosan as a gene carrier in vitro and in vivo. Progress in Polymer Science, **2007**. *32(7)*: p. 726-753.

19.Kiang, T., et al., Formulation of chitosan-DNA nanoparticles with poly(propyl acrylic acid) enhances gene expression. Journal of Biomaterials Science-Polymer Edition, **2004**. *15(11)*: p. 1405-1421.

20.Wang, H.J., et al., Construction of a Novel Cationic Polymeric Liposomes Formed From PEGylated Octadecyl-Quaternized Lysine Modified Chitosan/Cholesterol for Enhancing

Storage Stability and Cellular Uptake Efficiency. Biotechnology and Bioengineering, **2010**. *106(6)*: p. 952-962.

21.Jintapattanakit, A., V.B. Junyaprasert, and T. Kissel, The Role of Mucoadhesion of Trimethyl Chitosan and PEGylated Trimethyl Chitosan Nanocomplexes in Insulin Uptake. Journal of Pharmaceutical Sciences, **2009**. *98(12)*: p. 4818-4830.

22.Zhao, X.L., et al., Octaarginine-modified chitosan as a nonviral gene delivery vector: properties and in vitro transfection efficiency. Journal of Nanoparticle Research, **2011**. *13(2)*: p. 693-702.

23.Satoh, T., et al., 6-Amino-6-deoxy-chitosan. Sequential chemical modifications at the C-6 positions of N-phthaloyl-chitosan and evaluation as a gene carrier. Carbohydrate Research, **2006**. *341(14)*: p. 2406-2413.

24.Pack, D.W., et al., Design and development of polymers for gene delivery. Nature Reviews Drug Discovery, **2005**. *4(7)*: p. 581-593.

25.Zhang, X.Z., et al., Chitosan based oligoamine polymers: Synthesis, characterization, and gene delivery. Journal of Controlled Release, **2009**. *137(1)*: p. 54-62.

26.Kim, T.H., et al., Efficient gene delivery by urocanic acid-modified chitosan. Journal of Controlled Release, **2003**. *93(3)*: p. 389-402.

27.Wang, D.X., et al., Tetrahedral silicon-centered imidazolyl derivatives: Promising candidates for OLEDs and fluorescence response of Ag (I) ion. Journal of Organometallic Chemistry, **2010**. *695(21)*: p. 2329-2337.

28.Chan, P., et al., Synthesis and characterization of chitosan-g-poly(ethylene glycol)-folate

as a non-viral carrier for tumor-targeted gene delivery. Biomaterials, **2007**. *28(3)*: p. 540-549.

29.Mao, H.Q., et al., Chitosan-DNA nanoparticles as gene carriers: synthesis, characterization and transfection efficiency. Journal of Controlled Release, **2001**. *70(3)*: p. 399-421.

30.Heyes, D.M., System size dependence of the transport coefficients and Stokes-Einstein relationship of hard sphere and Weeks-Chandler-Andersenfluids. Journal of Physics-Condensed Matter, **2007**. *19(37)*.

31.Amal, R., J.A. Raper, and T.D. Waite, Fractal Structure of Hematite Aggregates. Journal of Colloid and Interface Science, **1990**. *140(1)*: p. 158-168.

32.Corsi, K., et al., Mesenchymal stem cells, MG63 and HEK293 transfection using chitosan-DNA nanoparticles. Biomaterials, **2003**. *24(7)*: p. 1255-1264.

33.Bi, X.J., et al., Dynamic characterization of recombinant Chinese Hamster Ovary cells containing an inducible c-fos promoter GFP expression system as a biomarker. Journal of Biotechnology, **2002**. *93(3)*: p. 231-242.

34.Brugnerotto, J., et al., An infrared investigation in relation with chitin and chitosan characterization. Polymer, **2001**. *42(8)*: p. 3569-3580.

35.Cavalheiro, E.T.G. and L.S. Guinesi, Influence of some reactional parameters on the substitution degree of biopolymeric Schiff bases prepared from chitosan and salicylaldehyde. Carbohydrate Polymers, **2006**. *65(4)*: p. 557-561.

36.Wang, J.T., X.X. Jin, and J. Bai, Synthesis and antimicrobial activity of the Schiff base from chitosan and citral. Carbohydrate Research, **2009**. *344(6)*: p. 825-829.

37.Nanbu, N., Y. Sasaki, and F. Kitamura, In situ FT-IR spectroscopic observation of a room-

temperature molten salt vertical bar gold electrode interphase. Electrochemistry Communications, **2003**. *5(5)*: p. 383-387.

38.Walba, H. and R.W. Isensee, Spectrophotometric Study of the Hydrolysis Constants of the Negative Ions of Some Aryl Imidazoles. Journal of the American Chemical Society, **1955**. *77(21)*: p. 5488-5492.

39.Park, J.W., K.H. Choi, and K.K. Park, Acid-Base Equilibria and Related Properties of Chitosan. Bulletin of the Korean Chemical Society, **1983**. *4(2)*: p. 68-72.

40.Choosakoonkriang, S., et al., Biophysical characterization of PEI/DNA complexes. Journal of Pharmaceutical Sciences, **2003**. *92(8)*: p. 1710-1722.

41.Zhu, A.P., J.H. Liu, and W.H. Ye, Effective loading and controlled release of camptothecin by O-carboxymethylchitosan aggregates. Carbohydrate Polymers, **2006**. *63(1)*: p. 89-96.

42.Zhu, A.P., et al., Interaction between O-carboxymethylchitosan and dipalmitoyl-sn-glycero-3-phosphocholine bilayer. Biomaterials, **2005**. *26(34)*: p. 6873-6879.

43.Lu, B., et al., Chitosan based oligoamine polymers: Synthesis, characterization, and gene delivery. Journal of Controlled Release, **2009**. *137(1)*: p. 54-62.

44.Chae, S.Y., et al., Deoxycholic acid-conjugated chitosan oligosaccharide nanoparticles for efficient gene carrier. Journal of Controlled Release, **2005**. *109(1-3)*: p. 330-344.

45.He, Z.Y., et al., Development of glycyrrhetinic acid-modified stealth cationic liposomes for gene delivery. International Journal of Pharmaceutics, **2010**. *397(1-2)*: p. 147-154.

46.Kean, T. and M. Thanou, Biodegradation, biodistribution and toxicity of chitosan. Advanced Drug Delivery Reviews, **2010**. *62(1)*: p. 3-11.

47.Yamano, S., J.S. Dai, and A.M. Moursi, Comparison of Transfection Efficiency of Nonviral Gene Transfer Reagents. Molecular Biotechnology, **2010**. *46(3)*: p. 287-300.

48.Leong, K.W., Polymeric controlled nucleic acid delivery. Mrs Bulletin, **2005**. *30(9)*: p. 640-646.

49.Appelhans, D., et al., Hyperbranched PEI with Various Oligosaccharide Architectures: Synthesis, Characterization, ATP Complexation, and Cellular Uptake Properties. Biomacromolecules, **2009**. *10(5)*: p. 1114-1124.

50.Kievit, F.M., et al., PEI-PEG-Chitosan-Copolymer-Coated Iron Oxide Nanoparticles for Safe Gene Delivery: Synthesis, Complexation, and Transfection. Advanced Functional Materials, **2009**. *19(14)*: p. 2244-2251.

51.Pack, D.W., D. Putnam, and R. Langer, Design of imidazole-containing endosomolytic biopolymers for gene delivery. Biotechnology and Bioengineering, **2000**. *67(2)*: p. 217-223.

52.Benns, J.M., et al., pH-sensitive cationic polymer gene delivery vehicle: N-Ac-poly(L-histidine)-graft-poly(L-lysine) comb shaped polymer. Bioconjugate Chemistry, **2000**. *11(5)*: p. 637-645.

53.Midoux, P. and M. Monsigny, Efficient gene transfer by histidylated polylysine pDNA complexes. Bioconjugate Chemistry, **1999**. *10(3)*: p. 406-411.

54.Luo, D. and W.M. Saltzman, Enhancement of transfection by physical concentration of DNA at the cell surface. Nature Biotechnology, **2000**. *18(8)*: p. 893-895.

55.Ishii, T., Y. Okahata, and T. Sato, Mechanism of cell transfection with plasmid/chitosan complexes. Biochimica Et Biophysica Acta-Biomembranes, **2001**. *1514(1)*: p. 51-64.

56.Lavertu, M., et al., High efficiency gene transfer using chitosan/DNA nanoparticles with specific combinations of molecular weight and degree of deacetylation. Biomaterials, **2006**. *27(27)*: p. 4815-4824.

57.Adler, A.F. and K.W. Leong, Emerging links between surface nanotechnology and endocytosis: Impact on nonviral gene delivery. Nano Today, **2010**. *5(6)*: p. 553-569.

58.Dean, D.A., D.D. Strong, and W.E. Zimmer, Nuclear entry of nonviral vectors. Gene Therapy, **2005**. *12(11)*: p. 881-890.

59.Tullis, G.E., et al., Transfection of mammalian cells using linear polyethylenimine is a simple and effective means of producing recombinant adeno-associated virus vectors. Journal of Virological Methods, **2006**. *138(1-2)*: p. 85-98.

60.Tait, A.S., et al., Transient production of recombinant proteins by chinese hamster ovary cells using polyethyleneimine/DNA complexes in combination with microtubule disrupting anti-mitotic agents. Biotechnology and Bioengineering, **2004**. *88(6)*: p. 707-721.

Chapter 4 Exploring N-Imidazolyl-O-Carboxymethyl Chitosan for High Performance Gene Delivery

Bingyang Shi, Zheyu Shen, Hu Zhang, Jingxiu Bi*, Sheng Dai*

School of Chemical Engineering, The University of Adelaide, Adelaide, SA 5005, Australia

Biomacromolecules 2012, 13, 146−153/ DOI: 10.1021 / bm201380e

STATEMENT OF AUTHORSHIP

Exploring N-Imidazolyl-O-Carboxymethyl Chitosan for High Performance Gene Delivery

Bingyang Shi, Zheyu Shen, Hu Zhang, Jingxiu Bi*, Sheng Dai*

School of Chemical Engineering, The University of Adelaide, Adelaide, SA 5005, Australia

Biomacromolecules 2012, 13, 146−153/ dx.doi.org/10.1021/bm201380e

By signing the Statement of Authorship, each author certifies that their stated contribution to the publication is accurate and that permission is granted for the publication to be included in the candidate's thesis.

Bingyang Shi (Candidate)

Performed experiments, analysed results and wrote the manuscript.

I hereby certify that the statement of contribution is accurate.

*Signed..... .....Date.*15/08/2013 .....

Zheyu Shen

Assisted in writing the manuscript..

I hereby certify that the statement of contribution is accurate.

*Signed..... .....Date.*15/08/2013 .....

Hu Zhang

Assisted in writing the manuscript..

I hereby certify that the statement of contribution is accurate.

Signed.....Date.....

Jingxiu Bi

Supervised development of work and assisted in writing the manuscript.

I hereby certify that the statement of contribution is accurate.

Signed.....Date.....

Sheng Dai

Supervised development of work and assisted in writing the manuscript.

I hereby certify that the statement of contribution is accurate and I give permission for inclusion of the paper in the thesis.

Signed.....Date.....

Shi, B., Shen, Z., Zhang, H. Bi, J. & Dai, S. (2012) Exploring N-Imidazolyl-O-Carboxymethyl Chitosan for high performance gene delivery.
Biomacromolecules, v. 13(1), pp. 146-153

Chapter 5 Endosomal pH Responsive Polymer for Efficient Cancer-Targeted Gene Delivery

Bingyang Shi, Hu Zhang, Sheng Dai*, Jingxiu Bi*

School of Chemical Engineering, The University of Adelaide, Adelaide, SA 5005, Australia

Submitted to Langumir, July 2013

STATEMENT OF AUTHORSHIP

Endosomal pH Responsive Polymer for Efficient Cancer-Targeted Gene Delivery

Submitted, July 2013

By signing the Statement of Authorship, each author certifies that their stated contribution to the publication is accurate and that permission is granted for the publication to be included in the candidate's thesis.

Bingyang Shi (Candidate)

Designed, carried out the experiments and wrote the manuscript.

I hereby certify that the statement of contribution is accurate.

*Signed..... .....Date...*15/08/2013*.....*

Hu Zhang

Assisted in writing the manuscript.

I hereby certify that the statement of contribution is accurate.

*Signed.....Date...*15/08/2013*.....*

Sheng Dai

Supervised development of work and assisted in writing the manuscript.

I hereby certify that the statement of contribution is accurate.

*Signed.....Date...*15/08/2013*.....*

Jingxiu Bi

Supervised development of work and assisted in writing the manuscript.

I hereby certify that the statement of contribution is accurate and I give permission for inclusion of the paper in the thesis.

*Signed.....Date...*15/08/2013
.....

Endosomal pH Responsive Polymer for Efficient Cancer-Targeted Gene Delivery

5.1 Introduction

Gene therapy is becoming promising for cancer treatment due to the rapid development of knowledge in elucidating the molecular basis of cancers, as well as the availability of the complete sequence information of the human genome. [1] One of the most improvements for cancer treatment is targeted gene therapy, that is, deliver the therapeutic nucleic acid into the chromosomes of cancer cells to regulate or replace abnormal genes. [2] However, it is difficult to obtain satisfactory therapeutic efficiency for naked nucleic acids without carrier/vectors since gene delivery in eukaryotic cells is a multiple-step process and therapeutic nucleic acid has to overcome a series of barriers including cell uptake, endosome escape, endoplasmic gene transport and nucleus entry for successful gene therapy. Therefore, the development of safe, efficient and specific delivery vectors for transporting therapeutic genes to specific cells or tissues is one of the biggest challenges in gene therapy.

Chitosan has been considered to be a potential candidate as nucleic acid carrier since it is known as a biocompatible, biodegradable, and low-toxicity biomaterial with cationic charges. However, the poor water solubility, low transfection efficiency and non-specificity of chitosan must be overcome before its end-use in gene delivery. Fortunately, chitosan provides several functional groups along its backbone for further modification, so that the final property of the modified chitosan can be tailored.[3] Imidazole is a functional segment of several biomolecules (such as histidine). It has been reported that polymers incorporating an imidazole ring show enhanced gene transfection efficiency due to the imidazole ring can improve the gene loading capability of the carrier as binding site.[4] Imidazole-chitosan (EICS) has been developed via EDC chemistry and displays an improved performance in gene

delivery.[5] However, the poor water solubility at physiological pH and non-specificity of EICS limits its biomedical application. On the other hand, Schiff-base (-N=C-) is a pH sensitive functional group that contains a carbon-nitrogen double bond. The pKa of Schiff-base is between 10.6 and 16.0 at 25 ^{o}C, rendering it can be fully protonated at physiological pH. [6] Therefore, the introduction of Schiff-base can improve the water solubility of gene carriers. In addition, the Schiff-base can be hydrolyzed at endosomal pH (pH 6.5 decreases to 5.0 from early to late endosome),[7] which could be used as an intracellular microenvironment responsive linkage to control the release of gene cargo.

Targeting capability is very important in gene delivery. A promising vector should be the one that efficiently conveys genes to specific target tissues with minimal toxicity. Internalization of the gene carrier could be enhanced by coupling targeting ligands of specific cells or tissues, taking advantage of endocytosis pathways.[8] Using this strategy, a variety of ligands, such as antibodies, growth factors or irons, can be used to facilitate the uptake of carriers into target cells.[9] Among these targeted ligands mentioned above, folic acid (FA) is a sensitive and smart one for targeting cancer cells since the folate receptor (FR) is over-expressed on the surface of cancer cells, but not expressed in most normal cells. Thus, the conjugation of FA to gene carriers can render the carrier has specific targeting capability and enhance cell uptake via the receptor-mediated endocytosis. [10]

In this study, folic acid functionalized Schiff-base linked imidazole-chitosan (FA-SLICS) was synthesized through introducing imidazole to the backbone of chitosan by the formation of Schiff-base and then grafting folic acid to the Schiff-base linked imidazole-chitosan (Figure 5.2). We hypothesize that the water solubility of FA-SLICS should be improved at physiological pH since the protonated Schiff-base and imidazole ring. Furthermore, FA-SLICS should be pH sensitive and the loaded gene will released within the endosomal pH range because of the pH-sensitive Schiff-base linkage. Importantly, FA-SLICS should be able

to specifically deliver loaded gene to FA positive (FA^+) tumour cells because of the introduction of folic acid to the modified chitosan (Figure 5.1). To verify our hypothesis, DNA binding and protection capability, particle size and zeta potentials, pH controlled gene loading and release efficiency, cytotoxicity, and targeted gene delivery capability of FA-SLICS were systematically examined.

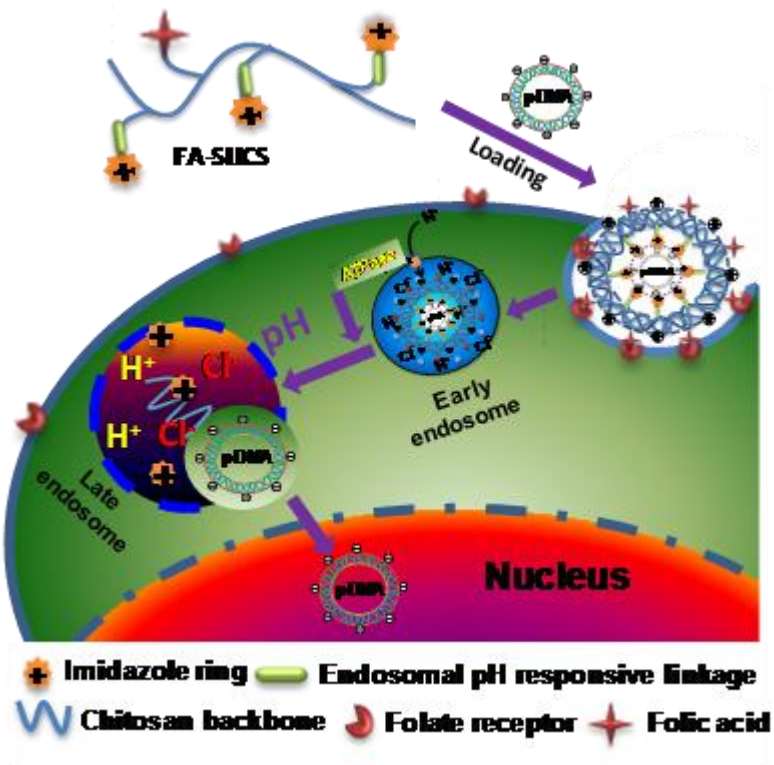

Figure 5.1 The intracellular microenvironment responsive polymer mediated gene deliver.

5.2 Experimental Section

5.2.1 Materials.

Chitosan (molecular weight ~ 200 kDa, degree of acetylation ~ 90%), EDC (1-ethyl-3-(3-dimethy- laminopropyl) carbodiimide), NHS (N-hydroxysulfosuccinimide) and folic acid were purchased from Acros (New Jersey, USA). QIAGEN Maxi kit was obtained from Qiagen (Boncaster, Australia). Plasma membrane and nuclear labelling kit, nucleic acid stains

dimer sampler were purchased from Life Technologies (Mulgrave, Australia). Fetal bovine serum (FBS), trypsin-EDTA, penicillin-streptomycin (PS) mixture, RPMI 1640 cell culture medium, phosphate buffered saline (PBS), TAE (tris-acetate), agarose and Lipofectamin™ 2000 reagent were purchased from Gibco-BRL (Grand Island, USA). Sucrose, folic acid, gel red, *3*-(*4*, *5*-dimethylthiazol-*2*-yl)-*2*, *5*-diphenyltetrazolium bromide (MTT), kanamycin, *4*-imidazolecarboxaldehyde (ICD) and other chemicals/solvents were purchased from Sigma-Aldrich (St. Louis, MO).

5.2.2 Plasmid DNA Preparation.

The pEGFP-N1 plasmid expressing the Enhanced Green Fluorescent Protein (EGFP) as biomarker was prepared in *E. coli* DH5α strain and extracted using a QIAGEN Maxi kit. The integrity and purity of the prepared plasmid DNA was analysed using 0.8% agarose gel electrophoresis and the DNA concentration was determined using a Jasco UV-vis spectrophotometer (Tokyo, Japan) at the fixed wavelengths of 260 and 280 nm.[11] The plasmid DNA was further labelled by fluorescent dye (YOYO-1) at a molar ratio of 1 molecular dye to 100 nucleic acid base pairs for following cellular uptake study.

5.2.3 Synthesis of FA-SLICS.

The synthesis of FA-SLICS polymers was described in Figure 5.2. The Schiff-base linked imidazolyl chitosan (SLICS) was synthesized and purified. Briefly, chitosan (0.5 g, 2 mmol glucosamine repeat unit) was dissolved in 15 mL deionized water, pH was adjusted to 6 using 1 M HCl and stand at 65 ^{o}C overnight. *4*-imidazolecarboxaldehyde (0.192 g, 2 mmol) was dissolved in 10 mL deionized water, and then it was dropwisely added into the chitosan solution during a 20 min period. The mixture was stirred at room temperature for another 4 h. The solutions were condensed and precipitated in excessive amount of anhydrous acetone. The products were filtered, rinsed thrice with anhydrous acetone, and vacuum-dried at room temperature. Various SLICS polymers were prepared by changing the amounts of feed *4*-

imidazolecarboxaldehyde to chitosan to change the substitution degree of *4*-imidolecarboxaldehyde (details shown in Table 5.1).

SLICS polymers were further reacted with folic acid using carbodiimide chemistry. Taking the synthesis of FA-SLICS-1 for example, NHS/EDC (0.737mg/1.227mg, 0.0064 mmol) and folic acid (1.4 mg, 0.0032mmol) were added to 5 mL deionized water at pH 9.0 and stirred at room temperature for 1 h. It was then mixed with SLICS-1 (30 mg, 0.16 mmol free amino group, pH 7). The reaction mixture was stirred in darkness at room temperature for 16 h. pH value of the reaction mixture was brought to 9.0 by adding NaOH solution (0.1 M) and the reaction mixture was dialyzed against deionized water (pH 9.0) for 3 d, followed by the dialysis against deionized water (pH 7.4) for another 3 d. The obtained FA-SLICS polymers were lyophilized and the characterization of resulting polymers was conducted by using various analytical techniques as explaining in the following (details shown in Table 5.1).

5.2.4 Determination of Imidazolyl and Folic Acid Substitutions.

UV-visible spectro-photometer (UV-1601, SHIMADZU) was used to determine the substitution of *4*-imidolecarboxaldehyde and folate along the chitosan backbone since imidazolyl and folate have specific absorption peaks at 257 nm and 363nm, respectively. After setting up the calibration curves at pH 7, the imidazolyl substitution degrees of the synthesized FA-SLICS were determined with the absorption peaks at 257 nm, and then folate substitutions in the synthesized FA-SLICS were determined by the absorption peaks at 363 nm according to the Beer-Lambert's law.[12] The path length was 1 cm.

5.2.5 FTIR and ^{1}H-NMR Spectroscopy.

The infrared spectrometer (IR) spectra of chitosan, SLICS and FA-SLICS were examined using a Thermo NICOLET 6700 Fourier Transform Infrared Spectrometer (FTIR) at room temperature. ^{1}H-NMR experiments were recorded using a 600 MHz Bruker NMR in D_2O.

5.2.6 FA-SLICS and Plasmid DNA (pDNA) Binding Interaction.

The loading capability of nucleic acid to the FA-SLICS was evaluated by agarose gel electrophoresis using naked pDNA as the model cargo and control. Various polyplexes were prepared by mixing FA-SLICS polymers with 0.2 μg pDNA at different mixing charge ratios (N/P of polymers to pDNA, amine group to phosphate group). The polymer/pDNA polyplexes were prepared at pH 7.2, and kept at room temperature for 20 min before being loaded onto 0.8 wt% agarose gel in a Tris–acetate (TAE) running buffer and electrophoresed at 80 V for 60 min. The resulting pDNA migration patterns were read under UV irradiation (G-BOX, SYNGENE).

5.2.7 The Nucleic Acid Protection Capability of FA-SLICS Assay Against DNase I.

FA-SLICS/pDNA polyplexes were prepared at different N/P ratios and then incubated with DNase I (25 μL,160 units/mL) in DNase/Mg^{2+} digestion buffer (50 mM, Tris-HCl, pH 7.6, and 10 mM $MgCl_2$) at 37 ^{o}C for 30 min using free pDNA (0.2 μg) as the negative control. The degradation of the pDNA was investigated by 0.8 wt% agarose gel with a Tris–acetate (TAE) running buffer and electrophoresed at 80 V for 60 min. The resulting pDNA migration patterns were read under UV irradiation.

5.2.8 Particle Size and Zeta-potential of FA-SLICS/pDNA Polyplexes.

The particle size and zeta potential of the FA-SLICS/pDNA polyplexes prepared at different charge ratios were measured by a Malvern Zetasizer (Malvern Inst. Ltd. UK) at pH 7.2, equipped with a four-side clear cuvette or ZET 5104 cell at room temperature.[13] For all polyplexes, the concentration of pDNA was kept at 5 μg/mL. For the particle size analysis, cumulant method was used to convert intensity-intensity autocorrelation functions to apparent particle sizes according to the Stokes-Einstein relationship.[14] The Smuloschowski model was used to convert electrophoresis mobility to zeta potential.[15] Ten parallel runs were carried out

for each measurement and the final data were obtained based on statistical analysis.

5.2.9 Ethidium Bromide (EtBr) Exclusion Assay.

The pDNA condensation was measured by exclusion of EtBr method.[16] Briefly, 4 μg DNA was mixed with the gradually increased amounts of FA-SLICS to a final volume of 280 μL at different N/P ratios (polymer to pDNA) under the condition of pH 7. After incubation for 30 min at room temperature, 20 μL of a 0.1 mg/mL EtBr solution was added to the polymer/DNA polyplexes solution and the solutions were mixed intensively. Fluorescence was measured using a fluorescence plate reader (LS 50 B; Perkin- Elmer, Rodgau-Jugesheim, Germany) at 518 nm excitation and 605 nm emission wavelengths. Analytical results are presented as relative fluorescence intensity values, where 1 represents the fluorescence of naked DNA with EtBr and without polycation, and 0 represents the remaining fluorescence of non-intercalating EtBr.

5.2.10 Gene Release *in Vitro.*

FA-SLICS/pDNA polyplexes prepared at various N/P ratios of 5, 10, 20 were incubated at 37 °C with DMEM at pH 7.2 for 30 min. The pH values of FA-SLICS/pDNA polyplexes were adjusted to 7, 6 and 5, respectively. At each pH value, the complex suspension was centrifuged at 20,000×g for 30 min and the supernatant was quantified for pDNA content by spectrofluorimetry after the addition of Hoechst 33258 (20 μl, 1mmol/μl). [17]

5.2.11 Evaluation of Cytotoxicity.

Normal cell (CHO) and cancer cells (HeLa and $HepG_2$) were cultured in DMEM medium supplied with 10% FBS in 96-well plates (200 μL /well) at a cell density of 1.0×10^5 cells/mL. After inoculation, the cells were allowed to adhere overnight at 37 ^oC in a humidified 5% CO_2-containing atmosphere. The growth medium was replaced with 200 μL fresh medium containing FA-SLICS polymers at final concentrations of 0.5, 1, 3, 5, 10, 20, 30, 50 μg/mL.

Cells were then incubated for 48h before 10 μL of MTT (5.0 mg/mL in PBS) was added to each well for the evaluation of cell viability. After incubating for another 4 h at 37 ^{o}C, the growth medium was replaced by 150 μL of dimethyl sulfoxide (DMSO) to ensure complete solubilization of the formed formazan crystals. Finally, the absorbance was determined using the Biotek Microplate Reader (Biotek, USA) at a wavelength of 570 nm.[18]

5.2.12 Assessment of Intracellular Uptake.

HeLa and $HepG_2$ cells at a concentration of 2×10^5 cells/well were cultured in 6-well plates loaded with cover-glass slides for 24 h. 4 μg YOYO-1 labelled pDNA was loaded on to the different gene carriers (chitosan, L-PEI, SLICS-2 and FA-SLICS-2) at various charge ratios (N/P) of 10.0, 5.0, 10.0 and 10.0 to form polymer/pDNA polyplexes. Cells were incubated with polymer/pDNA polyplexes for another 4 h and then the polyplexes were removed by washing the cells with PBS for three times before fixing with 4% formaldehyde. The cell membrane and nucleus were separately stained by 100 μL of Alexa Fluor 594 (5.0 μg/mL) and Hoechst 33258 (2 μM) for 15 min at 37 °C. The cells were further washed with PBS for three times and incubated with 500 μl PBS, and kept at room temperature for further analysis. The fluorescent images were observed by a confocal laser scanning microscope (Leica Confocal 1P/FCS) equipped with a 405 nm diode laser for Hoechst 33258, a 488 nm argon ion laser for YOYO-1 and a 561 diode laser for Alexa Fluor 594. The high magnification images were obtained with a 100 × objective. Optical sections were averaged 4 times to reduce noise, and images were processed using Leica Confocal software.

5.2.13 Cell Culture and Gene Delivery.

HeLa and $HepG_2$ cells were seeded in 24-well plates and cultured in complete DMEM supplemented with 10% fetal bovine serum (FBS) at 37^{o}C in a humidified incubator, in the presence of 5% CO_2. After 24 h culturing, the medium was replaced with fresh 200 μL culture medium with and without FBS, respectively. Meanwhile, the polymer/pDNA

polyplexes, which were prepared by incubating FA-SLICS or SLICS polymers and pDNA at various N/P ratios at room temperature for 20 min, were added to each well. After 6 h incubation, the cultured medium was replaced by 1 mL fresh complete culture medium with 10% FBS and the cells were further incubated for another 42 h.

5.2.14 GFP Expression Analysis by Fluorescent Microscopy and Flow Cytometry.

Green fluorescent protein (GFP) expression level can be evaluated by fluorescence microscopic analysis. Briefly, living cells were rinsed 3 times by 1× PBS and visualized *in situ* by the detection under an epi-fluorescence microscope (Multi-photon Microscope, Nikon) connected to a CCD camera (RS Photometrics). A band pass filter (BP 485/20) was chosen for excitation and a 520 nm long pass filter were used for emission as barrier filter in viewing emission. Digitalized photographs were stored and analysed by using the Bio-Rad Radiance 2000MP Visualising System. The green fluorescence intensity was also detected directly by a FACSCalibur flow cytometry (Becton Dickinson), and the transfection efficiency was calculated by the percentage of positive cells, using non-transfection cells (mock cells) as the negative control. Briefly, cells were harvested by the digestion of trypsin after 42 h post-transfection. 1×10^6 cells were washed with 2% FCS/PBS buffer, and centrifuged at 1000 rpm for 5 min. The cells were stained by propidium iodide (400 μL, 0.5 μg /mL) in 1×PBS. Approximately $1\text{-}2\times10^4$ cells were analysed at the rate of 200 ~ 600 cells per second. CellQuest3.3 software was used for data analysis. [19]

5.2.15 Statistical Analysis.

Data obtained from our experiments are represented as mean ± SE (standard error). Statistical analysis of the numerical variables was performed using a two-sample, two-tailed t-test. A value of $p < 0.05$ is considered to be significant.

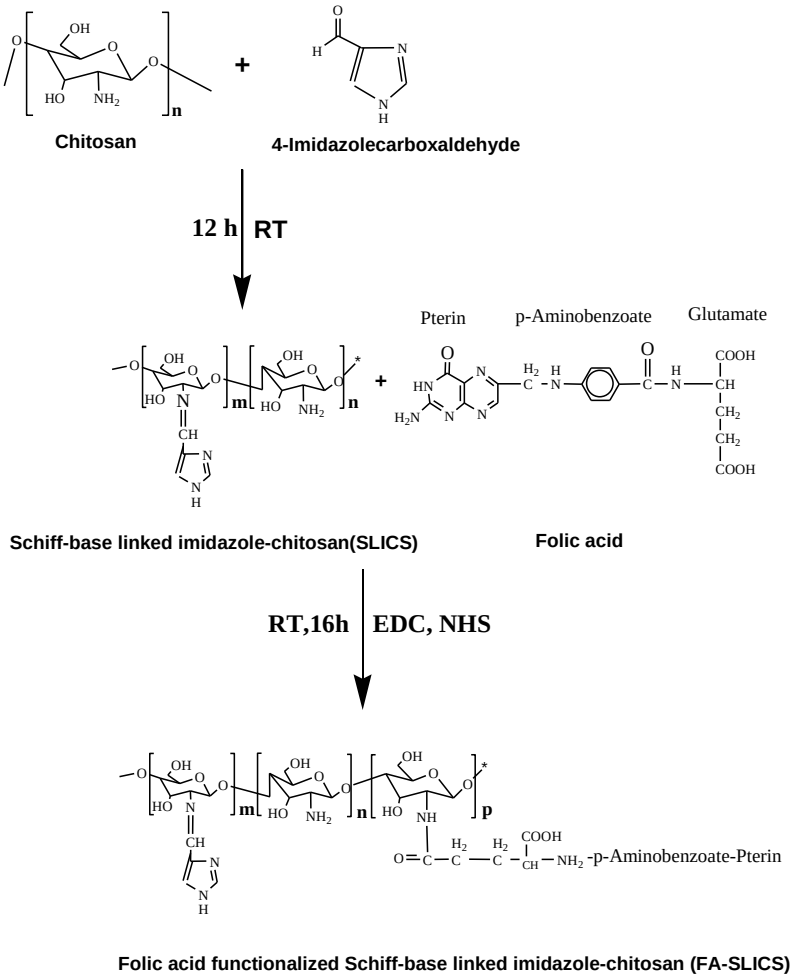

Figure 5.2 Schematic representation for the synthesis of folic acid functionalized Schiff-base linked imidazole-chitosan (FA-SLICS).

5.3 Results and Discussion

5.3.1 Synthesis and Characterization.

To improve the water solubility and gene binding capability of chitosan under a physiological condition, functional imidazole groups were introduced to the 2-*N* position of chitosan *via* the formation of Schiff-base linkage. Different amounts of *4*-imidazolecarboxaldehyde were reacted with chitosan at room temperature to obtain a series of Schiff-base linked imidazole-chitosan (SLICS) with the imidazolyl substitutions ranging from 3.35% to 79.20% (Table 5.1, Figure 5.3, 5.4 and 5.5).

In order to increase the specificity and selectivity of the SLICS carriers to FR+ tumour cells, folate groups were further coupled to the SLICS polymers via the EDC-mediated reaction (Figure 5.2). The feed molar ratio was set as 1 to 50 (γ-carboxyl groups of folic acid to primary amine groups of SLICS), and the developed polymer were named FA-SLICS-1, -2 and -3. From the UV-vis absorption of FA-SLICS polymers at the wavelength of 363 nm, the percentages of folic acid substitution are found to be 0.874%, 0.504% and 0.253% for FA-SLICS-1, -2 and -3 respectively (Table 1, Figure 5.3 and 5.4). The feed molar ratio of 1:50 was chosen in the reaction because we noticed that the water solubility of FA-SLICS polymers is poor in neutral pH at the feed ratios higher than 0.02 since excessive amounts of carboxyl group of folic acid were introduced along the SLICS backbone. The successful conjugation of folic acid to SLICS was further confirmed by the FT-IR and ^{1}H-NMR measurement (Figure 5.6 and 5.7). For chitosan, the basic characteristic peaks at 1590 cm^{-1} (N-H bending) and 1080 cm^{-1} (C-O- stretching) are evident.[20] The SLICS-2, prepared by the formation of Schiff-base between chitosan and imidazole, presents a strong absorption band at 1634 cm^{-1} attributing to the C=N vibration.[21] The peak at 1570 and 1405cm^{-1} are assigned to the in-plane C–C and C–N, and N-H stretching vibration of the imidazolyl rings.[22] Comparing with SLICS-2, the characteristic band of folic acid at 1725 cm^{-1} is attributed to the α-carboxyl groups (-COOH) of FA-SLICS-2, which indicates the successful folic acid conjugation.[23] The peak of C=O amide bond at 1659 cm^{-1} is wider because it is overlapped by the spectra peak of the C=N vibration at 1634 cm^{-1}, which also helps to confirm the reaction between folate and SLICS. In addition, ^{1}H-NMR was used to further elucidate the chemical structure of the FA-SLICS. From the ^{1}H-NMR analysis, the chemical shifts for the H atoms of chitosan are located within the δ range of 2.00 to 4.80 ppm. The successful conjugation of the imidazole ring to chitosan is evident from the presence of signals ranging from δ 7.8 to 9.6 ppm. Additionally, the appearance of chemical shift at δ 7.4 - 7.6 ppm is

contributed to the formed amide linkage between folic acid and SLICS (Figure 5.7).

Table 5.1 Details on the FA-SLICS polymer preparation.

Sample Name	Feed Ratio[a]	Imidazolyl Substitution (mol/mol %)	Feed Ratio[b]	Folic Acid Substitution (mol/mol %)
FA-SLICS-1	1:10	3.35	1:50	0.874
FA-SLICS-2	1:1	55.06	1:50	0.504
FA-SLICS-3	2:1	79.20	1:50	0.253

a) Feed ratio of the aldehyde group to the amine group on chitosan.

b) Feed ratio of the γ-carboxyl group of folic acid to the primary amine group of SLICS.

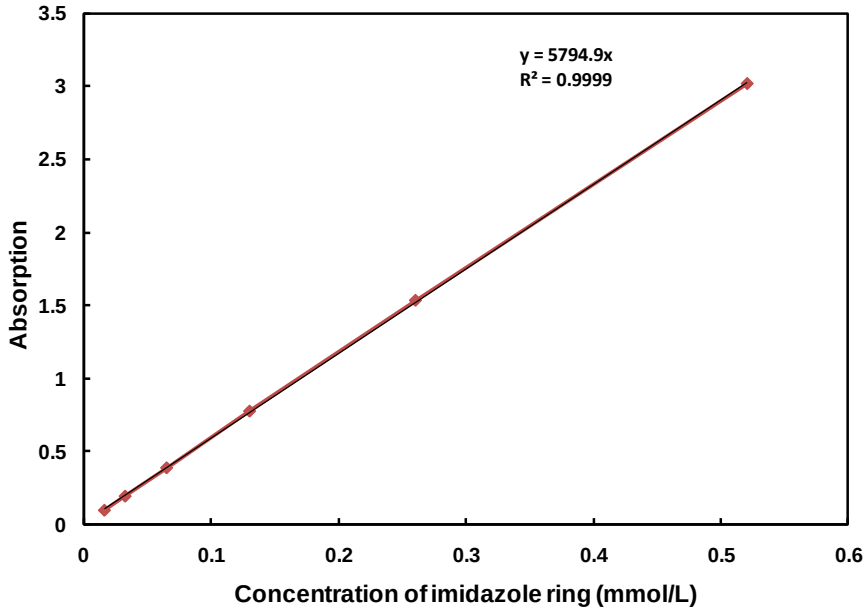

Figure 5.3 Calibration curve of imidazole group at the wavelength of 257 nm.

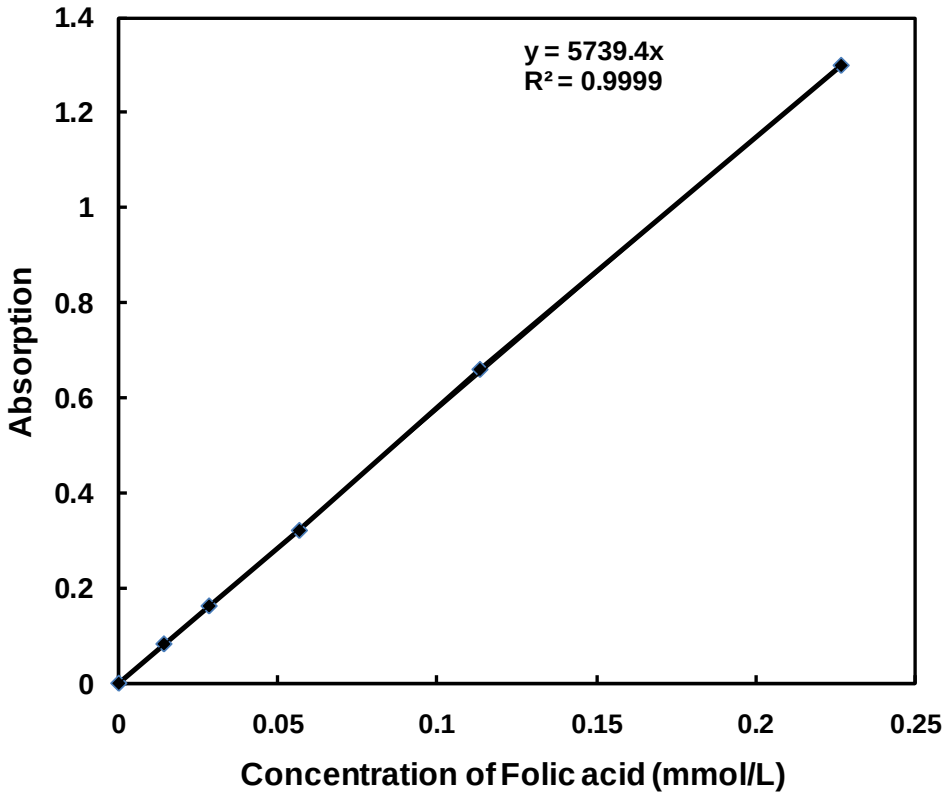

Figure 5.4 Calibration curve of folate group at the wavelength of 363 nm.

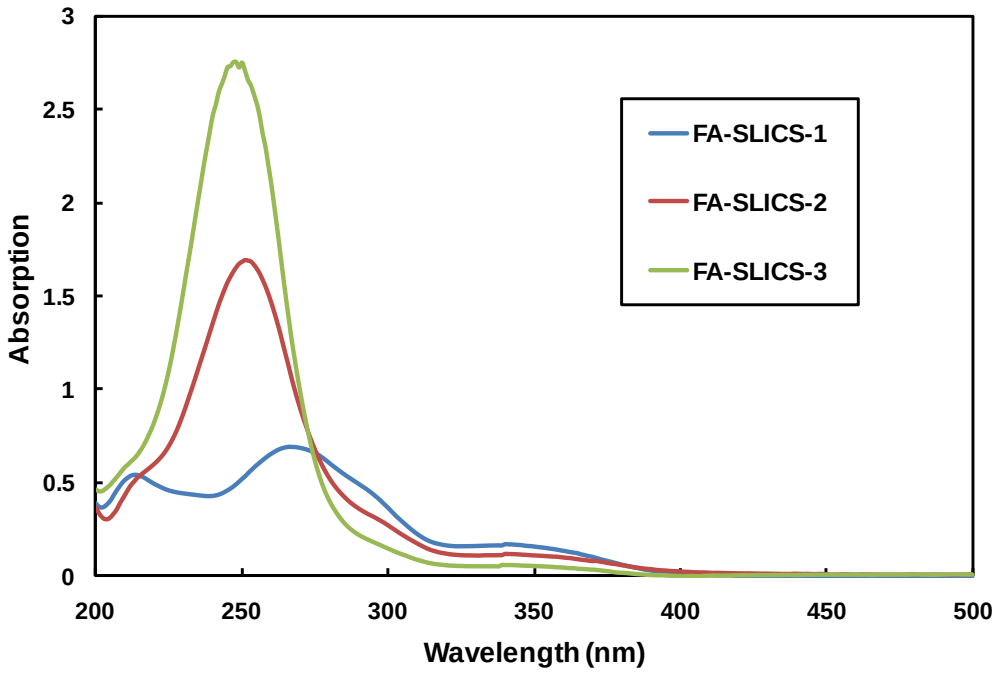

Figure 5.5 UV absorption of the synthesized FA-SLICS polymers.

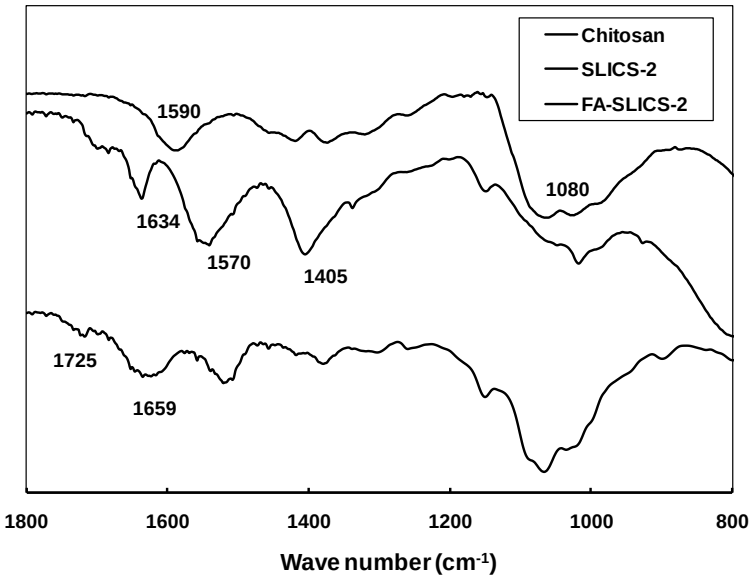

Figure 5.6 Comparison on the FTIR spectra of chitosan, SLICS-2 and FA-SLICS-2.

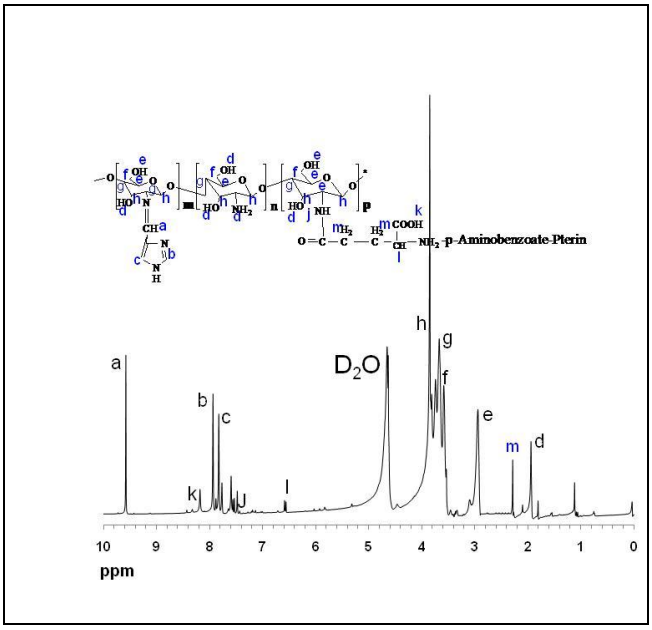

Figure 5.7 The ^{1}H-NMR of the FA-SLICS in D_2O.

5.3.2 Nucleic Acid Binding Ability Assay.

Nucleic acid loading ability is a curial parameter for evaluating gene carriers.[24] The nucleic acid binding ability of FA-SLICS with different degrees of imidazolyl and folate substitutions were examined by gel retardation assays using naked pDNA as model nucleic acid and

negative control. As shown in Figure 5.8A, the electrophoresis mobility of pDNA decreases with increasing in the mixing charge (N/P) ratios of FA-SLICS to pDNA, and pDNA can be completely retarded at the charge ratios ranging from 3 to 50 for all FA-SLICS polymers. For the FA-SLICS-1 with 3.35% imidazolyl and 0.87% folic acid substitution, free pDNA can be observed below the N/P ratio of 1, but disappears when the N/P ratio is above 3. For the other two polymers (FA-SLICS-2 and 3) with higher degrees of imidazolyl substitution (55.6% and 79.2%) and lower degrees of folate substitution (0.504% and 0.253%), free pDNA bands can only be observed at the charge ratios of 0.5 and 1, and the pDNA signals are much weaker than those of FA-SLICS-1. Free pDNA disappears at the charge ratio above 1. The experimental results indicate that the higher imidazolyl substitution, the stronger gene binding abilities, due to the presence of protonated Schiff-base and imidazolyl which can improve pDNA binding affinity. The more amino groups along chitosan backbones are substituted by the imidazole rings via Schiff-base linkers, the more pDNA can be bound to form polyplexes in neutral pH solution. The improved electrostatic attraction dominates high gene loading capability of FA-SLICS polymers.

5.3.3 DNase I Digestion Assay.

Gene delivery is a multiple-step procedure and the polyplexes have to overcome a series of barriers in successful DNA transport. Therefore, the gene protection ability against digestion is another key factor for gene carrier design since various nuclease exist in cells or *in vivo*. The protection capability of FA-SLICS to nucleic acid against nuclease degradation was identified using pDNA as model nucleic acid and DNase I as a model nuclease. As Figure 5.8B shows, 0.2 μg of naked pDNA is completely degraded after incubating with 200 U/mL of excessive DNase I at 37 ^{o}C for 30 min as evident from the disappearance of gel intensity. However, only half of the pDNA is degraded for the FA-SLICS-1/pDNA polyplex at the N/P ratio of 0.5, whereas no pDNA digestion can be observed at the N/P ratios from 3 to 80 under

the same digestion condition. It can be explained that at higher N/P ratios, more FA-SLICS-1 polymers are bounded to pDNA and form polyplexes which are able to protect pDNA against DNase I digestion. In addition, pDNA can be fully protected against the digestion of DNaseI by FA-SLICS-2 or FA-SLICS-3 beyond an N/P ratio of 1. Obviously, FA-SLICS-2 and FA-SLICS-3 have stronger pDNA protection capability than FA-SLICS-1 due to their higher binding ability with pDNA. As such, FA-SLICS is effective in the protection of pDNA at physiological condition since the real nuclease concentration *in vivo* is much lower than our experimental DNase concentration.[25]

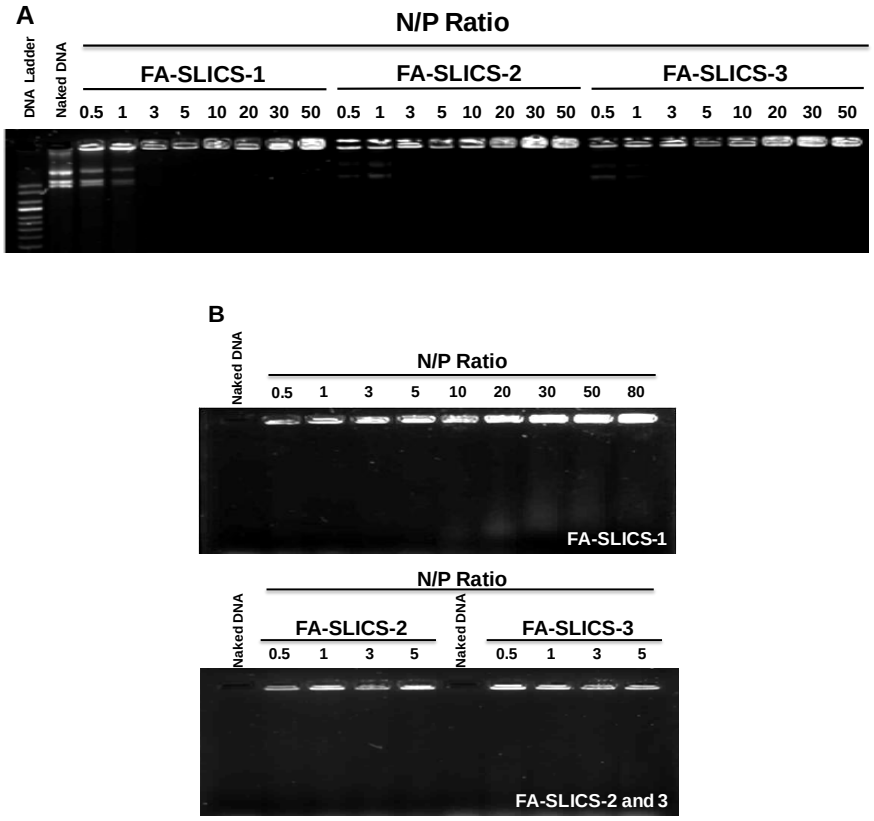

Figure 5.8 Evaluation of nucleic acid binding and protection capability of FA-SLICS. A: Nucleic acid binding ability assay; B: Nucleic acid protection ability assay against DNase I. The polymer/DNA polyplexes were prepared at various charge ratios (N/P), pH 7.0. Agarose gel electrophoresis was run with 0.8% agarose in Tris-acetate running buffer.

5.3.4 Particle Size and Zeta Potential.

The endocytic machinery and cell membrane have well-defined geometries and flexibility

that restrict the entry of incompatible particles. Small particles (50 - 200nm) can be up-taken via the endosome mediated endocytosis and large particles may be preferentially trafficked through a slow, non-degradable, caveolae-mediated route.[26] Therefore, the control of polyplex particle size is crucial for gene delivery. Various FA-SLICS/pDNA polyplexes were prepared by mixing pDNA with FA-SLICS polymers at different mixing N/P ratios. The sizes of polyplexes were examined using dynamic light scattering (DLS), and the cumulant approach was used to analyse scattered light intensity-intensity autocorrelation functions. As shown in Table 5.2, the apparent particle sizes of the FA-SLICS/pDNA polyplexes decrease with the increase of the N/P ratios from 0.5 to 30 for all FA-SLICS polymers. In addition, the apparent sizes of polyplexes reduce while the degree of imidazolyl substitution increases, which is attributed to the stronger polymer/pDNA electrostatic interaction and the formation of more compact structure. The pK_a value of the imidazole ring is 14.2 at 25 ^oC,[27] and the pK_a for Schiff-base is between 10.6 and 16.0 at 25 ^oC.[6] Both of them are higher than that of the amino groups (6.2 at 25 ^oC).[28] The presence of secondary and ternary amino groups significantly enhances the binding interaction between the FA-SLICS and negative charged biomacromolecules such as pDNA.

Zeta potential is a ubiquitous particular parameter that is important for understanding cell uptake mechanism and transfection efficiency. It is generally believed that low positively charged nanoparticles perform better for *in vitro* transfection due to their binding capability to negatively charged proteoglycans on cell surfaces.[29] Optimization of a non-viral carrier often involves an adjustment of the charge ratios of cationic polymers to anionic pDNAs, aiming to balance the competing effects of cellular binding and uptake, pDNA protection and release, and the polyplex size and stability. The zeta potentials of the polyplexes in water at seven different mixing ratios are compared in Figure 5.9. Electrostatic interaction dominates the formation of polyplexes between negatively charged pDNA and positively charged FA-

SLICS. The zeta potentials of polyplexes are negative at smaller mixing ratios of FA-SLICS to pDNA and increase to about zero with a mixing N/P ratio of 2. It turns to positive with further increase in the amount of FA-SLICS and later levels off at the mixing N/P ratios beyond 5. The shift in the zeta potentials with mixing charge ratio is attributed to the strong binding of FA-SLICS and pDNA, which agrees well with previous gel electrophoresis analysis (Figure 5.8). The zeta potential values are influenced by the substitution of imidazole ring and the formation of Schiff base, as well as the concentration of FA-SLICS. At a fixed mixing ratio, with increasing the degrees of substitution, more negative charges along pDNA backbones are neutralized, which is confirmed from the lower zeta potential values. On the other hand, the presence of folic acid may neutralize some of positive charges of SLICS, which further results in the decrease in zeta potential. It has been reported that the presence of slightly positive charges on the polyplex surface is useful for gene delivery due to its minor damage to cells and easy entry into cells via endocytosis.[30]

Table 5.2 Particle sizes of the FA-SLICS/pDNA polyplexes at various mixing charge ratios.

Charge ratio (N/P)	FA-SLICS-1 (nm)	FA-SLICS-2 (nm)	FA-SLICS-3 (nm)
0.5	320±36	315±32	310±26
1	262±33	253±21	242±23
3	255±26	230±20	218±19
5	246±33	195±15	178±13
10	204±30	155±14	140±20
20	188±28	126±16	116±13
30	180±22	91±12	80±11

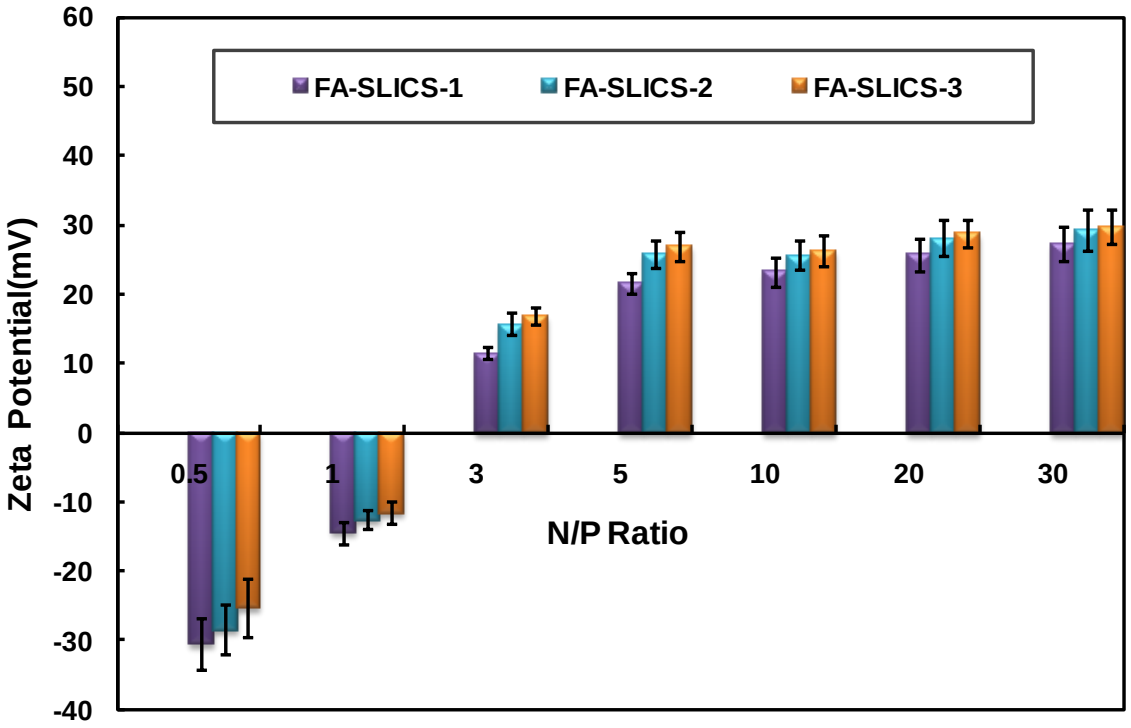

Figure 5.9 Zeta potentials of the FA-SLICS/pDNA polyplexes prepared by different charge ratios (N/P) of FA-SLICS to pDNA at pH 7.0 and 25 ^{o}C. For all measurements, the DNA concentration was fixed at 5 μg/mL.

5.3.5 Gene Loading and Release *in Vitro.*

The gene loading efficiency of FA-SLICS was examined by EtBr exclusion assay using pDNA as model nucleic acid. The binding sites of pDNA can be competitively occupied by FA-SLICS polymers and EtBr, and EtBr becomes fluorescent after binding with pDNA. Therefore, the pDNA unoccupied by FA-SLICS polymers can be examined by detecting the fluorescent intensity of EtBr. The naked pDNA without polymers was used as control, where the relative fluorescent intensity (RFI) is regarded as 1. As shown in Figure 5.10A, after adding polymers to the pDNA, the RFI gradually decreases from 1 to 0.1 with the increment of the N/P ratio from 0.5 to 20. This indicates pDNA are competitively occupied by FA-SLICS polymers to form the polymer/pDNA complexes. The more sites of DNA have been occupied, the lower the RFI is.

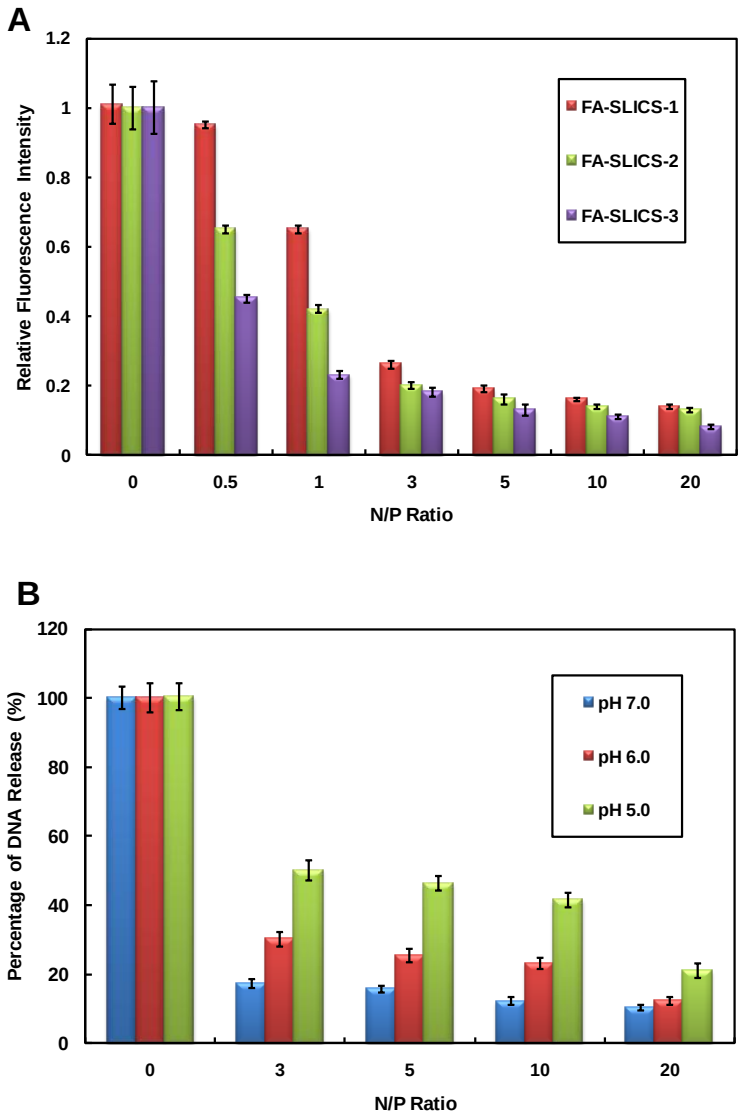

Figure 5.10 Gene loading and release *in vitro*. A: Gene load efficiency of FA-SLICS by EtBr exclusion assay. B: *In vitro* gene release profile from FA-SLICS-2 at various pH values.

To simulate the gene release process from the FA-SLICS polymers triggered by pH change in cells, gene release profiles from FA-SLICS polymers were further assessed with the Hoechst 33258 exclusion assay using pDNA as model nucleic acid. Hoechst 33258 can interact with the binding site of free pDNA released from FA-SLICS/pDNA polypolexes, which results in detectable fluorescence. Therefore, the released pDNA can be monitored by examining the fluorescent intensity (The RFI of the system without FA-SLICS is defined as 100%, while the system without Hoechst 33258 is defined as 0). FA-SLICS-2/pDNA

polyplexes were prepared at various N/P ratios under physiological condition, and the pH values of the release medium were controlled at 7, 6 and 5. As Figure 5.10B shows, at a fixed N/P ratio, the released pDNA increases within the dropping pH from 7 to 5. On the other hand, at a fixed pH value, the released pDNA decreases as the N/P ratio increases. Taking the N/P ratio of 10 as an example, the ratio of released pDNA is less than 20% at pH 7, increases slightly at pH 6, and further increases to more than 40% at pH 5. The results suggest about 40% of pDNA can be released from FA-SLICS-2 when the pH decreases from 7 to 5 due to the pH sensitive linkage between imidazole ring and chitosan.[7] It has been reported that endosomes are formed after the receptor-mediated endocytosis, which provides an environment for materials to be sorted before reaching the degradable lysosomes.[31] The pH of the endosomal environment decreases to about 5 when early endosomes mature into late stage before fusing with lysosomes.[32] Therefore, the loaded nucleic acid cargos on the FA-SLICS should be gradually released in vivo associated with the pH fluctuation in endosomes, which resulting in enhanced gene delivery efficiency.

5.3.6 Cell Toxicity.

To evaluate the cytotoxicity of FA-SLICS, a variety of cells (CHO, HeLa and $HepG_2$ cells) were incubated with FA-SLICS in a broad concentration range (1.0-50.0 μg/ml), using linear PEI and lipofectamine 2000 as the positive controls and chitosan as a negative control. Figure 5.11 shows the results of 24 h culture against CHO, HeLa and $HepG_2$ cells. FA-SLICS polymers have no significant toxicity to all the three types of cell incubated at the concentration range of 0 to 20 μg/mL and the cell viabilities are above 90%. With further increase in the concentrations of FA-SLICS polymers to 50 μg/mL, negligible toxicity can be observed for normal cells (CHO cells) with the average cell viability over 95%, cell viabilities of FA-SLICS-2 and FA-SLICS-3 fall to about 87% for cancer cells (HeLa and $HepG_2$ cells). For comparison, the cytotoxicity of linear PEI (25kDa) and lipofectamine 2000,

which are most commonly used commercial gene carriers, were also examined. Both commercial gene vectors show toxicity against cancer cell lines (HeLa cells and $HepG_2$) and normal cells (CHO), and the viabilities are less than 60% when the concentration of vectors were above 10 μg/mL (Figure 5.11). The MTT assay results strongly indicate that FA-SLICS polymers have no significant toxicity to both normal cells (CHO) and cancer cells (HeLa and $HepG_2$) due to the good biocompatibility of chitosan, imidazolyl and folic acid.

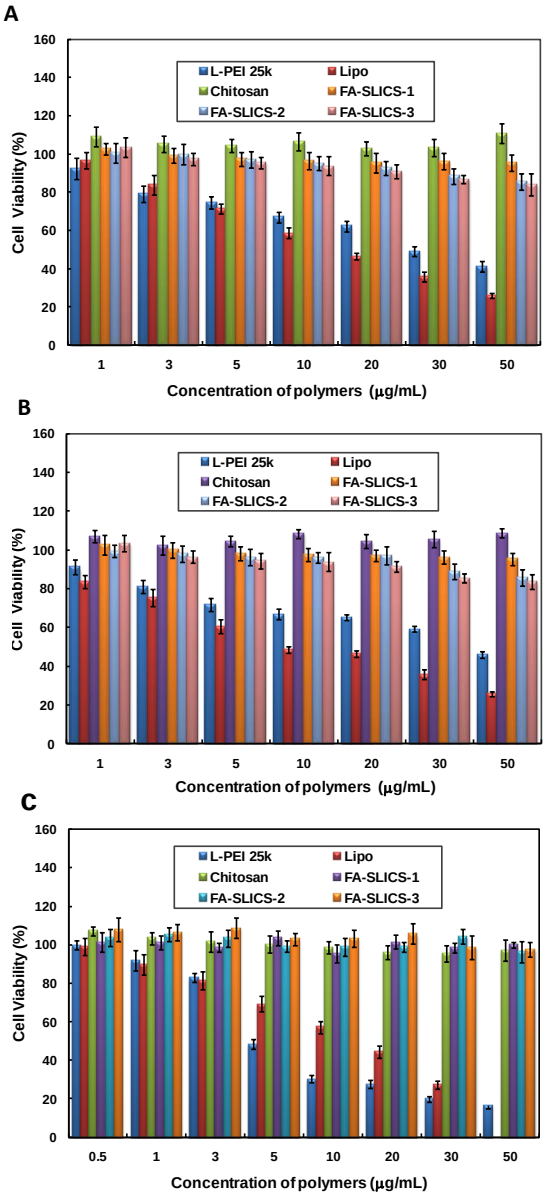

Figure 5.11 Cytotoxicity of FA-SLICS polymers comparing with the linear PEI and lipofectamine 2000. A: Cell viability of CHO cells; B: Cell viability of HeLa cells; C: Cell viability of $HepG_2$. The absorption was measured at 570 nm using a microplate reader (n = 3).

5.3.7 Cellular Uptake of Polymer/DNA Polyplexes.

To analyze the cell uptake of nucleic acid delivered using functional polymer vectors, pDNA was labelled by YOYO-1 with green fluorescence as a model nucleic acid. The labelled pDNA was delivered with SLICS-2 or FA-SLICS-2 into HeLa and $HepG_2$ cells at the N/P of 10 using chitosan and L-PEI as positive controls. To identify the location of pDNA, cell membrane and nucleus were stained by Alexa Fluor 594 (red fluorescence) and Hoechst 33258 (blue fluorescence), respectively. The images were captured with a confocal microscopy at 4 h post transfection. As shown in Figure 5.12A, the green fluorescence of labelled pDNA can be found in both cytoplasm and nucleus of HeLa cells after 4 h pDNA delivery except for chitosan. The fluorescence intensity of labelled pDNA in HeLa cells delivered by FA-SLICS-2 is higher than that of SLICS-2 and L-PEI, which demonstrates that the gene delivery capability of FA-SLICS-2 is higher than that of SLICS-2 due to the presence of folic acid, which may be due to the FR mediated endocytosis in the cellular uptake process of FR positive cells, such as HeLa.

To further identify the targeted function of FA-SLICS, the nucleic acid delivery capability of SLICS-2 and FA-SLICS-2 was also examined with FR negative cells ($HepG_2$) using L-PEI and chitosan as positive controls. The fluorescence intensity of labelled pDNA in $HepG_2$ cells delivered by FA-SLICS-2 is similar to that of SLICS-2 resulting from lack of the FR mediated cellular uptake pathway for the polymer/pDNA polyplexes, but slightly higher than that of L-PEI, which may be due to better biocompatibility of chitosan supported gene carrier and results in efficient pDNA release in delivery course (Figure 5.12B). However, much weaker green fluorescence of labelled plasmid DNA can be found in cells after 4 h delivery with chitosan comparing with that delivered by FA-SLICS. Therefore, both the pDNA delivery and targeted abilities of chitosan have been significantly improved after introducing imidazole Schiff-bases and folates onto the backbone of chitosan.

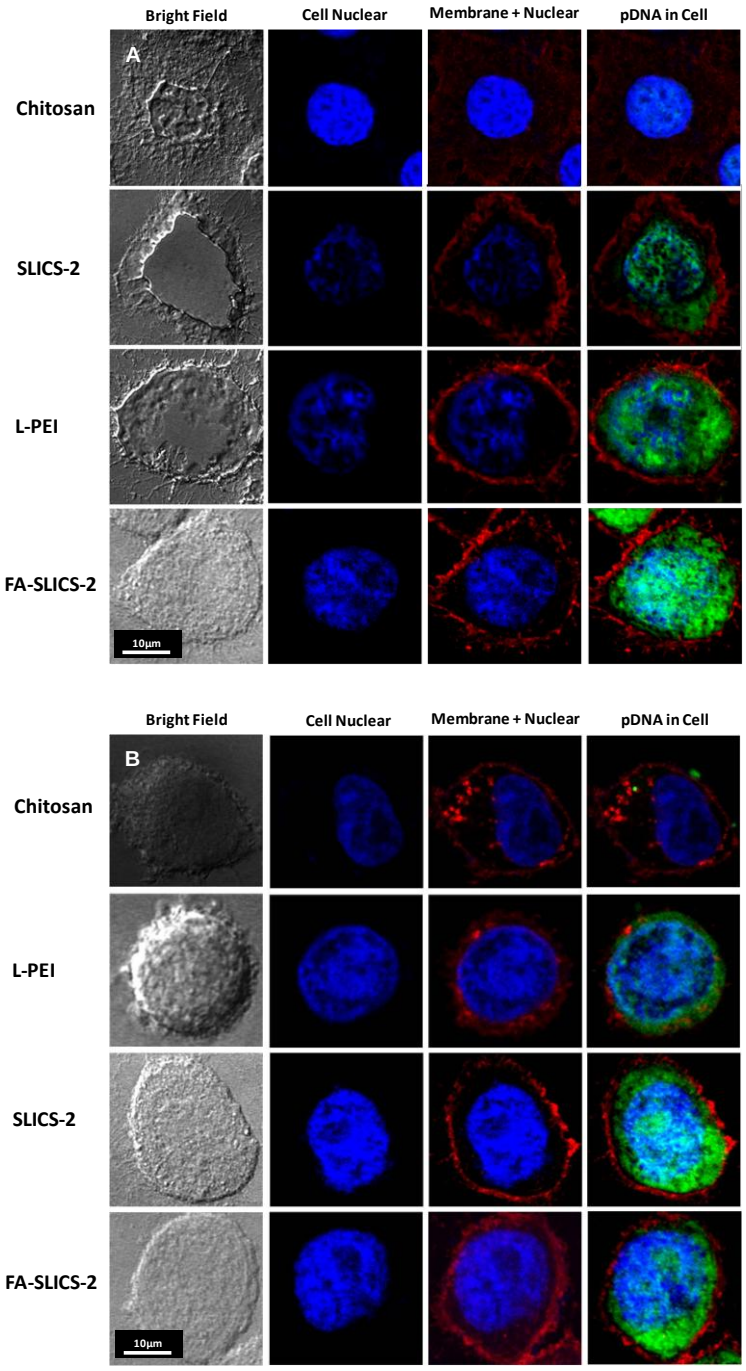

Figure 5.12 Cellular uptake of YOYO-1-labeled pDNA in HeLa and $HepG_2$ with the delivery of gene vectors: chitosan, L-PEI, SLICS-2 and FA-SLICS-2. A: HeLa cell (FR positive); B: $HepG_2$ cell (FR negative). Cells were incubated with ploymer/pDNA polyplexes for 4 h in 6-well plate at the DNA concentration of 4 μg/well. Cells were visualized using a confocal 1P/FCS inverted microscope after cell membrane and nucleus were stained with 100 μL of Alexa Fluor 594 (5.0 μg/mL) and Hoechst 33258 (2 μM).

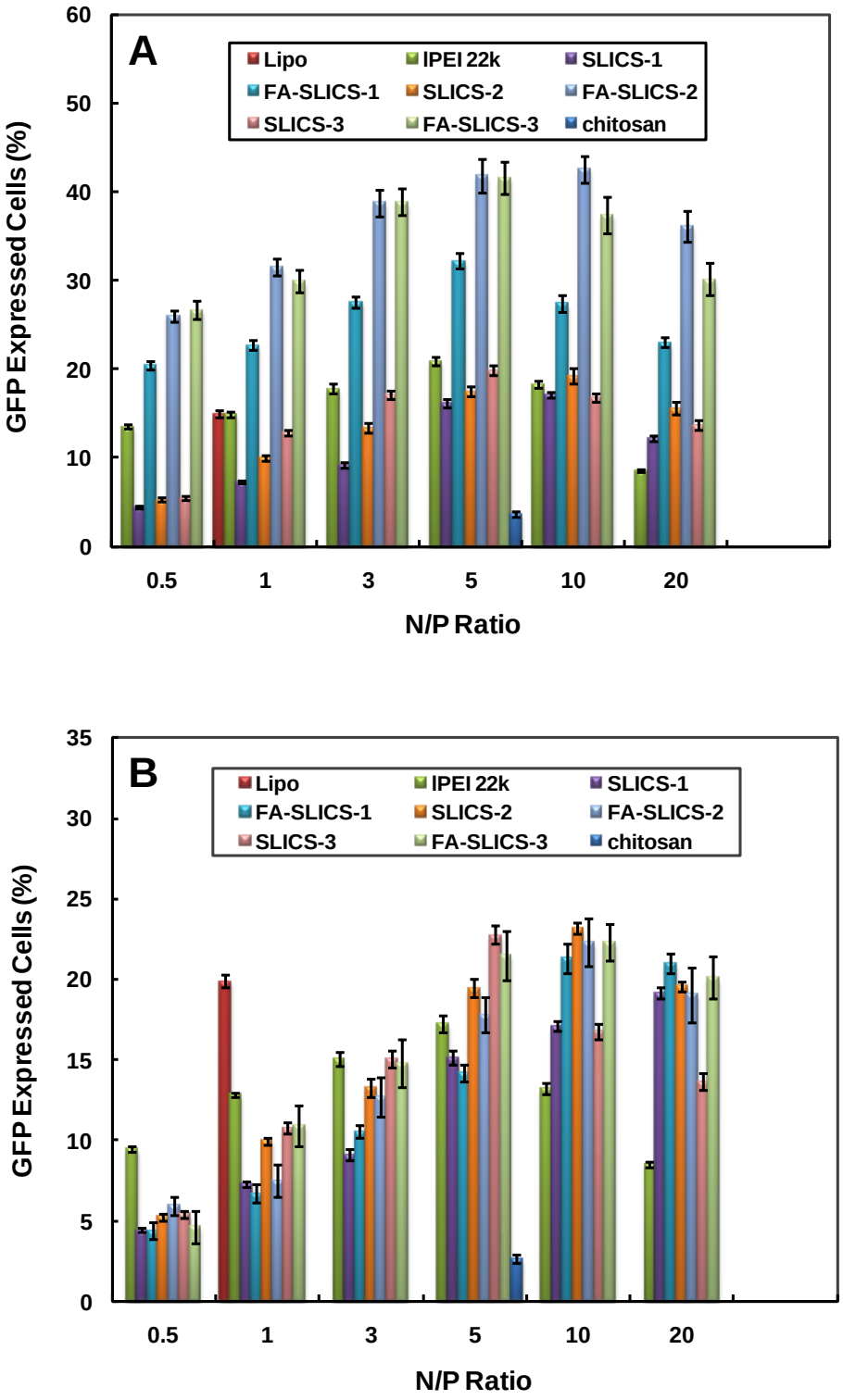

Figure 5.13 Cell transfection by the polymer/pDNA polyplexes at various charge (N/P) ratios. A: HeLa cells; B: $HepG_2$ cells. Transfection was performed at a dose of 1 μg of plasmid DNA per well in a 24-well plate. The transfection efficiency was calculated by percentage of positive cells with a FACSCalibur flow cytometry using non-transfection cell as negative control.

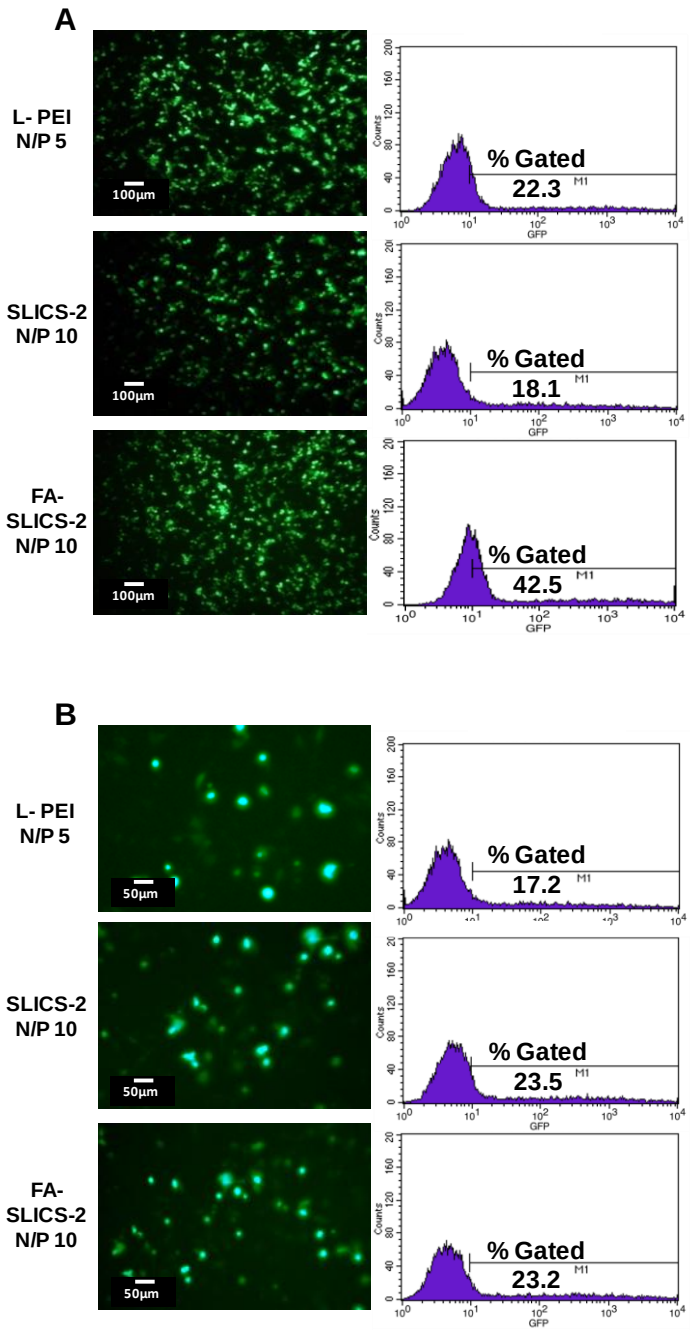

Figure 5.14 Fluorescent images and flow cytometry analyzed graphs of GFP expressed cell distribution. A: HeLa cells; B: HepG2 cells.

5.3.8 Gene Delivery.

To determine the cell transfection efficiency of FA-SLICS, nucleic acid delivery capability was evaluated by transferring pDNA into mammalian cells *in vitro*. Transfection experiments were carried out against FR positive tumour cells (HeLa) and FR negative cells ($HepG_2$) for

examining the target capability of FA-SLICS.[33] As Figure 5.13 shows, the transfection efficiency of FA-SLICS is significantly higher than that of SLICS in FR positive HeLa cells, but similar to that of SLICS for FR negative $HepG_2$ cells. Taking FA-SLICS-2 as an example, the highest transfection efficiency is 42.5% for FR positive HeLa cells, which is 2.5 times higher than that of SLICS-2 (42.5% vs. 18.1%). On the other hand, the highest transfection efficiencies of FA-SLICS-2 and SLICS are very close (23.2% vs. 23.5%) (Figure 5.14). The transfection efficiencies of the FA-SLICS are much higher than those of SLICS with FA positive HeLa cells due to the introduction of folic acid to the backbone of chitosan. Folate receptors on the cell membrane can improve the cellular uptake of folic acid-conjugated nanoparticle through receptor-mediated cellular pathway because folic acid has a highly specific affinity to folate receptors.[10] Thus, the folic acid endued higher transition efficiency of FA-SLICS was lost for FR negative $HepG_2$ cells since the FR deficiency on the cell membrane of $HepG_2$ cells. In addition, the highest cell transfection efficiencies of FA-SLICS are higher than those of commercial gene vectors (lPEI 22k and lipofectamine 2000) not only with FR positive HeLa cells but also with FR negative $HepG_2$ cells, which may be due to the high gene loading and intracellular microenvironment responsive gene release of FA-SLICS.

To further confirm the specific targeted ability of FA-SLICS, FR positive HeLa cells and FR negative $HepG_2$ cells were transfected by FA-SLICS-2/pDNA in various free folic acid contained cell culture medium (0 - 1.0 μM/mL). Interestingly, the transfection efficiency of FA-SLICS-2 is 42.2% without free folic acid in HeLa cells, deceases to 27.3% at a free folic acid concentration of 0.3 μM/mL, and continues to decease to around 20% when the free folic acid concentration increases to 1 μM/mL in the culture medium (Figure 5.15). However, the transfection efficiencies of FA-SLICS-2 and SLICS-2 are similar for FR negative $HepG_2$ cells (Figure 5.15). The above results demonstrate that the cellular uptake of FA-SLICS/pDNA polyplexes is mainly via potocytosis, a folate receptor-mediated endocytosis.

The free folic acid competes with FA-SLICS in binding to the receptors on the cell membrane, resulting in reduction of the amount of FA-SLICS/pDNA internalized into cells leading to a decrease in transfection efficiency. To evaluate the effect of serum to cell transfection of the developed FA-SLICS polymers, $HepG_2$ cells were transfected with FA-SLICS-2 (chosen as a model gene carrier) under different conditions (with and without serum). The experiment results show that the presence of serum in cell culture medium has no significant effect to transfection efficiencies (42.9% vs. 42.1%) (Figure 5.16), indicating that the FA-SLICS can be potentially used as a gene carrier *in vivo*. Therefore, FA-SLICS is an efficient ligand equipped gene carrier for FR^+ tumor cells and could be potentially used for targeted cancer gene therapies.

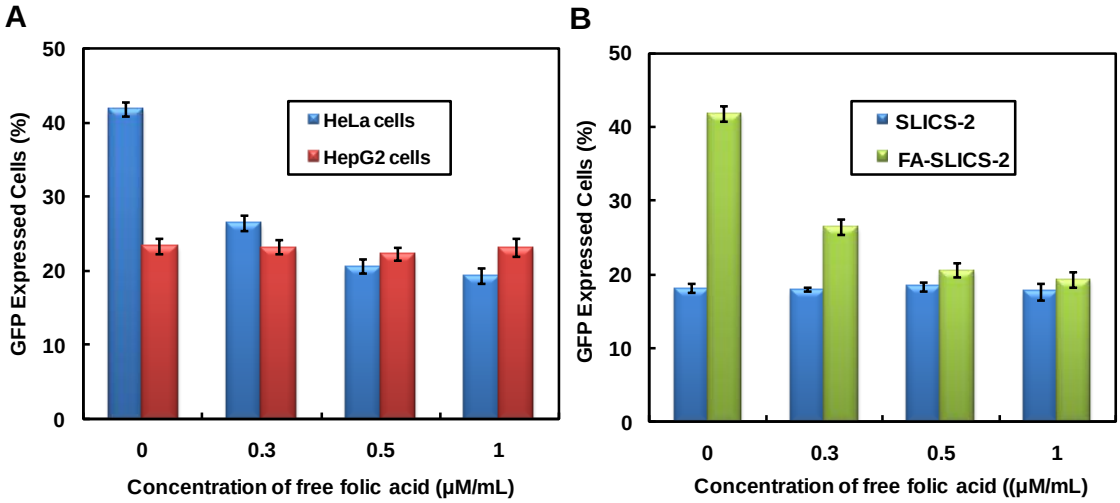

Figure 5.15 Folic acid competition study. A: Cell transfection efficiency at different folic acid concentration using FA-SLICS-2 at N/P of 10 against HeLa and $HepG_2$ cells. B: Cell transfection efficiency at different folic acid concentration using FA-SLICS-2 and SLICS at N/P of 10 against HeLa cells.

5.4 Conclusion

In this study, we successfully developed a novel intracellular microenvironment responsive targeted delivery system for cancer gene therapy, folic acid functionalized Schiff-base linked imidazole-chitosan (FA-SLICS). FA-SLICS is efficient in gene delivery, due to its strong

nucleic acid binding capability for cargo loading and endosome pH sensitive nucleic acid delivery mechanism for controllable cargo release. Furthermore, FA-SLICS has low toxicity to cells resulting from the excellent biocompatibility of chitosan, imidazolyl and folic acid. Most importantly, FA-SLICS is a promising targeted gene carrier for FR positive tumor gene therapy since the folic acid on its backbone can trigger FR-mediated cellular uptake pathway. Therefore, FA-SLICS is potentially an efficient and safe gene vector which can be used in FR positive tumour targeted gene therapy.

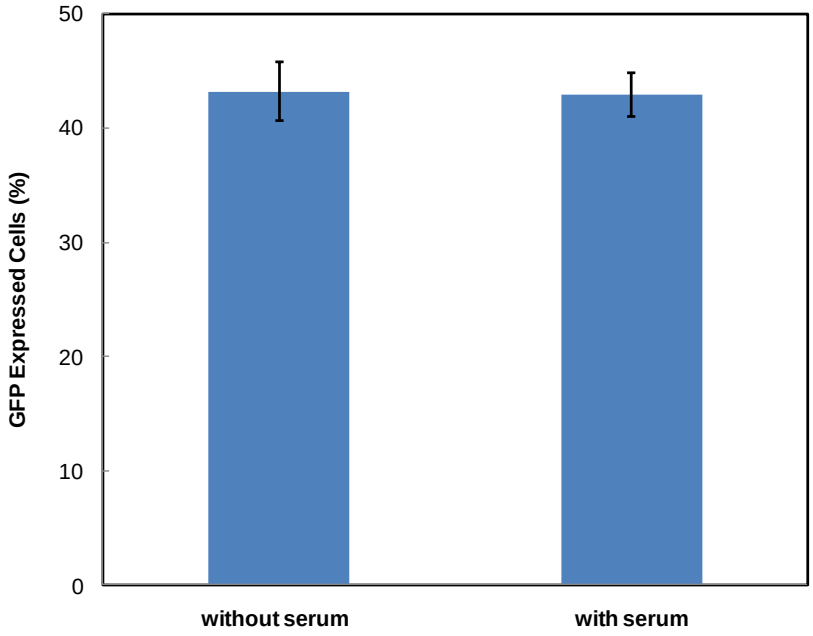

Figure 5.16 Comparison of cell transfection efficiency of FA-SLICS-2 with HeLa cells under different conditions (with and without serum).

Reference

1 Benson, J. D.; Chen, Y. N. P.; Cornell-Kennon, S. A.; Dorsch, M.; Kim, S.;Leszczyniecka, M.; Sellers, W. R.; Lengauer, C. Validating Cancer Drug Targets. Nature **2006**, *441*, 451-456.

2 Katherine A. H. Gene therapy: The moving finger. Nature **2005**, *435*, 477-479.

3 Dang, J. M.; Leong, K. W.; Natural Polymers for Gene Delivery and Tissue Engineering. Adv. Drug Delivery Rev. **2006**, *58*, 487-499.

4 Pack, D. W.; Hoffman, A. S.; Pun, S.; Stayton, P. S. Design and Development of Polymers for Gene Delivery. Nat. Rev. Drug Disco. **2005**, *4*, 581-593.

5 Kim, T. H.; Ihm, J. E.; Choi, Y. J.; Nah, J. W.; Cho, C. S. Efficient Gene Delivery by Urocanic Acid-modified Chitosan. J. Controll. Release **2003**, *93*, 389-402.

6 Cordes, E. H.; Jencks, W. P. The Mechanism of Hydrolysis of Schiff bases Derived from Aliphatic Amines. J. Am. Chem. Soc. **1963**, *18*, 2843-2848.

7 Jin, Y.; Song, L.; Su, Y.; Zhu, L.; Pang, Y.; Qiu, F.; Tong, G.; Yan, D.; Zhu, B.; Zhu, X. Oxime Linkage: A Robust Tool for the Design of pH-Sensitive Polymeric Drug Carriers. Biomacromolecules **2011**, *12*, 3460-3468.

8 Tang, Q.; Cao, B.; Wu, H.; Cheng, G. Selective Gene Delivery to Cancer Cells Using an Integrated Cationic Amphiphilic Peptide. Langmuir **2012**, *28*, 16126–16132.

9 Kamaly, N.; Xiao, Z.; Valencia, P. M.; Radovic-Morenob, A. F.; Farokhzad, O. C. Targeted Polymeric Therapeutic Nanoparticles: Design, Development and Clinical Translation. Chem. Soc. Rev. **2012**, *41*, 2971–3010.

10 Sudimack, J.; Lee, R. J., Targeted Drug Delivery via the Folate Receptor. Adv. Drug Delivery Rev. **2000**, *41*, 147-162.

11 Shen, Z.Y.; Shi, B.Y.; Zhang, H.; Bi, J.X.; Dai, S. Exploring Low-positively Charged Thermo sensitive Copolymers as Gene Delivery Vectors. Soft Matter, **2012**, *8*, 1385-1392.

12 Ingratta, M.; Hollinger J.; Duhamel, J. A Case for Using Randomly Labeled Polymers to Study Long-Range Polymer Chain Dynamics by Fluorescence. J. Am. Chem. Soc. **2008**, *130*, 9420–9428.

13 Mao, H. Q.; Roy, K.; Troung-Le, V. L.; Janes, K. A.; Lin, K. Y.; Wang, Y., August, J. T.; Leong, K. W. Chitosan-DNA Nanoparticles as Gene Carriers: Synthesis, Characterization and Transfection Efficiency. J. Controll. Release **2001**, *70*, 399-421.

14 Heyes, D. M. System Size Dependence of the Transport Coefficients and Stokes–Einstein Relationship of Hard Sphere and Weeks–Chandler–Andersen Fluids. J. Phys-Condens Matt. **2007**, *19*, 376106-376114.

15 Adamczyk, Z.; Zaucha, M.; Zembala, M. Zeta Potential of Mica Covered by Colloid Particles: A Streaming Potential Study. Langmuir, **2010**, *26*, 9368–9377.

16 Ho, Y. C.; Liao, Z. X.; Panda, N.; Tang, D. W.; Yu, S. H.; Mi, F. L.; Sung, H. W. Self-organized Nanoparticles Prepared by Guanidine- and Disulfide -modified Chitosan as a Gene Delivery Carrier. J. Mater. Chem. **2011**, *21*, 16918–16927.

17 Zhao, X.; Yin, L.; Ding, J.; Tang, C.; Gu, S.; Yin, C.; Mao, Y. Thiolated Trimethyl Chitosan Nanocomplexes as Gene Carriers with High *in Vitro* and *in Vivo* Transfection Efficiency. J. Controlled Release **2010**, *144*, 46-54.

18 Cai, X.; Zhang, J.; Ouyang, Y.; Ma, D.; Tan, S.; Peng, Y. Bacteria-Adsorbed Palygorskite Stabilizes the Quaternary Phosphonium Salt with Specific-Targeting Capability, Long-Term Antibacterial Activity, and Lower Cytotoxicity. Langmuir **2013**, *29*, 5279–5285.

19 Bi, J. X.; Wirth, M.; Beer, C.; Kim, E. J.; Gu, M. B.; Zeng, A. P. Dynamic Characterization of Recombinant Chinese Hamster Ovary Cells Containing an Inducible *c-fos* Promoter GFP Expression System as a Biomarker. J. Biotechnol. **2002**, *93*, 231-242.

20 Brugnerotto, J.; Lizardi, J.; Goycoolea, F. M.; Arguelles-Monal, W.; Desbrieres, J.; Rinaudo, M. An infrared investigation in relation with chitin and chitosan characterization.

Polymer **2001**, *42*, 3569-3580.

21 Guinesi, L. S.; Cavalheiro, E. T. G. Influence of Some Reactional Parameters on the Substitution Degree of Biopolymeric Schiff bases Prepared from Chitosan and Salicylaldehyde. Carbohyd. Polym. **2006**, *65*, 557-561.

22 Nanbu, N.; Sasaki, Y.; Kitamura, F. In Situ FT-IR Spectroscopic Observation of a Room Temperature Molten Salt Gold Electrode Interphase. Electrochem. Commun. **2003**, *5*, 383-387.

23 Mohapatra, S.; Mallick, S. K.; Maiti, T. K.; Ghosh, S. K.; Pramanik, P. Synthesis of Highly Stable Folic Acid Conjugated Magnetite Nanoparticles for Targeting Cancer Cells. Nanotechnology **2007**, *18*, 385102-385111.

24 Franceschi, S.; Bordeau, O.; Millerioux, C.; Perez, E.; Vicendo, P.; Rico-Lattes, I.; Moisand, A. Highly Compacted DNA-polymer Complexes Obtained via New Polynorbornene Polycationic Latexes with Lactobionate Counterion. Langmuir **2002**, *18*, 1743–1747.

25 Chim, Y. T. A.; Lam, J. K. W.; Ma, Y.; Armes, S. P.; Lewis, A. L.; Roberts, C. J.; Stolnik, S.; Tendler, S. J. B.; Davies, M. C. Structural Study of DNA Condensation Induced by Novel Phosphorylcholine-Based Copolymers for Gene Delivery and Relevance to DNA Protection. Langmuir **2005**, *21*, 3591–3598.

26 Adler, A. F.; Leong, K. W. Emerging Links between Surface Nanotechnology and Endocytosis: Impact on Nonviral Gene Delivery. Nano Today **2010**, *5*, 553-569.

27 Walba, H.**;** Isensee, **R.** W. Spectrophotometric Study of the Hydrolysis Constants of the Negative Ions of Some Aryl Imidazoles. J. Am. Chem. Soc. **1955**, *77*, 5488-5492.

28 Castro, E. A.; Salas, M.; Santos, J. G. Concerted Mechanism of the Reactions of Secondary Alicyclic Amines with O-ethyl S-(2, 4, 6-trinitrophenyl) Thiocarbonate. J. Org. Chem. **1994**, *59*, 30–32.

29 Hess, G. T.; Humphries IV, W. H.; Fay, N. C.; Payne, C. K. Cellular Binding, Motion, and Internalization of Synthetic Gene Delivery Polymers. BBA – Molecul. Cell Res. **2007**, *1773*, 1583-1588.

30 Yamano, S.; Dai, J. S.; Moursi, A. M. Comparison of Transfection Efficiency of Nonviral Gene Transfer Reagents. Molecul. Biotechnol. **2010**, *46*, 287-300.

31 Grant, B. D.; Donaldson, J. G. Pathways and Mechanisms of Endocytic Recycling. Nat Rev Mol Cell Biol. **2009**, *10*, 597-608.

32 Akinic, A.; Thomas, M.; Klibanov, A. M.; Langer, R. Exploring Polyethylenimine-mediated DNA Transfection and the Proton Sponge Hypothesis. J Gene Med. **2005**, *7*, 657-663.

33 Trachootham, D.; Alexandre, J.; Huang, P. Targeting Cancer Cells by ROS-mediated Mechanisms: a Radical Therapeutic Approach? Nat. Rev. Drug Discov. **2009**, *8*, 579-591.

Chapter 6 Intracellular Microenvironment Responsive Polymer: A Multiple-stage Transport Platform for High-performance Gene Delivery

Bingyang Shi, Hu Zhang, Sheng Dai, Xin Du, Jingxiu Bi*, Shizhang Qiao*

School of Chemical Engineering, The University of Adelaide, Adelaide, SA 5005, Australia

Submitted to *Small*, August 2013

STATEMENT OF AUTHORSHIP

Intracellular Microenvironment Responsive Polymer: A Multiple-stage Transport Platform for High-performance Gene Delivery

By signing the Statement of Authorship, each author certifies that their stated contribution to the publication is accurate and that permission is granted for the publication to be included in the candidate's thesis.

Submitted, August 2013

Bingyang Shi (Candidate)

Designed, carried out the experiments and wrote the manuscript.

I hereby certify that the statement of contribution is accurate.

*Signed..... .....Date..*15/08/2013*.....*

Hu Zhang

Assisted in writing the manuscript.

I hereby certify that the statement of contribution is accurate.

*Signed.....Date..*15/08/2013*.....*

Sheng Dai

Supervised development of work and assisted in writing the manuscript.

I hereby certify that the statement of contribution is accurate.

*Signed.....Date....*15/08/2013*.....*

Jingxiu Bi

Supervised development of work and assisted in writing the manuscript.

I hereby certify that the statement of contribution is accurate and I give permission for inclusion of the paper in the thesis.

Signed.....Date.....15/08/2013
.....

Shizhang Qiao

Supervised development of work and assisted in writing the manuscript.

I hereby certify that the statement of contribution is accurate and I give permission for inclusion of the paper in the thesis.

Signed.....Date.....15/08/2013
.....

Shi, B., Zhang, H., Dai, S., Du, X., Bi, J. & Qiao, S. (2013) Intracellular microenvironment responsive polymer: a multiple-stage transport platform for high-performance gene delivery.
Small, v. 10(5), pp. 871-877

Chapter 7 Conclusions and future directions

Gene therapy has become a promising treatment for genetic diseases due to the development of the genetics and biomolecules. However, the future gene therapy is seriously limited by the lack of development of excellent gene carriers. Advanced delivery systems continue to grow in sophistication, leading to enhanced specificity and applicability for nucleic acid delivery. The drawback of this progress is that the ability to broadly apply these new materials to different fields, either in gene delivery or other areas like short interfering RNA (siRNA) and drug delivery, diminishes with each level of enhanced specificity. Nucleic acids are not only restricted to pDNA. For example, small duplex RNA sequences have gained prominence as a new form of nucleic acid therapeutic. These small duplex RNA, orsiRNA , can inhibit protein synthesis within a cell through the RNA-interference pathway. It is not clear whether the design criteria traditionally used to generate new DNA-delivery reagents will translate to the design of materials for different nucleic acid classifications, and clever new generations of materials and constructs have begun to be developed for such purposes. From a technology standpoint, the combinatorial approach described for the development of nanoscale materials span only a small fraction of the potential parameter space that could be created from the large number of available building blocks. It is apparent that the high-throughput, combinatorial synthesis work reported to date falls short of fully understanding the structure–function relationships that governs DNA delivery. The future of the field will bring to bear new synthetic and robotic methods to increase the total number of structures that can be investigated. In addition, the incorporation of statistical and predictive computational methods at the library design phase could help lessen the synthetic burden by helping investigators choose the library components in a more rational and thorough fashion.

In this phD project, a serial of functional polymers, named chitosan supported imidazole

Schiff-base (CISB), N-imidazolyl-O-carboxymethyl chitosan (IOCMCS), folic acid factionalized Schiff-base linked imidazole chitosan (FA-SLICS), have been designed and successfully developed as gene carriers based on the modification of chitosan. Additionally, a new strategy for promoting endoplasmic gene delivery and nucleus uptake has been proposed by developing pH-sensitive Schiff-base linked imidazole biodegradable polymers. This delivery system can efficiently load nucleic acids at a neutral pH, release imidazole-gene complexes from the polymer backbones at intracellular endosmal pH, transport nucleic acids into nucleus through multiple-stage intracellular gene delivery, and thus leads to a high cell transfection efficiency. These smart polymers display good biocompatibility, multiple-functions, and efficient gene delivery efficiency as gene carriers. Hence they have promising potential applications in future gene delivery and enhance the development of gene therapy.

The rapid development of advanced nucleic acid delivery and the investigation of intracellular gene transport mechanism *in vitro* have constructed an excellent base for gene therapy. In addition, the exploring of knowledge in elucidating the molecular basis of genetic decieases, as well as the availability of the complete sequence information of the human genome render gene therapy to be potentially powerful tool for the treatment of human diseases. However, most of well defined gene delivery systems are needed to be furthrer examined *in vivo* and the mechanisms of gene delivery at animal level are still unclear, which seriously limits the clinical application of the developed gene delivery systems. Thus, the resulting gene delivery systems in this PhD project should be further evaluated at animal level and applied in clinical gene therapy in the future. In addition, the intracellular multiple-stage gene delivery mechanism suggested in this PhD project is also need to be further evaluated with other cells, especially primary cells to better guide the design and advanced gene delivery system.

List of publications published during PhD candidate

1. Shi, B.Y, Zhang, S.X, Wang, Y.H, Zhuang, Y.P, Chu, J. Shi, X.L, Bi, J.X. and Guo, M.J. Expansion of mouse sertoli cells on microcarriers. Cell Prolif. 2010, 43, 275-286.(IF, 2.7)
2. Shi, B.Y, Deng, L, Shi, X.L, Dai, S, Zhang, H, Wang, Y.H, Bi, J.X, and Guo, M.J, The enhancement of neural stem cell survival and growth by co-culturing with expanded sertoli cells in vitro. Biotechnol Prog. 2011, 28, 196-205.(IF, 2.4)
3. Deng, L, Shi, B.Y.*, Zhuang, Y.P, Shi, X.L, and Guo, M.J*, Performance and mechanism of neuroleukin in the growth and survival of embryonic neural stem cells in a co-culture system. Cell Transplant, 2012, **DOI**: 10.3727/096368913X663578 **(*Co-corresponding author**) (IF, 6.2)
4. Shi, B.Y, Zhang, H, Shen, Z.Y, Bi, J.X. and Dai, S. Developing a chitosan supported imidazole Schiff-base for high efficient gene delivery. Polym. Chem. 2013, 4, 840-850. (IF, 5.3)
5. Shen, Z.Y, Zhang, H, Shi, B.Y, Bi, J.X. and Dai, S. Exploring thermal reversible hydrogels for stem cell expansion in three-dimension. Soft Matter, 2012, 8, 7250-7257. (IF, 4.5)
6. Shen, Z.Y, Shi, B.Y, Zhang, H, Bi, J.X. and Dai, S. Exploring low-positively charged thermo sensitive copolymers as gene delivery vectors. Soft Matter, 2012, 8, 1385-1392. (IF, 4.5)

7. Shi, B.Y, Shen, Z.Y, Zhang, H, Bi, J.X. and Dai, S. Exploring N-Imidazolyl-O-Carboxym -ethyl chitosan for high performance gene delivery. Biomacromolecules, 2012, 13, 146-153. (IF, 5.5)
8. Du, X†., Shi, B.Y†., .Liang, J, Bi, J.X., Dai, S. and Qiao, S.Z. Developing functionalized dendrimer-like silica nanoparticles with hierarchical pores as advanced delivery nanocarriers. Adv. Mater., 2013, 25, 5981-5985. (**Co-first author**) (Highlighted by ***China Materials Reviews***).(IF, 14.8)
9. Shi, B.Y. , Zhang, H., Dai, S., Du, X., Bi, J.X. and Qiao S.Z. Intracellular microenvironment responsive polymer: A multiple-stage transport platform for high-performance gene delivery. Small, 2013, DOI:10.1002/smll.201302430.
10. Shi, B.Y., Zhang, M., Bi, J.X., Dai, S. Development of a novel folic acid chitosan supported imidazole Schiff base for tumor targeted gene delivery system and drug therapy. Journal of Controlled Release, 2013, DOI: 10.1016/j.jconrel.2013.08.244.

List of publications included in this thesis

Shi, B.Y Shen, Z.Y, Zhang, H, Bi, J.X. and Dai, S. Exploring N-Imidazolyl-O- Carboxym - ethyl chitosan for high performance gene delivery. *Biomacromolecules*, 2012, **13**, 146-153.

Shi, B.Y, Zhang, H, Shen, Z.Y, Bi, J.X. and Dai, S. Developing a chitosan supported imidazole Schiff-base for high efficient gene delivery. *Polym. Chem*. 2013, **4**, 840-850.

Shi, B., Shen, Z., Zhang, H. Bi, J. & Dai, S. (2012) Exploring N-Imidazolyl-O-Carboxymethyl Chitosan for high performance gene delivery.
Biomacromolecules, v. 13(1), pp. 146-153

Polymer Chemistry

RSC Publishing

PAPER

View Article Online
View Journal | View Issue

Developing a chitosan supported imidazole Schiff-base for high-efficiency gene delivery†

Cite this: *Polym. Chem.*, 2013, **4**, 840

Bingyang Shi, Hu Zhang, Zheyu Shen, Jingxiu Bi* and Sheng Dai*

A chitosan supported imidazole Schiff-base (CISB) has been developed to be used as the vector for high performance gene delivery. Introducing the imidazole Schiff-base to the branch of chitosan could improve its water solubility and gene binding ability under physiological conditions, and thus significantly enhance gene delivery capability due to the formation of Schiff-bases (azomethines) and the substitution of imidazole functional groups along chitosan backbones. Gel electrophoresis and light scattering results show that the CISB could effectively bind plasmid DNA (pDNA) and protect pDNA from DNase I digestion in solution. The CISB does not induce remarkable cytotoxicity against HEK 293 cells and can enhance delivery of pDNA into cytoplasm and nucleus efficiently. A transfection efficiency of 70% can be reached after systematically optimizing cell transfection conditions. Therefore, the CISB is a promising gene delivery vector due to its high solubility in physiological pH, strong gene binding and protection capability, low cytotoxicity, good biodegradability, and high efficiency in gene delivery and cell transfection.

Received 6th July 2012
Accepted 9th October 2012

DOI: 10.1039/c2py20494k

www.rsc.org/polymers

Introduction

Gene therapy can be defined as the treatment of human diseases by delivering therapeutic genes into patients' abnormal cells or tissues, and it has been intensively investigated over the last 15 years.[1] Gene delivery systems mainly employ viral and non-viral vectors. Viral vectors, such as adenoviruses and retroviruses, have been widely used due to their higher transfection efficiency than non-viral vectors.[2,3] However, viral vectors are not ideal candidates due to their various limitations, such as, random insertion into host genome, toxic immunological and inflammatory reactions.[4] The non-viral vector gene delivery system has attracted great attention because of the potential for limited immunogenicity, the ability to accommodate and deliver large-size genetic materials, and the capability of its chemical structure modification.[5] The most attractive non-viral vectors are cationic lipids and cationic polymers, which are safer and more amenable to large-scale production. In comparison, the application of cationic lipids is limited due to their toxicity and relatively low transfection efficiency.[6] On the other hand, cationic polymer carriers are widely accepted because of their higher ability to complex DNA and interact with cells. Additionally, the polyplex formation between cationic polymers and DNA molecules is able to effectively prevent DNA from nuclease degradation.[7] To date, a variety of cationic polymers, such as poly(2-dimethylaminoethyl methacrylate) (PDMAEMA),[8] gelatin,[9] polybrene,[10] tetraminofullerene[11] and poly(L-lysine) (PLL),[12] have been broadly studied for gene delivery purposes. The high charge density gives rise to an increase not only in gene transfection efficiency, but also in the cytotoxicity. Moreover, the non-biodegradability of synthetic cationic polymers might result in polymer accumulation in cells or body after repeated administrations.

Schiff-base is a compound with a functional group that contains a carbon–nitrogen double bond with the nitrogen atom connected to an aromatic or alkyl group, but not hydrogen. Schiff-bases are widely investigated as one of the imine type compounds because of their structural variety and specific molecular properties. Compounds containing Schiff-base functional groups have been involved in many biochemical processes, drug development and functional biomaterials.[13,14] The pK_a of a Schiff-base (–N=C–) is between 10.6 and 16.0 at 25 °C, and it can be fully protonated at physiological pH.[15] In addition, it has been reported that Schiff-base can enhance gene-binding ability due to its imine characteristic.[16,17] Since one polymer contains many repeat units, the polymer supported Schiff-bases should be a good candidate as the gene carrier in gene delivery. However, to our knowledge, almost no relevant study has been reported.

Chitosan is an important biomaterial due to its biocompatibility, biodegradability, low cytotoxicity, and high cationic charge

School of Chemical Engineering, The University of Adelaide, Adelaide, SA 5005, Australia. E-mail: s.dai@adelaide.edu.au; jingxiu.bi@adelaide.edu.au; Fax: +61 8 8313 4373; Tel: +61 8 8313 1015

† Electronic supplementary information (ESI) available: Calibration curve of the imidazole groups at a wavelength of 257 nm, UV absorption of the synthesized CISB polymers, FT-IR spectrum, ^{1}H-NMR of CISB-2 in D_2O, SEM image of the CISB-2/pDNA polyplexes, the buffer capacity of various polymers, and gene transfection efficiency measured by using a flow cytometer are provided. See DOI: 10.1039/c2py20494k

density.[18] The poor water solubility at moderate pH and low gene transfection efficiency of chitosan make it not suitable to be used as a non-viral gene delivery carrier. However, chitosan involves both hydroxyl and amino functional groups along its backbone, which allows further chemical modification to tailor the physicochemical properties of chitosan so as to satisfy various end-used applications.[19] In gene delivery applications, proton-sponge ability is crucial for exploring off-the-shelf materials as the gene carriers. It would be desirable for efficient gene carriers to mimic the proton-sponge mechanism, which requires the buffering capacity between the physiological and lysosomal pH range. Imidazole exhibits the required proton-sponge property and is the functional moiety of many biomolecules (such as histidine).[20] Therefore, the conjugation of imidazole to the branch of chitosan should increase its gene transfection efficiency without sacrificing the biocompatibility and biodegradability. In the literature, the gene delivery vector based on the imidazolyl modified chitosan has been developed recently,[21] where the *N*-imidazolyl-chitosan molecules are synthesized by coupling the amino groups of chitosan and urocanic acid *via* the EDC (*N*-(3-dimethylaminopropyl)-*N*-ethylcarbodiimide) chemistry. The synthesized *N*-imidazolyl-chitosan has been used for small interfering RNA (si-RNA) delivery for the potential treatment of lung diseases[22] and targeted gene delivery in the nervous system.[23] For those *N*-imidazolyl-chitosans, the imidazolyl groups are linked to the chitosan backbone by the formation of amide bonds. However, the amide linkage might be easily digested by enzymes *in vivo*.[24,25] In addition, the solubility of *N*-imidazolyl-chitosan is poor in the physiological pH.[21,23]

Based on previous studies, we hypothesize that the Schiff-base linked imidazole and chitosans might have obvious advantages (such as high solubility in neutral pH, satisfying gene binding and protection ability, and good gene delivery capability), and should be a more efficient gene delivery vector. Here, we synthesized various chitosan-supported imidazole Schiff-bases (CISBs) and systematically examined their gene binding and protection capability, nucleic acid delivery ability and cell transfection efficiency. It was found that the CISB is a potentially safe and efficient vector in gene therapy.

Results and discussion

Synthesis and characterization of chitosan supported imidazole Schiff-bases (CISBs)

In this study, the imidazole rings are introduced to the 2-*N* position of chitosan *via* the reaction of the amino group of chitosan and the aldehyde group of 4-imidazolecarboxaldehyde at room temperature, where Schiff-base functional groups are formed (Scheme 1). Both Schiff-bases and imidazole rings can be protonated in aqueous medium and give the ternary and secondary amines.[25] The presence of Schiff-bases and imidazole rings along chitosan backbones makes the resulting CISB polymers possess higher solubility in a wide pH range (6–10) and stronger gene binding capability than the unmodified chitosan at a neutral pH.

Different amounts of 4-imidazolecarboxaldehyde were reacted with chitosan at room temperature with the feed molar ratios of 4-imidazolecarboxaldehyde to the amino groups of chitosan ranging from 1 : 5 to 2 : 1 (Table 1). The degrees of imidazole Schiff-base substitution on chitosan were determined by UV-vis measurements based on the imidazolyl absorption at 257 nm (water, pH 7) (Fig. S1, ESI†). According to the Lambert–Beer's law, the imidazole Schiff-base substitutions are found to be 3.4%, 55.0% and 79.2% for the above synthesized CISB polymers: CISB-1, CISB-2, and CISB-3 (Fig. S2, ESI†).

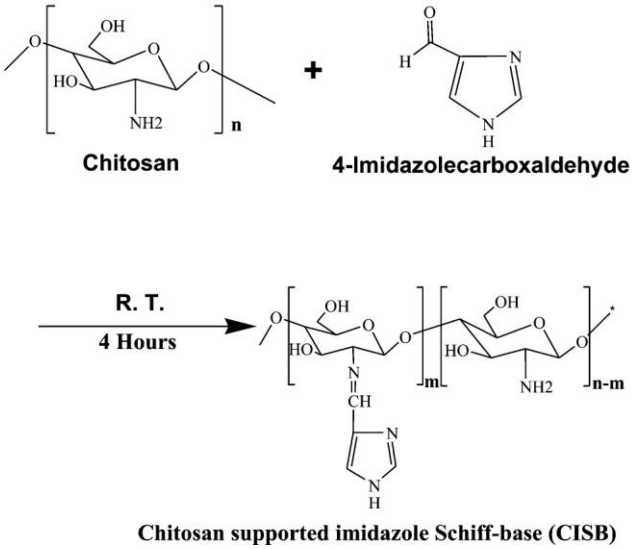

Scheme 1 Scheme for the synthesis of chitosan supported imidazole Schiff-bases (CISBs).

The conjugation of imidazole rings to chitosan *via* the Schiff-base functional group is further confirmed by the FTIR. For chitosan, the characteristic peaks at 1598 cm^{-1} (N–H bending) and 1080 cm^{-1} (C–O– stretching) are evident.[26] The weak peak at 1655 cm^{-1} is attributed to the stretching of C=O associated with the non-fully deacetyl residuals. For the CISB samples, a strong absorption band at 1634 cm^{-1} is presented, which is attributed to the vibration of the –C=N– in the Schiff-base.[27,28] Such a characteristic peak cannot be observed in the IR spectra of chitosan as a control. The peaks at 1577 cm^{-1} and 1405 cm^{-1} can be assigned to the in-plane C–C and C–N, and N–H stretching vibrations of the imidazole ring (Fig. S3, ESI†).[29] Additionally, the ^{1}H-NMR was used to further elucidate the chemical structure of the CISB. From the ^{1}H-NMR analysis, the chemical shifts of the H atoms of chitosan are located within the δ range of 2.00 to 4.80 ppm. The chemical shifts of the H atoms of the imidazole ring are located within the δ range of 7.60–8.20 ppm. The successful conjugation of the imidazolyl to chitosan is evident from the chemical shift δ at 9.72 ppm (–*H*C=N–) (Fig. S4, ESI†).[30,31]

Table 1 Synthesis and characterization of the CISB polymers

Nomenclature	Reaction ratio[a]	Imidazolyl substitution (%)
CISB-1	1 : 5	3.35
CISB-2	1 : 1	55.06
CISB-3	2 : 1	79.20

[a] The feed molar ratio of 4-imidazolecarboxaldehyde to the amine group of chitosan.

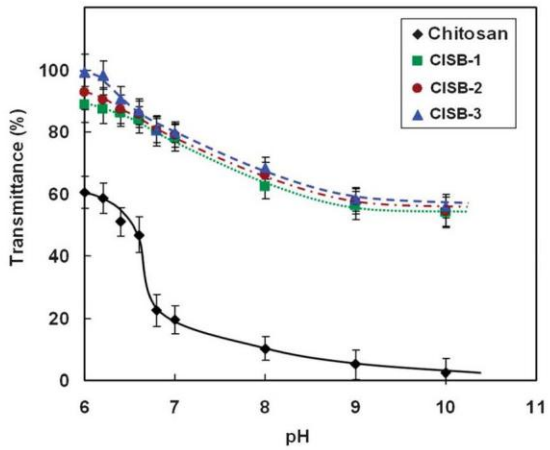

Fig. 1 Comparison of the solubility of chitosan and various CISB polymers at different pHs as measured by light transmittance study at a fixed wavelength of 600 nm and at 25 °C.

The solubility of the CISB in aqueous media was examined by light transmittance as shown in Fig. 1. Chitosan is soluble in water at pH lower than 6, beyond that, it becomes water-insoluble, where the transmittance in the pH range of 6 to 10 is less than 20%. However, the CISB samples are soluble in a broader pH range. The transmittance of the CISB polymers slightly decreases in the pH range of 6 to 9, and keeps constant beyond that with an average transmittance of more than 60%. Obviously, the solubility of the CISB samples is much higher than that of chitosan. On the other hand, it is noticed that the trends of transmittance *vs.* pH are not much different for those three CISB samples although they have different degrees of imidazole Schiff-base substitutions which indicates that both the formed Schiff-bases and the substituted imidazole rings are able to alter the solubility of chitosan. The substitution degree of these two functional groups in CISB-1 (3.4%) is enough to destroy the intermolecular H-bond and improve the solubility of chitosan. The increase of the solubility may be ascribed to different pK_a values of various ammonium functional groups. The pK_a value of the imidazole ring is 14.2 and the pK_a of the Schiff-base is between 10.6 and 16.0 at 25 °C,[22] compared with the pK_a of 6.2 for the amino group of chitosan.[32,33] The higher pK_a indicates the presence of more protonated positive charges in solution, and thus enhances the solubility of the CISB in a broad pH range. In addition, the substitution of the imidazole Schiff-base along the chitosan backbone can effectively eliminate the chitosan–chitosan interaction, which results in the increase in solubility. Due to the increase of water solubility under biological and physiological conditions, the applications of the CISB in gene delivery can be improved, such as the resulting polymers make it possible to prepare the polymer and pDNA polyplexes at neutral pH. However, when the *N*-imidazolyl-chitosan is used as a gene carrier, such polyplexes can only be prepared around pH 5 due to its relatively poor water solubility at a neutral pH.[21,22] The structure of the polyplexes prepared at pH 5 might be different when they are used under physiological conditions.

Nucleic acid binding and DNase I digestion assays

The gene binding capabilities of various CISB samples were examined by gel retardation assays using a naked plasmid DNA as a control. Fig. 2A shows the electrophoretic mobility of pDNA in the presence of different amounts of various CISB polymers. The experimental results show that the electrophoretic mobility of pDNA is retarded by increasing the dose of CISB polymers, especially at a mixing weight ratio of polymer to pDNA above 3. (The weight ratio of 1 equals to the N/P molar ratios of 2.02, 1.61 and 1.48 for CISB-1, CISB-2 and CISB-3, respectively.) By comparing with the electrophoretic mobility of reference pDNA shown in Fig. 2A, the retention of pDNA at the top of the gel in the presence of CISB polymers suggests that all pDNA have been complexed with CISB polymers in the mixing weight ratio range of 3 to 80. On the other hand, the pDNA gel retardation for those three CISB polymers is different when the mixing weight ratios are smaller than 3. For CISB-1 with a low degree (3.4%) of imidazole substitution, free plasmid DNA can be observed within the weight ratios of 0.5 to 1 (equal to the N/P of 1.0 to 2.0). Beyond that, free pDNA bands are not visible. Kim and Ghosn have examined *N*-imidazolyl-chitosan for gene delivery,

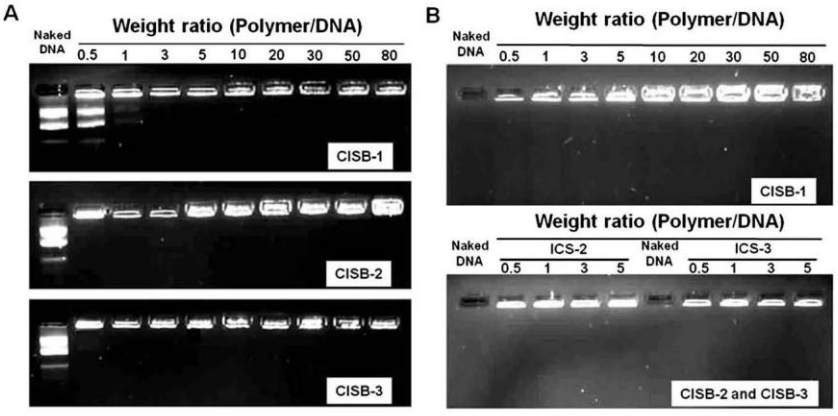

Fig. 2 Nucleic acid binding and protection ability assays of the CISB polymers by agarose gel electrophoresis using 0.8% agarose in Tris–acetate running buffer. (A) Nucleic acid binding ability assays; (B) nucleic acid protection capability assays against DNase I.

where the imidazole rings were conjugated to the chitosan using an amide linkage *via* the EDC chemistry.[21,23] The gene binding ability of CISB-1 is similar to that of *N*-imidazolyl-chitosan with a higher degree of imidazolyl substitution (27.7%). Obviously, the protonated Schiff-base moieties in the CISB can enhance gene binding/loading capability.[21] For the CISB samples (CISB-2 and CISB-3) with higher degrees (55.06% and 79.20%) of imidazole substitution, free pDNA bands cannot be observed even at a weight ratio of 0.5. Therefore, the polymer/pDNA polyplexes formation strongly depends on the extent of imidazole Schiff-base substitution along chitosan backbones.

Preliminary studies have demonstrated a low binding capability of chitosan to genes due to its low solubility and the weak intermolecular interaction between the primary amino groups of chitosan and the phosphates of DNA.[34] However, the biocompatibility and biodegradability of chitosan are attractive in biological applications. To improve the performance of chitosan in gene delivery, various chemical modifications have been developed. Lu *et al.* synthesized various oligoamine polymers based on chitosan, with which free DNA could be fully retarded at a weight ratio of 4.5.[35] Chae *et al.* synthesized the deoxycholic acid-conjugated chitosan oligosaccharide, which was able to bind free DNA (0.2 μg) and form their stable polyplexes at a weight ratio of 1.0.[36] From our study, the gene binding ability of the CISB polymers with higher degree of imidazole Schiff-base substitution (CISB-2 and CISB-3) is stronger than that of *N*-imidazolyl-chitosan, deoxycholic acid-conjugated chitosan oligosaccharide and oligoamine chitosan. It is similar to that of linear PEI (25 kDa), which can eliminate free DNA beyond an N/P molar ratio of 3.[37] For the CISBs, it can be explained that both the formed Schiff-bases and the substituted imidazole rings have stronger binding affinity with pDNA after protonation. The more the amino groups along chitosan backbones are substituted by the imidazole Schiff-bases, the stronger the polymer/pDNA polyplexes are formed in a solution dominated by electrostatic attraction. Additionally, the presence of Schiff-bases in CISB polymers is crucial to not only enhance gene-binding ability, but also to increase water solubility. Therefore, the imidazole Schiff-base chitosan has obvious advantages as a potential gene delivery vector over chitosan.

The representative effect of the CISB polymers on protecting plasmid DNA from DNase degradation was examined using DNase I as a model enzyme. The experimental results are shown in Fig. 2B. When 0.2 μg naked pDNA is incubated with excessive DNase I (200 U mL^{-1}) at 37 °C, naked pDNA are completely degraded within 30 min as evident from a significant drop in DNA gel intensity. Under the same digestion conditions, only approximately half of the pDNA is degraded for the CISB-1/pDNA polyplex at a mixing weight ratio (polymer to DNA) of 0.5, whereas no DNA digestion can be observed at the weight ratios of 5 to 80. The degree of pDNA degradation decreases at the mixing weight ratio range of 0.5 to 5. The formation of CISB/pDNA polyplexes can effectively protect DNA from DNase I digestion. The polyplexes formed at higher mixing weight ratios have a higher DNA protection ability against DNase I since more pDNAs have been bound to CISB polymers. In addition, plasmid DNA can be fully protected from DNase I digestion using CISB-2 or CISB-3 at weight ratios higher than 0.5. It means that CISB-2 or CISB-3 has a stronger pDNA protection capability than CISB-1 due to their higher gene binding capability. As such, all CISB samples are able to protect pDNA from digestion under physiological conditions where the nuclease concentration is much lower than our experimental DNase concentration.[38]

Particle sizes and zeta potentials of CISB/pDNA polyplexes

The polyplexes were prepared by mixing plasmid DNA with various CISB samples at different mixing weight ratios (from 0.5 to 100) at pH 7. The sizes of the CISB/pDNA polyplexes were measured by dynamic light scattering (DLS), and the cumulant approach was used to analyze the intensity–intensity autocorrelation functions of scattered light. As shown in Fig. 3A, for all CISB samples, the apparent *z*-averaged particle size of the

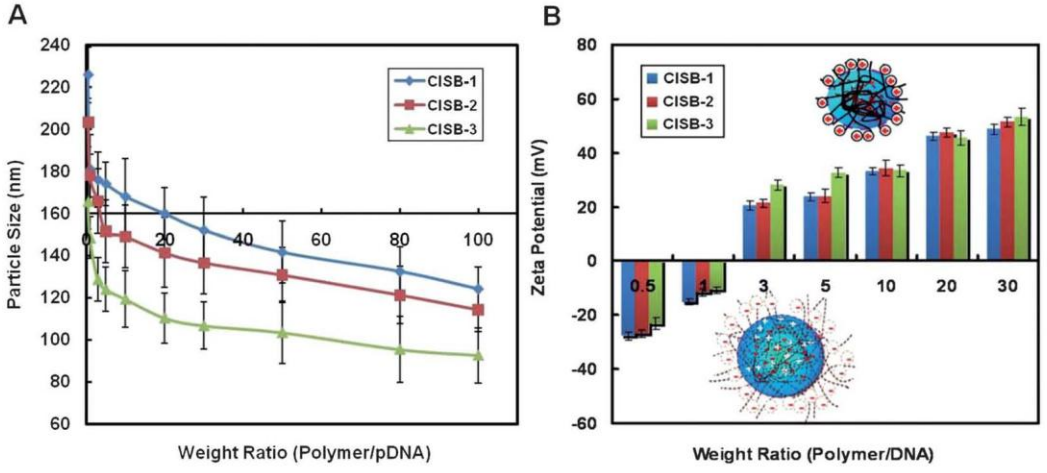

Fig. 3 Particle sizes and zeta-potentials of the CISB/pDNA polyplexes prepared at different mixing ratios of CISB to pDNA in 0.9 wt% NaCl solution at pH 7.2, 25 °C. (A) Particle sizes of the CISB/pDNA polyplexes; (B) zeta-potentials of the CISB/pDNA polyplexes. For all measurements, the DNA concentration was fixed at 5 μg mL^{-1}. The insets in (B) are the possible representative microstructures of the polyplexes at low and high mixing ratios.

polyplexes decreases nearly to half with the increment of the mixing weight ratios of CISB and pDNA from 0.5 to 100. The range of the polyplexes diameter is between 100 and 200 nm when the weight ratio is above 1, which is further confirmed by SEM analysis (Fig. S5, ESI†). On the other hand, the apparent *z*-averaged polyplex size reduces with an increase in the degree of imidazole Schiff-base substitution, which indicates that more compact polyplexes are formed in solution due to the presence of stronger polymer and pDNA electrostatic attraction. After protonation, both the formed Schiff-base and the substituted imidazole rings can interact with negatively charged pDNAs. The enhanced intermolecular binding interaction results in a decrease in the size of the polyplexes.

The zeta-potential is relevant to the overall net charges of the CISB/pDNA polyplexes and it is one of the major factors influencing polyplex biodistribution and transfection efficiency in gene delivery.[39] Fig. 3B compares the zeta-potentials of the polyplexes at different mixing weight ratios. Due to the presence of phosphate ions, the plasmid DNA is negatively charged. After protonation, the CISB is positively charged. Electrostatic interaction dominates the formation of CISB/pDNA polyplexes in solution. At a lower mixing ratio of CISB to pDNA, the polyplexes are negatively charged since the positive charges of the CISB are not enough to balance all negative charges of pDNA. With an increase in the CISB concentration, the zeta-potentials of the polyplexes tend to be less negative at the mixing weight ratio of 1. With further increase in CISB concentrations, the zeta-potential turns into positive and keeps stable at the mixing weight ratios beyond 20. The change of the zeta-potentials with the CISB concentration is attributed to the electrostatic attraction between CISB and pDNA in various CISB/pDNA polyplexes. Moreover, the zeta-potentials are also influenced by the degree of imidazole Schiff-base substitution in the CISB. At a fixed mixing ratio, with the increment of substitution degree, more negative charges along pDNA backbones can be neutralized as evident from their higher zeta-potential values.

The zeta-potentials of the polyplexes increase with an increase in the mixing ratios of CISB to pDNA and the degrees of imidazole Schiff-base substitution. This is due to the formation of different structured polyplexes. At a small mixing ratio or degree of substitution, the amounts of the CISB positive charges are not enough to neutralize all negative charges of pDNA resulting in a core–shell structure of the polymer/DNA polyplexes where the complexed polymer/pDNA core is surrounded by a corona layer composed of negatively charged plasmid DNA residuals which can be digested by DNase. With an increase in the mixing ratio of polymer to plasmid DNA or the degree of substitution, the zeta-potential of the polyplexes turns into positive. The positive zeta-potential indicates that the CISB positive charges are excessive for pDNA binding interaction and the formation of CISB/pDNA polyplexes with a core–shell structure whose corona layer is made up of the residual positive charges from the excessive CISB, which leads to the gel retardation and DNase resistance. In addition, the formation of core–shell structures significantly enhances the stability of the polyplexes and avoids agglomeration. At the same time, slightly positive charges on the polyplex surface are helpful for gene delivery since relatively low positive charges can facilitate

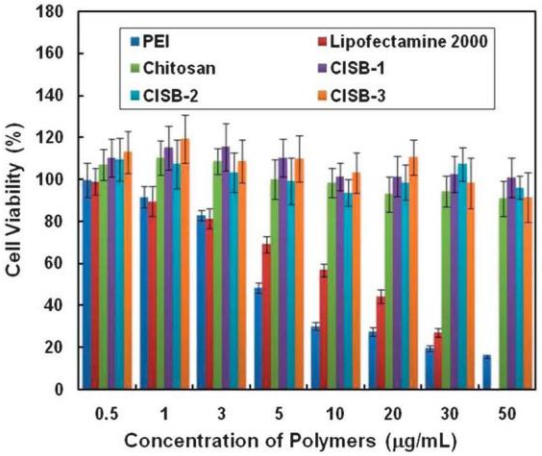

Fig. 4 Comparison of the cytotoxicity of L-PEI, lipofectamine 2000, chitosan and various CISB polymers against HEK 293 cells. The absorbance was read at 570 nm using a microplate reader ($n = 3$).

an easy entry into cells *via* the endocytosis but cause negligible or minor damage to cells.[40] Therefore, the synthesized CISB can be expected to have great potential applications for gene transfection.

Cell cytotoxicity

Cell toxicity of the CISB polymers has to be examined before exploring their biomedical applications. Fig. 4 compares the cytotoxicities of chitosan, CISB, linear PEI (L-PEI, 25 kDa) and lipofectamine 2000 against HEK 293 cells at a broad concentration range typically used in transfection experiments by MTT assays. A negligible effect of chitosan and different CISB polymers on cell viability can be observed with an average cell viability of over 90% at polymer concentrations ranging from 1 to 50 μg mL^{-1}. For comparison purpose, the cytotoxicities of L-PEI and lipofectamine 2000 were included. From Fig. 4, 30–50% of cells remain viable with an increase of L-PEI concentration from 5 to 20 μg mL^{-1}, and beyond an L-PEI concentration of 30 μg mL^{-1}, the cell viability is reduced to below 20%. Lipofectamine 2000 at a concentration of 10 μg mL^{-1} decreases the cell viability below 60%. The cell cytotoxicities of both chitosan and CISBs are lower than those of commercial gene delivery vectors. The low cell toxicity of the chitosan derivatives mainly results from the biocompatible characteristics of chitosan. Since the imidazole ring is an important biological building-block for many biomolecules (such as histidine),[20] the introduction of imidazole Schiff-base functional groups does not bring significant cytotoxicity to the CISBs.

Cellular uptake of polymer/DNA polyplexes

To analyze the cellular uptake of nucleic acid delivered using functional polymers as gene vectors, pDNA was used as a model gene, which was labeled with YOYO-1 with green fluorescence. In order to show the location of DNA, the cell membrane and nucleus were labeled with Alexa Fluor 594 (red fluorescence) and Hoechst 33258 (blue fluorescence), respectively. The labeled DNA

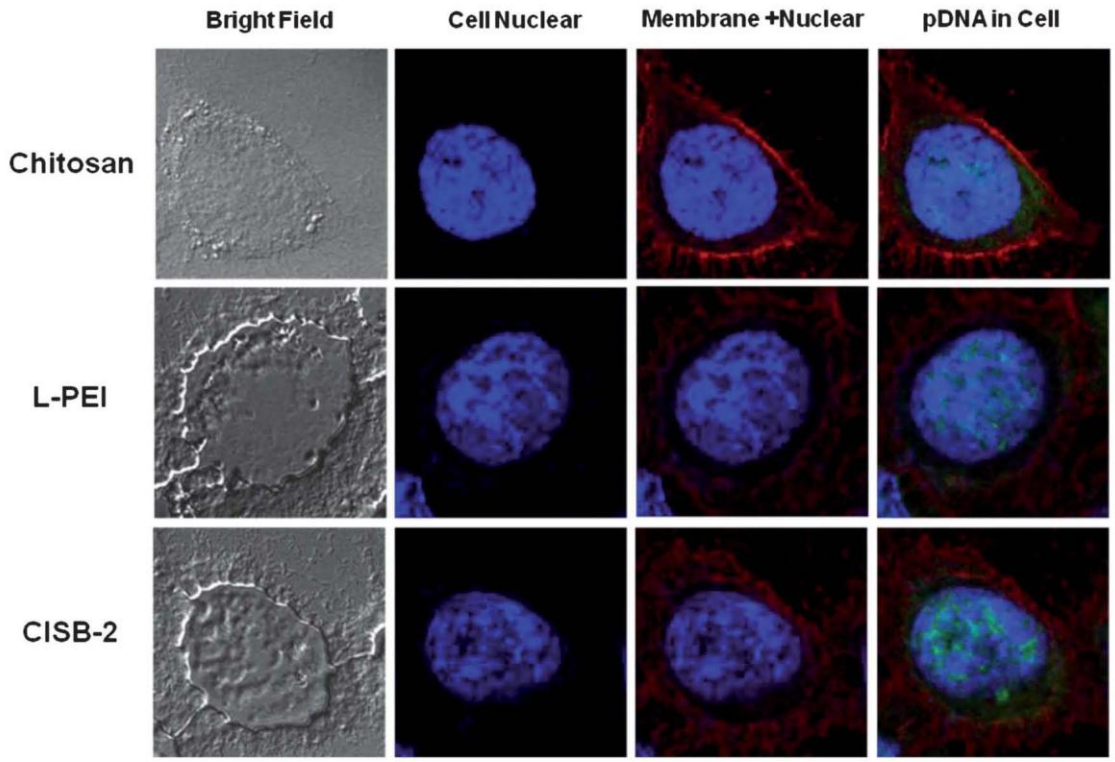

Fig. 5 Cellular uptake of YOYO-1-labeled pDNA in HEK 293 with the aid of gene vectors: chitosan, L-PEI and CISB-2. Cells were incubated with polymer/pDNA polyplexes for 3 h in a 6-well plate at the DNA concentration of 4 μg per well. Cells were visualized using a confocal 1P/FCS inverted microscope after cell membrane and nucleus were stained with 100 μL of Alexa Fluor 594 (5.0 μg mL^{-1}) and Hoechst 33258 (2 μM).

was delivered by CISB-2 into HEK 293 cells at the mixing weight ratio of 10 (N/P = 14.8) and analyzed with a confocal microscope at 3 h post-transfection using chitosan and L-PEI as positive controls. From Fig. 5, the green fluorescence of labeled plasmid DNA could be found in both cytoplasm and nucleus after 3 h delivery with CISB-2 and L-PEI, which indicates that the CISB can deliver gene not only to cytoplasm but also to cell nucleus. However, the fluorescence intensity of labeled pDNA in cell nucleus delivered by L-PEI is slightly lower than that of CISB-2, which might demonstrate that the gene delivery capability of CISB is a little higher than that of L-PEI. The images of pDNA intracellular distribution agree with the transfection efficiencies of both gene carriers which are shown in Fig. 6A. However, much weaker green fluorescence of labeled pDNA can be found in cells after 3 h delivery with chitosan comparing with that delivered by CISB-2. Therefore, the gene delivery ability of chitosan has been improved significantly by introducing the imidazole Schiff-base onto the backbone of chitosan.

Cell transfection of CISB *in vitro*

To successfully transfect cells, the pDNA must overcome a series of biological barriers. It should pass the surface membrane at first, and then go through the endocytic pathway before entering into the nucleus of the target cells, so as to get translated into functional proteins. pDNA can only be translated after overcoming all these barriers with the aid (nucleic acid protection and release) of gene delivery vectors, which are reflected in the transfection efficiency. The optimization of a non-viral gene carrier involves the adjustment on the mixing ratios of polymer vectors and pDNA aiming to balance the competing effects on cellular binding and uptake, DNA protection and release, and size and stability of vector/DNA polyplexes, which decide the final transfection efficiency.[41] In the following study, the DNA delivery efficiencies were evaluated and optimized by transferring plasmid DNA into mammalian cells *in vitro*.

Transfection experiments were carried out using HEK 293 as the host cell line. The CISB/pDNA (pEGFP-N1) polyplexes at different mixing weight ratios of 0.5 to 20 (keeping pDNA constant at 1 μg) were prepared and added to each well in a 24-well plate with RPMI1640 culture medium without fetal bovine serum (FBS). The cell transfection efficiencies of CISB polymers were assessed by flow cytometry at 72 h after transfection. The positive controls are chitosan, linear PEI and lipofectamine 2000, and the negative control is naked pDNA. The transfection efficiency is determined by the actual percentage of cells expressing green fluorescent protein compared to the mock transfection.

As shown in Fig. 6A, the transfection efficiency is dependent on the degree of substitution and the mixing ratio of polymer to pDNA. The cell transfection efficiency of the CISB-1/pDNA polyplexes increases slowly with the increment of the mixing weight ratio of CISB-1 to plasmid DNA (0.5 to 20). The highest achievable transfection efficiency is 27% at a mixing weight ratio of 20. The cell transfection efficiency of the CISB-3/pDNA polyplexes is around 19%, nearly identical at the mixing weight

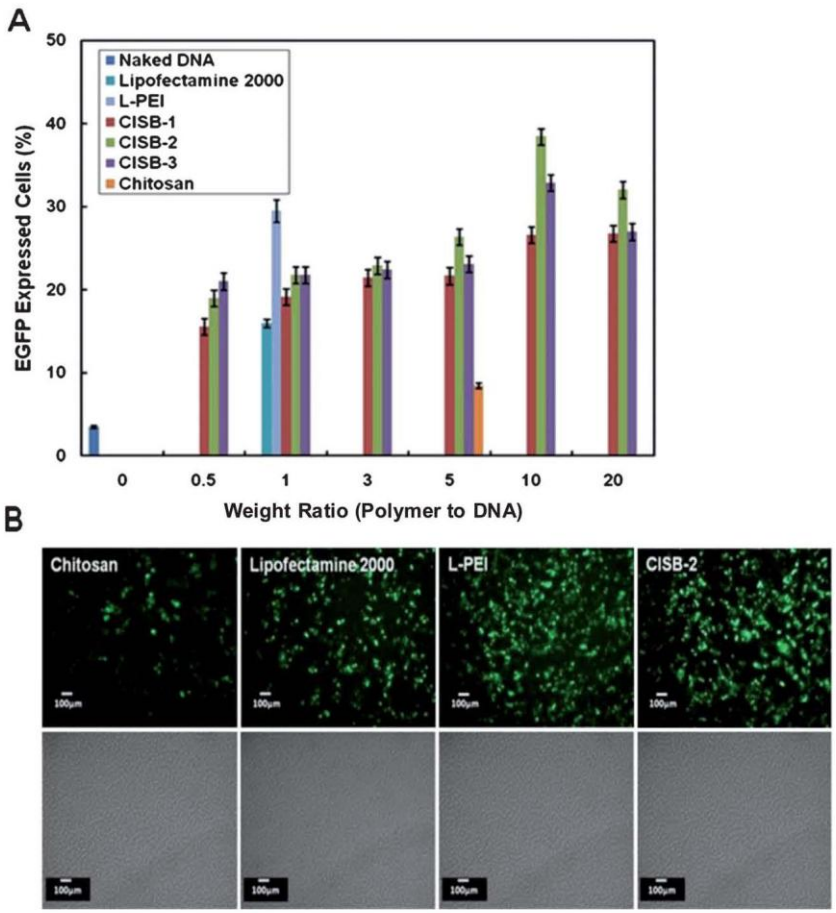

Fig. 6 (A) Transfection efficiencies of CISB/pDNA polyplexes determined by flow cytometry against HEK 293 cells at various mixing ratios with positive (L-PEI and lipofectamine 2000) and negative (naked pDNA) controls. (B) Fluorescent micrographs and light inverted micrograph of HEK 239 cells transfected with chitosan, lipofectamine 2000, L-PEI and CISB-2 at the weight ratio of polymer to DNA: 5.0, 1.0, 1.0 and 10.0. Transfection was performed at a plasmid DNA dose of 1 μg per well in 24-well plates, and all transfection efficiencies were determined at 72 h post-transfection. Data are shown as mean ± SE ($n = 3$).

ratio range from 0.5 to 5.0, but transfection efficiency sharply increases to 33% as the weight ratio changes from 5.0 to 10. For the CISB-2 vector, a transfection efficiency of 19% is obtained at a mixing weight ratio of 0.5, similar to that of CISB-3 at the mixing ratios of 1.0 to 3.0. The highest transfection efficiency of 39% is obtained at a mixing ratio of 10. The general trend for CISB vectors is that the transfection efficiency increases with the increment of the mixing ratio (CISB to pDNA) from 0.5 to 10 for all CISB polymers because the increase in the amount of positive charges in CISB facilitates the CISB/pDNA polyplex formation, which makes pDNA more stable and also enhances the binding to the negatively charged proteoglycans on the cell surface. As such, the improvement on the uptake of pDNA leads to an increase in gene transfection efficiency. On the other hand, the transfection efficiency decreases for CISB-2 and CISB-3 at high mixing weight ratios (10 and 20), but the decrease is not evident for CISB-1 due to its lower degree of imidazole Schiff-base substitution (Fig. 6A). An ideal gene vector should balance the abilities between protecting DNA from degradation and releasing DNA near or within the nucleus of the target cell. Since the polyplexes are formed based on electrostatic interaction, the final structure and properties of the CISB/pDNA polyplexes can be tailored by varying the amount of charge groups of gene carriers. High amounts of charged group can effectively prevent pDNA from degradation due to the formation of compact polyplex structure, but they can also inhibit pDNA release in nucleus.[42] A higher mixing ratio of CISB-2 or CISB-3 to plasmid DNA results in formation of tighter CISB/pDNA polyplexes, and thus decreases gene transfection efficiency. The similar inhibiting results have been observed while using L-PEI as a gene carrier.[43,44]

Fig. 6 compares the fluorescence images of the transfected HEK 293 cells using different gene delivery carriers (chitosan, Lipofectamine 2000, L-PEI-25K and CISB-2). In the positive controls of chitosan, lipofectamine 2000 and L-PEI, the cell transfection efficiencies of 9%, 16% and 30% are obtained (Fig. S6, ESI†), and the similar efficiency was also reported by Mao *et al.* using lipofectamine 2000 complexes to transfect HEK 293 cells.[38] The transfection efficiency is lower than that of CISB-2 at a weight ratio of 10 (39%) as confirmed by the fluorescence image analysis. Almost no naked DNA can be taken into cells and expressed in cells without the help and protection of gene carriers due to their negative charges and digestion of DNases.[42] The transfection efficiency of polymer/pDNA polyplexes

depends on the mixing ratios of polyplexes, which reach the balance of making polymer/pDNA polyplexes escape from the endo-/lysosomal compartment and pDNA release from polymer/pDNA polyplexes. It has been reported that high transfection efficiency of PEI is attributed to its ability of destabilizing the endosome and its high proton sponge effect.[44,45] CISB contains primary, secondary and tertiary amines, which results in a broad buffering range (Fig. S7, ESI†). Therefore, the CISB polymers have a similar proton sponge effect as PEI and thus can improve the polyplex release to cytoplasm after endocytosis.[46]

The concentration of pDNA at the cell surface has been suggested to be an important factor in non-viral gene delivery.[47] In order to optimize the concentration of plasmid DNA at the HEK 293 cell surface in the presence of a CISB deliver vector, CISB-2 is chosen as a model polymer. Different amounts of pDNA from 0.1 to 5.0 μg were mixed with CISB-2 at a fixed weight ratio of 10 (polymer to pDNA) and added to the wells of a 24-well culture plate with 1 mL culture medium. The transfection efficiency is determined at 72 h post-transfection. As shown in Fig. 7A, the transfection efficiency is measured up to 70% from 2.5% as the pDNA increases from 0.1 to 2.0 μg per well in the 24-well plate, which is also confirmed from the fluorescence images of the transfected cells (Fig. 7B). With further increase in the dose of pDNA from 2.0 to 5.0 μg per well in the 24-well plate, the increment in the transfection efficiency is minor (Fig. S8, ESI†). The results suggest that 2 μg mL^{-1} may be close to the maximum amount of pDNA complexed with CISB-2 which can be taken in by endocytosis and expressed in HEK 293 cells. Similar results have also been reported from other investigators. Ishii *et al.*[48] reported the optimal pDNA amount in SOJ cells transfection using a chitosan carrier is 2 μg mL^{-1} and Lavertu *et al.* obtained the optimal pDNA dose of 2.5 μg mL^{-1} in HEK 293 cell transfection using chitosan vectors.[49] Gene transfection is dominated by both forward and reverse transfection. For the forward transfection, the delivery of polyplexes to the cell surface is a diffusion-limited process, whereas the reverse transfection can pre-load polyplexes at high levels onto the cell–substrate interface through electrostatic or hydrophobic interaction. The optimal dose of pDNA at the cell surface for cell transfection may be between 2 and 2.5 μg mL^{-1} which depends on the types of cell and vector.[50]

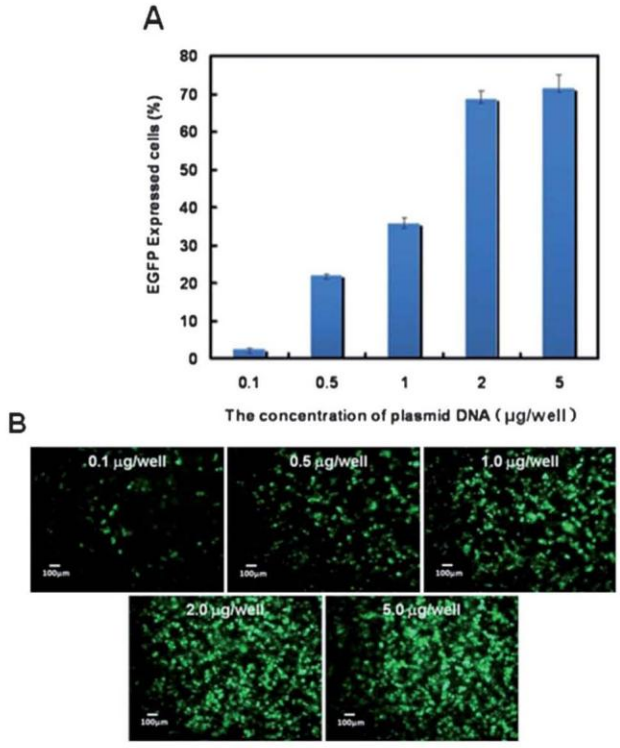

Fig. 7 (A) Transfection efficiencies of CISB-2/pDNA polyplexes determined by flow cytometry in HEK 293 cells with different pDNA concentrations at the fixed mixing weight ratio of 10 (polymer to plasmid DNA). (B) Fluorescence micrographs of the HEK 239 cells transfected with CISB-2/pDNA polyplexes at the fixed polymer to pDNA weight ratio of 10 and varying pDNA concentrations from 0.1 to 5.0 μg pDNA per well in a 24-well plate. All the transfection efficiencies were determined at 72 h post-transfection. Data are shown as mean ± SE ($n = 3$).

Recently, various gene delivery vectors have been developed and achieved gene transfection efficiency is from 36% to 59%. Trimethyl chitosan–cysteine conjugate (TMC–Cys) has been evaluated as a non-viral gene carrier with HEK 293 cells, which displayed the highest transfection efficiency of 36%.[51] Comb-shaped copolymers composed of nonionic hydrophilic dextran and cationic PDMAEMA (poly(2-dimethylaminoethyl methacrylate)) side chains were used for non-viral gene delivery, and a transfection efficiency of 37% was acquired for HEK 293 cells.[52] Cationic polymers composed of chitosan backbones and PDMAEMA side chains resulted in a transfection efficiency of 52% for HEK 293 cells.[53] The ternary copolymer composed by grafting linear PEI onto the block copolymer of poly(L-lysine) and poly(ethylene glycol) gave a transfection efficiency of 59% for HEK 293 cells.[54] In this study, a transfection efficiency of 70% can be reached for the HEK 293 cells using CISB-2 as the gene carrier, which is higher than that of *N*-imidazolyl-chitosan.[22]

Conclusions

In this paper, functional biocompatible polymer supported imidazole Schiff-bases have been developed for gene delivery applications. Due to the introduction of Schiff-base and imidazole functional groups to chitosan backbones, water solubility, gene binding and protection capacity, cell uptake and gene delivery capability are significantly improved. The enhancement in water solubility and pDNA binding capability is ascribed to the presence of more nitrogen atoms with different protonation capabilities (Schiff-base and imidazole functional groups). The resulting polymers retain the basic characteristics of chitosan (non-cytotoxic and biodegradable). CISB-2 shows higher transfection efficiency and low cytotoxicity against HEK293 cells than commercial transfection carriers such as linear PEI and lipofectamine 2000. The transfection efficiency can reach up to 70% after systematical optimization. The results demonstrate that the CISB polymers have great potential in gene therapy.

Experimental

Materials

Chitosan (molecular weight ~200 kDa, degree of acetylation: 90%) was purchased from Acros (New Jersey, USA). The

plasmid DNA pEGFP-N1 (4.7 kb) encoding green fluorescent protein gene with a cytomegalovirus (CMV) promoter was kindly supplied by Dr Julian Adams (Flinders University, Australia). QIAGEN Maxi kit was obtained from Qiagen (Boncaster, Australia). Fetal bovine serum (FBS), trypsin–EDTA, penicillin–streptomycin (PS) mixture, RPMI 1640 cell culture medium, phosphate buffered saline (PBS), TAE (Tris–acetate), agarose and Lipofectamin™ 2000 reagent were purchased from Gibco-BRL (Grand Island, USA). Dimeric cyanine nucleic acid stains, live plasma membrane and nuclear labeling kit were purchased from Molecular Probes (Grand Island, USA). Sucrose, gel red, 3-(4,5-dimethylthiazol-2-yl)-2,5-diphenyltetrazolium bromide (MTT), kanamycin, 4-imidazolecarboxaldehyde (ICD) and other chemicals or solvents were purchased from Sigma-Aldrich.

Plasmid DNA preparation

The pEGFP-N1 plasmid was prepared in *E. coli* DH5 α strain and extracted using the QIAGEN Maxi kit. The integrity and purity of the prepared plasmid DNA (pDNA) were analyzed using 0.8% agarose gel electrophoresis, and the DNA concentration is determined by using a Jasco UV-vis spectrophotometer (Japan) at the fixed wavelength of 260 and 280 nm.[55] Plasmid DNA was fluorescently labeled with the intercalating nucleic acid stain YOYO-1 with a molar ratio of 1 dye molecule per 100 base pairs for 60 min at RT in the dark for cellular uptake study.

Synthesis of chitosan supported imidazole Schiff-base (CISB)

Chitosan (0.5 g, 2 mmol glucosamine repeat unit) was dissolved in 15 mL deionized water, adjusted to pH 4 using 0.1 M HCl and incubated at 65 °C overnight. In a typical experiment for the CISB-1 synthesis, 4-imidazolecarboxaldehyde (0.0192 g or 0.2 mmol) was dissolved in 15 mL deionized water, and charged dropwise to the chitosan solution over a 20 min period. The reaction mixture was stirred at room temperature for 4 h and then condensed using a rotary evaporator. The concentrated polymer solution was precipitated in excess amount of anhydrous acetone. The products were filtered, rinsed thrice with anhydrous acetone, and vacuum-dried at room temperature. Different CISB samples were prepared by charging various amounts of 4-imidazolecarboxaldehyde. The resulting polymers are noted as CISB-1 (feed ratio of 4-imidazolecarboxaldehyde to amine ~1 : 5), CISB-2 (1 : 1) and CISB-3 (2 : 1). The obtained CISB samples were subjected to FTIR and ^{1}H-NMR analysis.

Imidazole Schiff-base substitution

A UV-visible spectrophotometer (UV-1601, SHIMADZU) was used to determine the percentage of imidazole Schiff-base along chitosan backbone. The imidazolyl moiety has a maximal absorption at the wavelength of 257 nm. The standard absorption calibration curve was set up, and the percentages of the imidazole Schiff-base substitution in the above-synthesized CISB polymers were determined using the UV absorbance at 257 nm through the Beer–Lambert's law.[56] The UV path length was 1 cm.

FTIR and ^{1}H-NMR

The IR spectra of chitosan and the CISB samples were examined using a Thermo NICOLET6700 Fourier Transform Infrared Spectrometer (FTIR) at room temperature. The ^{1}H-NMR experiments were recorded using a 600 MHz Bruker NMR in D_2O.

Polymer solubility

The solubility of chitosan and its derivatives were evaluated at different pH, where 1 mg mL^{-1} chitosan or CISB sample was first dissolved in 0.2 wt% acetic acid aqueous solution. The pH of various polymer solutions was adjusted by the addition of NaOH solution. The transmittances of the polymer solutions were monitored as functions of pH using a UV-vis spectrophotometer equipped with a 1 cm quartz cell at a fixed wavelength of 600 nm.[57]

Nucleic acid binding assay

The binding interaction of pDNA to CISB was examined using agarose gel electrophoresis. The polyplexes contain CISB and 0.2 μg plasmid DNA at various mixing weight ratios (W/W of CISB to plasmid DNA). The weight ratio of 1 for CISB-1/pDNA, CISB-2/pDNA and CISB-3/pDNA corresponds to their N/P molar ratios of 2.02, 1.61, and 1.48. The polymer/pDNA polyplexes were prepared at pH 7.2, incubated at room temperature for 20 min before loading onto the 0.8 wt% agarose gel in a Tris–acetate (TAE) running buffer and electrophoresed at 80 V for 60 min. The resulting pDNA migration patterns were read under UV irradiation (G-BOX, SYNGENE).

Resistance of CISB/pDNA polyplexes against DNase I degradation

CISB/pDNA polyplexes were separately incubated with DNase I (4 units, 200 U mL^{-1}) in DNase/Mg^{2+} digestion buffer (50 mM, Tris–Cl, pH 7.6, and 10 mM $MgCl_2$) at 37 °C for 30 min using the free pDNA (0.2 μg) as the negative control. The degradation of pDNA was investigated by 0.8 wt% agarose gel in a Tris–acetate (TAE) running buffer and electrophoresed at 80 V for 60 min. The resulting pDNA migration patterns were read under UV irradiation.

Particle sizes and zeta-potentials of the CISB/pDNA polyplexes

The particle sizes and zeta potentials of the polyplexes prepared by mixing CISB and pDNA at different weight ratios and pH 7.2 was measured using a Malvern Zetasizer (Malvern Inst. Ltd. UK) equipped with either a four-side clear cuvette for particle size analysis or ZET 5104 cell[58] for zeta-potential measurement at 25 °C. The concentration of plasmid pDNA was kept at 5 μg mL^{-1}. For particle size analysis, a cumulant method was used to convert intensity–intensity autocorrelation functions to apparent particle sizes *via* the Stokes–Einstein relationship.[58] For electrokinetics, Smoluchowski model was used to convert electrophoresis mobility to zeta-potential.[59] 10 parallel runs were carried out for each measurement and the final data were obtained based on statistical analysis.

Evaluation of cytotoxicity

HEK 293 cells, kindly supplied by Dr Michael Brown at the Hanson Institute, Adelaide Royal Hospital, were cultured in RPMI 1640 medium supplied with 10% FBS in 96-well plates (200 μL medium per well) at a cell density of 1.0×10^5 cells per mL. After inoculation, the cells were allowed to adhere overnight at 37 °C in a humidified 5% CO_2-containing atmosphere. The growth medium was replaced with 200 μL fresh medium containing CISB polymers at final concentrations of 0.5, 1, 3, 5, 10, 20, 30 and 50 μg mL^{-1} using L-PEI (25K), lipofectamine 2000 and chitosan as positive controls (due to the low solubility of chitosan at neutral pH, 1 mg mL^{-1} chitosan stock solution was prepared at pH 6 and then mixed with RPMI 1640 cell culture medium at different volume ratios). Cells were then incubated for 24 h before 10 μL of MTT (5.0 mg mL^{-1} in PBS) was added to each well. After further incubation for additional 4.0 h at 37 °C, the growth medium was removed and 150 μL of dimethyl sulfoxide (DMSO) was charged to each well to ensure complete solubilization of the formed formazan crystals. Finally, the absorbance was determined using the Biotek Microplate Reader (Biotek, USA) at a wavelength of 570 nm.[60]

Assessment of cellular uptake by confocal laser scanning microscopy

The ability of vectors to transport pDNA into the cytoplasm and nucleus in HEK 293 cells was evaluated using a confocal laser scanning microscope. The HEK 293 cells were seeded at a concentration of 2×10^5 cells per well into 6-well plates loaded with cover-glass slides of 25 mm diameter and cultured for 24 h. 4 μg YOYO-1-labeled pDNA was loaded on the polymers (chitosan, L-PEI and CISB) at different weight ratios of 5.0, 1.0 and 10.0 to form polymer/pDNA polyplex. HEK 293 cells were incubated with the polymer/pDNA polyplexes for 3 h and then fixed with 4% formaldehyde. The polyplexes were removed and the cells were washed with PBS three times after transfection. The cell membrane and nucleus were stained with 100 μL of Alexa Fluor 594 (5.0 μg mL^{-1}) and Hoechst 33258 (2 μM) for 10 min at room temperature, the cells were further washed with PBS for three times and incubated with 200 μL PBS. The fluorescence images were observed with a confocal laser scanning microscope (Leica Confocal 1P/FCS) equipped with a 405 nm diode laser for Hoechst 33258, a 488 nm argon ion laser for YOYO-1 and a 561 diode laser for Alexa Fluor 594. High-magnification images were obtained with a 100× objective. Optical sections were averaged 4 times to reduce noise. Images were processed using Leica Confocal software.

Cell culture and gene transfection

HEK 293 cells were incubated in RPMI 1640 supplemented with 10% fetal bovine serum (FBS), streptomycin at 100 μg mL^{-1}, and penicillin at 100 U mL^{-1}. The cells seeded in 24-well plates were incubated at 37 °C in a humidified incubator in the presence of 5% CO_2. After 24 h culturing, the medium was replaced with 200 μL of culture medium in the absence of FBS. In the meantime, polymer/pDNA polyplexes, prepared by incubating the CISB polymers and plasmid DNA at various weight ratios at room temperature for 30 min, were added to each well. After 6 h incubation, the medium was replaced by 1 mL fresh complete culture medium with 10% FBS and the cells were further incubated for another 66 h.

GFP expression analysis by fluorescence microscopy and flow cytometry

For the fluorescence microscopic analysis of GFP (green fluorescent proteins) expression, living cells were rinsed in 1× PBS and visualized by *in situ* detection with an epi-fluorescence microscope (Multi-photon Microscope, Nikon) connected to a CCD camera (RS Photometrics). A band pass filter (BP 485/20) for excitation and a 520 nm long pass filter were used as a barrier filter in viewing emission. Digitalized photographs were stored and analyzed by using the Bio-Rad Radiance 2000MP Visualising System. On the other hand, the green fluorescence intensity was detected directly by a FACSCalibur flow cytometry (Becton Dickinson), and the transfection efficiency was calculated by percentage of positive cells using non-transfection cell as the negative control. Briefly, cells were harvested by the digestion of trypsin after post-transfection culture. 1×10^6 cells were washed with 2% FCS/PBS buffer, and centrifuged at 1000 rpm for 5 min. The cells were stained by 400 μL 0.5 μg mL^{-1} propidium iodide in 1× PBS. Approximately 1–2 $\times 10^4$ cells were analyzed at the rate of 200–600 cells per second. Cell Quest 3.3 software was used for data analysis.[55]

Statistical analysis

Data obtained from our experiments are represented as mean ± SE (standard error). Statistical analysis of the numerical variables was performed using a two-sample, two-tailed *t*-test. A value of $p < 0.05$ is considered to be significant.

Acknowledgements

We thank the financial support from the Australian Research Council (DP110102877). BS appreciates the support from the China Scholarship Council (CSC). We also thank Dr Michael Brown at the Royal Adelaide Hospital for providing HEK 293 cells.

Notes and references

1 R. Mulligan, *Science*, 1993, **260**, 926–932.
2 P. Blomberg and C. I. E. Smith, *Expert Opin. Biol. Ther.*, 2003, **3**, 941–949.
3 G. Y. Wu and C. H. Wu, *J. Biol. Chem.*, 1988, **263**, 14621–14624.
4 A. Mhashilkar, S. Chada, J. A. Roth and R. Ramesh, *Biotechnol. Adv.*, 2001, **19**, 279–297.
5 J. B. Zhou, J. Liu, C. J. Cheng, T. R. Patel, C. E. Weller, J. M. Piepmeier, Z. Z. Jiang and W. M. Saltzman, *Nat. Mater.*, 2012, **11**, 82–90.
6 D. Deshpande, P. Blezinger, R. R. Pillai, J. J. Duguid, B. B. Freimark and A. Rolland, *Pharm. Res.*, 1998, **15**, 1340–1347.

7 X. Gao and L. Huang, *Biochemistry*, 1996, **35**, 9286–9286.
8 F. Y. Dai, P. Sun, Y. J. Liu and W. G. Liu, *Biomaterials*, 2010, **31**, 559–569.
9 V. L. Truong, J. T. August and K. W. Leong, *Hum. Gene Ther.*, 1998, **9**, 1709–1717.
10 J. M. Russell, J. G. Duguid, K. Anwer, K. M. Barron, H. Nitta and A. P. Rolland, *Pharm. Res.*, 1996, **13**, 701–709.
11 H. Isobe, S. Sugiyama, K. Fukui, Y. Iwasawa and E. Nakamura, *Angew. Chem., Int. Ed.*, 2001, **40**, 3364–3369.
12 W. Zauner, M. Ogris and E. Wagner, *Adv. Drug Delivery Rev.*, 1998, **30**, 97–113.
13 A. J. Mazzarello, R. Vuilleumier, J. J. Panek and G. J. Ciccotti, *J. Phys. Chem. B.*, 2010, **114**, 242–253.
14 H. Chen and J. Rhodes, *J. Mol. Med.*, 1996, **74**, 497–504.
15 J. Liang, G. Steinberg, N. Livnah, M. Sheves and T. G. Ebrey, *Biophys. J.*, 1994, **67**, 848–854.
16 Y. Li and Z. Y. Yang, *Inorg. Chim. Acta*, 2009, **362**, 4823–4831.
17 D. Sadhukhan, A. Ray, S. Das, C. Rizzoli, G. M. Rosair and S. Mitra, *J. Mol. Struct.*, 2010, **975**, 265–273.
18 K. Y. Lee, I. C. Kwon, Y. H. Kim, W. H. Jo and S. Y. Jeong, *J. Controlled Release*, 1998, **51**, 213–220.
19 J. M. Dang and K. W. Leong, *Adv. Drug Delivery Rev.*, 2006, **58**, 487–499.
20 (*a*) P. Midoux and M. Monsigny, *Bioconjugate Chem.*, 1999, **10**, 406–411; (*b*) S. Asayama, M. Sudo, S. Nagaoka and H. Kawakami, *Mol. Pharmaceutics*, 2008, **5**, 898–901.
21 T. H. Kim, J. E. Ihm, Y. J. Choi, J. W. Nah and C. S. Cho, *J. Controlled Release*, 2003, **93**, 389–402.
22 B. Ghosn, A. Singh, M. Li, A. V. Vlassov, C. Burnett, N. Puri and K. Roy, *Oligonucleotides*, 2010, **20**, 163–172.
23 H. Oliveira, L. R. Pires, R. Fernandez, C. M. L. Martins, S. Simões and A. P. Pêgo, *J. Biomed. Mater. Res., Part A*, 2010, **95**, 801–810.
24 S. Tsukiji, M. Miyagawa, Y. Takaoka, T. Tamura and I. Hamachi, *Nat. Chem. Biol.*, 2009, **5**, 341–343.
25 R. Chandra and R. Rustgi, *Prog. Polym. Sci.*, 1998, **23**, 1273–1335.
26 J. Brugnerotto, J. Lizardi, F. M. Goycoolea, W. Argüelles-Monal, J. Desbrières and M. Rinaudo, *Polymer*, 2001, **42**, 3569–3580.
27 E. T. G. Cavalheiro and L. S. Guinesi, *Carbohydr. Polym.*, 2006, **65**, 557–561.
28 J. T. Wang, X. X. Jin and J. Bai, *Carbohydr. Res.*, 2009, **344**, 825–829.
29 N. Nanbu, Y. Sasaki and F. Kitamura, *Electrochem. Commun.*, 2003, **5**, 383–387.
30 D. B. Santo, F. Ignazio, L. Isabelle, A. D. Maria and J. M. Tobin, *J. Am. Chem. Soc.*, 1997, **119**, 9550–9557.
31 P. Piotr, S. Grzegorz, P. Radosław, B. Bogumil and B. Franz, *J. Mol. Struct.*, 2003, **658**, 193–205.
32 H. Walba and R. W. Isensee, *J. Am. Chem. Soc.*, 1955, **77**, 5488–5492.
33 J. W. Park, K. H. Choi and K. K. Park, *Bull. Korean Chem. Soc.*, 1983, **4**, 68–72.
34 A. P. Zhu, N. Fang, M. B. Chan-Park and V. Chan, *Biomaterials*, 2005, **26**, 6873–6879.
35 B. Lu, C. F. Wang, D. Q. Wu, C. Li, X. Z. Zhang and R. X. Zhuo, *J. Controlled Release*, 2009, **137**, 54–62.
36 S. Y. Chae, S. Son, M. Lee, M. K. Jang and J. W. Nah, *J. Controlled Release*, 2005, **109**, 330–344.
37 S. Choosakoonkriang, B. A. Lobo, G. S. Koe, J. G. Koe and C. R. Middaugh, *J. Pharm. Sci.*, 2003, **92**, 1710–1722.
38 H. Q. Mao, K. Roy, V. L. Troung-Le, A. Kevin, K. A. Janes, K. Y. Lin, Y. Wang, J. T. August and K. W. Leong, *J. Controlled Release*, 2001, **70**, 399–421.
39 T. Kean and M. Thanou, *Adv. Drug Delivery Rev.*, 2010, **62**, 3–11.
40 S. Yamano, J. S. Dai and A. M. Moursi, *Mol. Biotechnol.*, 2010, **46**, 287–300.
41 A. F. Adler and K. W. Leong, *Nano Today*, 2010, **5**, 553–569.
42 D. W. Park, D. Putnum and R. Langer, *Biotechnol. Bioeng.*, 2000, **67**, 598–606.
43 G. T. Hessa, W. H. H. Ivb, N. C. Fayb and C. K. Payneb, *Biochim. Biophys. Acta, Mol. Cell Res.*, 2007, **1773**, 1583–1588.
44 M. L. Forrest, G. E. Meister, J. T. Koerber and D. W. Pack, *Pharm. Res.*, 2004, **21**, 365–371.
45 N. P. Gabrielson and D. W. Pack, *Biomacromolecules*, 2006, **7**, 2427–2435.
46 K. W. Leong, *MRS Bull.*, 2005, **30**, 640–646.
47 D. W. Pack, D. Putnam and R. Langer, *Biotechnol. Bioeng.*, 2000, **67**, 217–223.
48 J. M. Benns, J. S. Choi, R. I. Mahato, J. S. Park and S. W. Kim, *Bioconjugate Chem.*, 2000, **11**, 637–645.
49 P. Midoux and M. Monsigny, *Bioconjugate Chem.*, 1999, **10**, 406–411.
50 D. Luo and W. M. Saltzman, *Nat. Biotechnol.*, 2000, **18**, 893–895.
51 X. Zhao, L. C. Yin, J. Y. Ding, C. Tang, S. H. Gu, C. H. Yin and Y. M. Mao, *J. Controlled Release*, 2010, **144**, 46–54.
52 Z. H. Wang, W. B. Li, J. Ma, G. P. Tang, W. T. Yang and F. J. Xu, *Macromolecules*, 2011, **44**, 230–239.
53 Y. Ping, C. D. Liu, G. P. Tang, J. S. Li, J. Li, W. T. Yang and F. J. Xu, *Adv. Funct. Mater.*, 2010, **20**, 3106–3116.
54 J. Dai, S. Zou, Y. Y. Pei, D. Cheng, H. Ai and X. T. Shuai, *Biomaterials*, 2011, **32**, 1694–1705.
55 J. X. Bi, M. Wirth, C. Beer, E. J. Kim, M. B. Gu and A. P. Zeng, *J. Biotechnol.*, 2002, **93**, 231–242.
56 D. X. Wang, Y. Z. Niu, Y. K. Wang, J. K. Han and S. Y. Feng, *J. Organ. Chem.*, 2010, **695**, 2329–2337.
57 P. Chan, M. Kurisawa, J. E. Chung and Y. Y. Yang, *Biomaterials*, 2007, **28**, 540–549.
58 D. M. Heyes, *J. Phys.: Condens. Matter.*, 2007, **19**, 1–8.
59 R. Amal, J. A. Raper and T. D. Waite, *J. Colloid Interface Sci.*, 1990, **140**, 158–168.
60 K. Corsi, F. Chellat, L. Yahia and J. C. Fernandes, *Biomaterials*, 2003, **24**, 1255–1264.

Supporting Information

Developing a Chitosan Supported Imidazole Schiff-base for High-Efficiency Gene Delivery

Bingyang Shi, Hu Zhang, Zheyu Shen, Jingxiu Bi* and Sheng Dai *

School of Chemical Engineering, The University of Adelaide, Adelaide, SA 5005, Australia

* Corresponding authors

E-mail: s.dai@adelaide.edu.au (SD) and jingxiu.bi@adelaide.edu.au (JB)

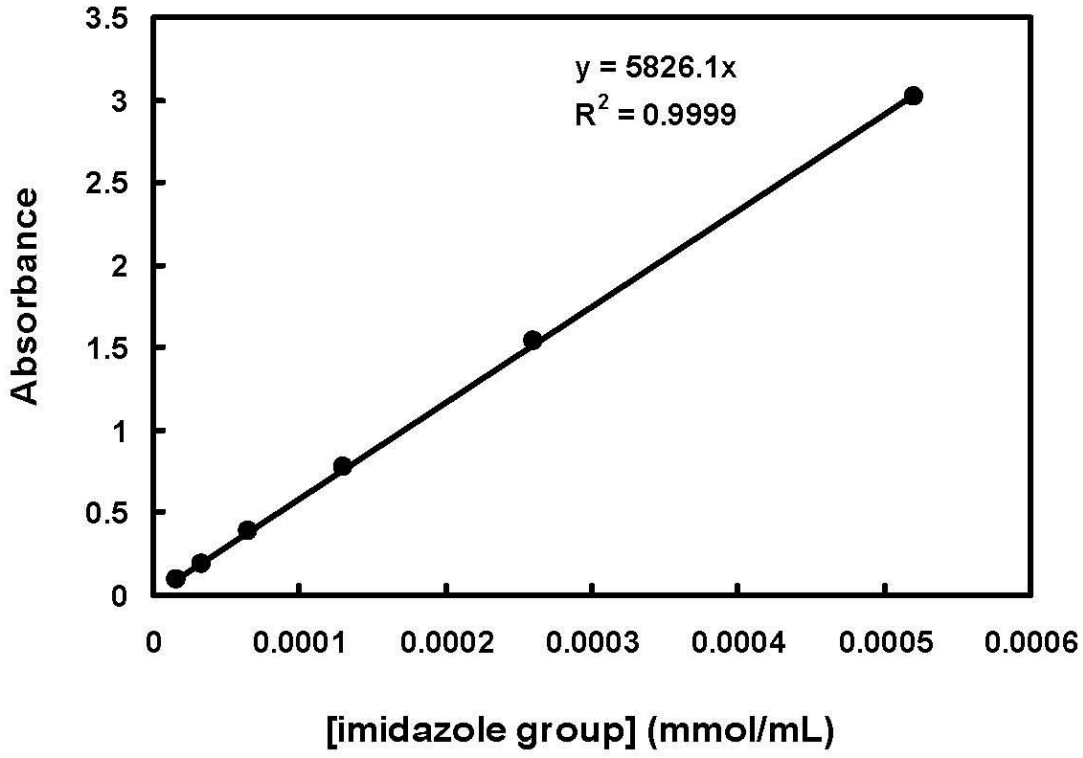

Figure S1. Calibration curve of imidazole groups at the wavelength of 257 nm.

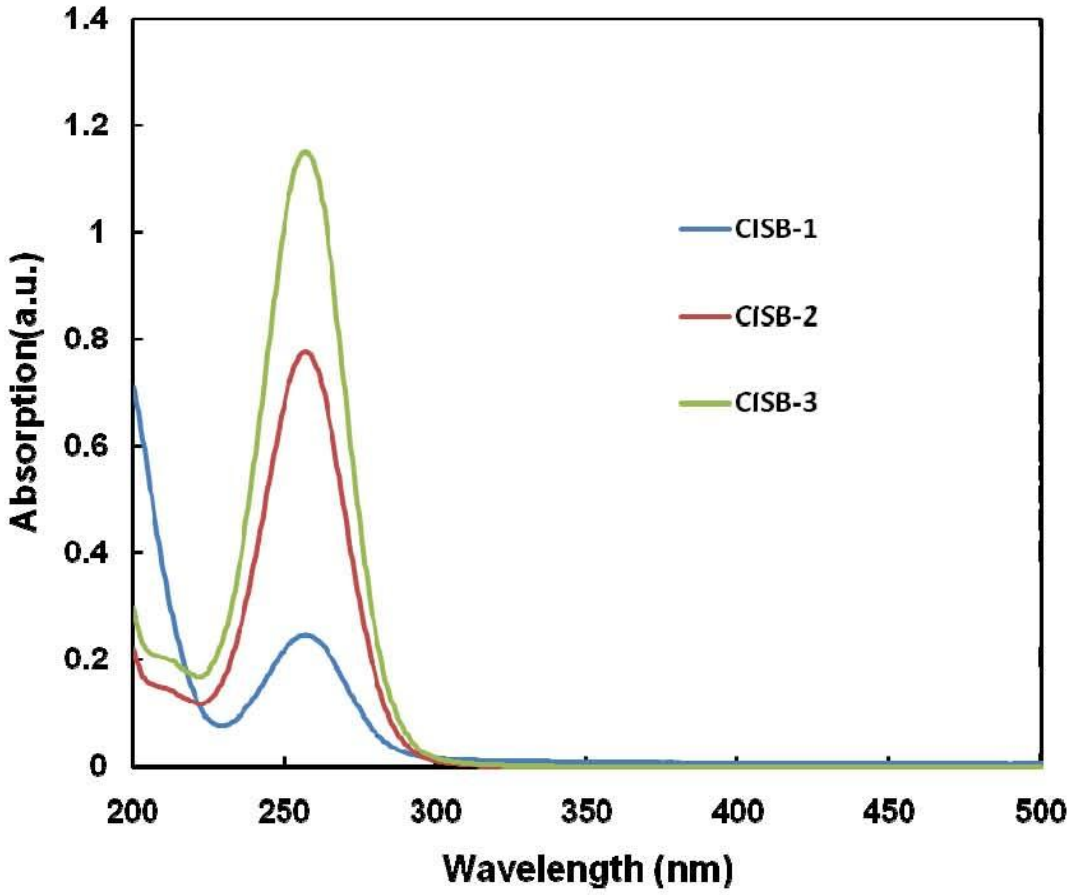

Figure S2. UV absorption of the synthesized CISB polymers.

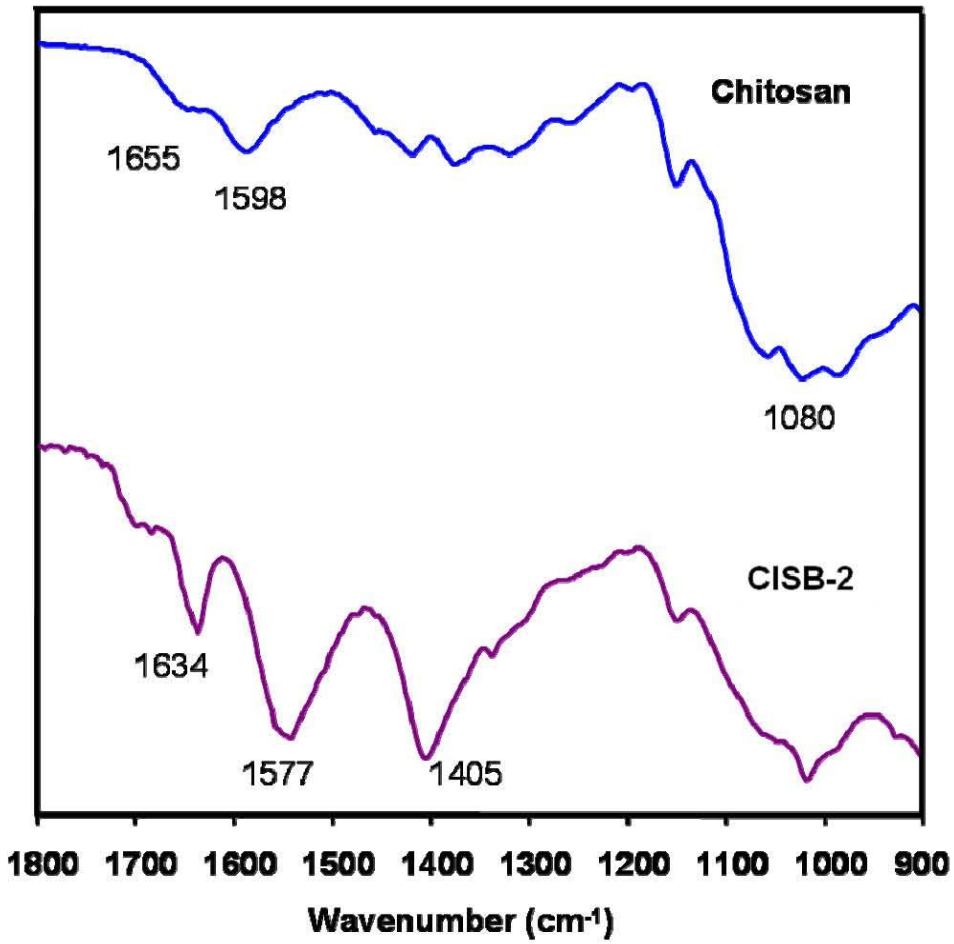

Figure S3. Comparison on the FTIR spectra of chitosan and CISBs.

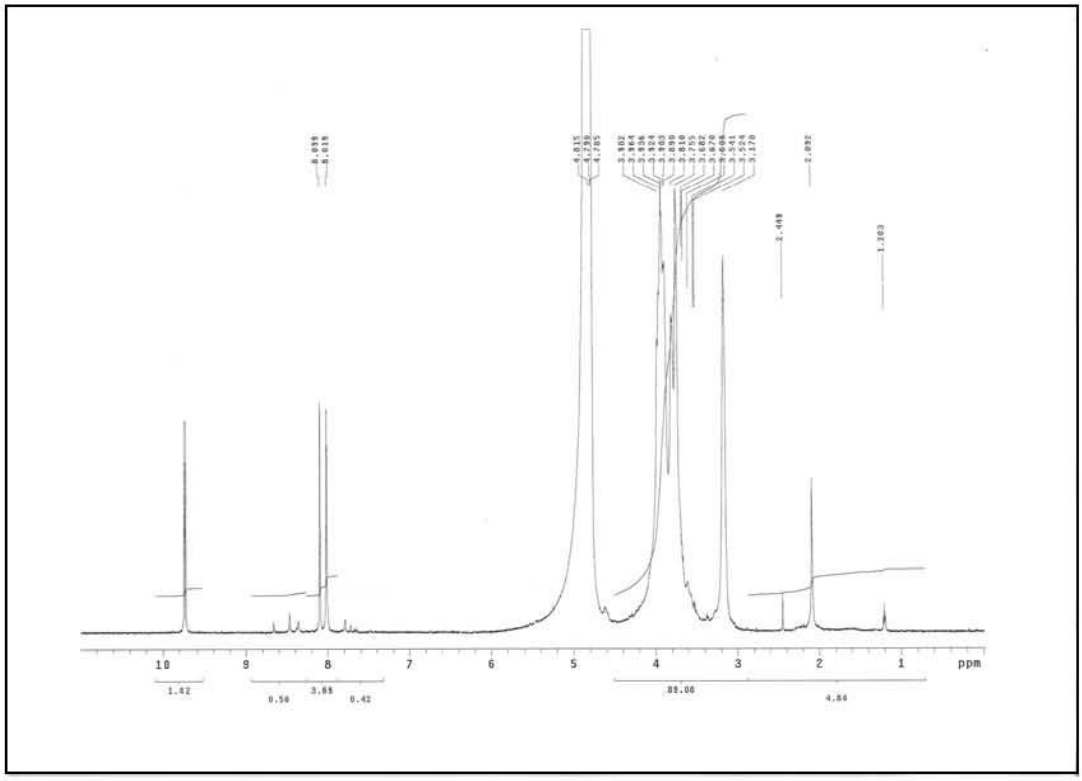

Figure S4. The ^{1}H-NMR of the CISB-2 in D_2O.

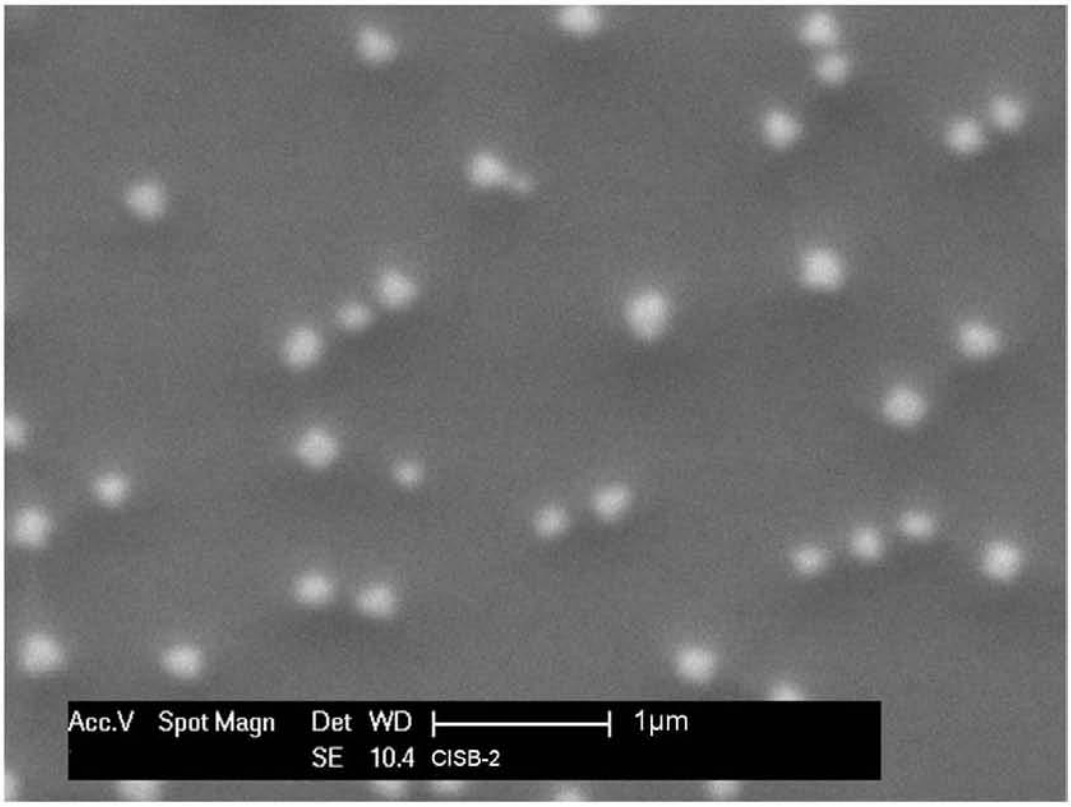

Figure S5. SEM image of CISB-2/pDNA polyplexes at the mixing weigh ratios of 10 (polymer to pDNA).

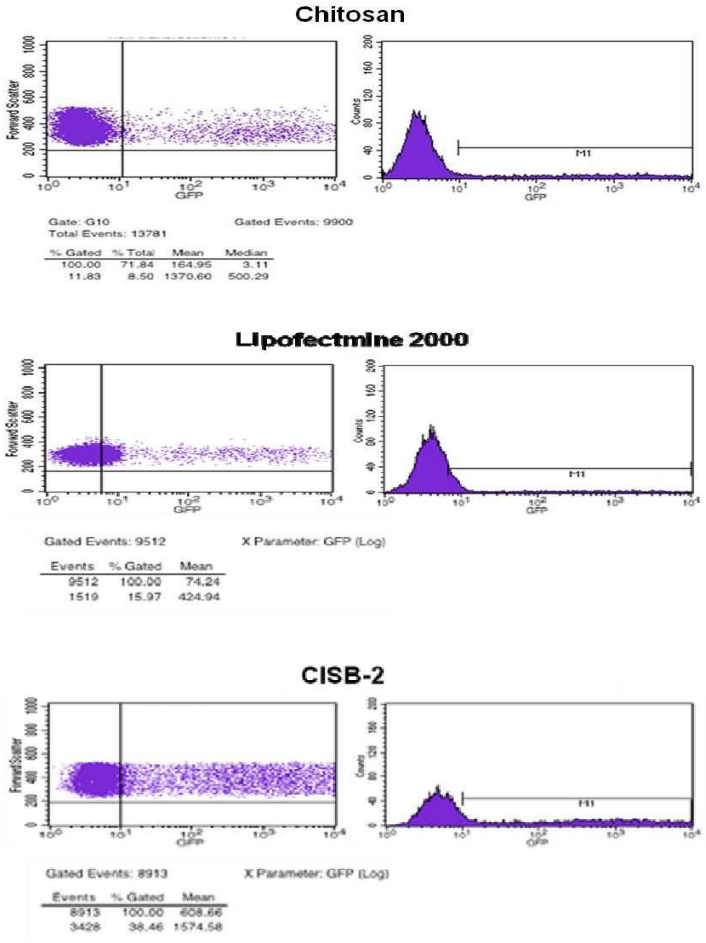

Figure S6. Gene transfection efficiency of the CISB-2 against the 293 cells measured by flow cytometer at the pDNA concentration of 1 μg/well in a 24-well plate using naked DNA as a negative control, Chitosan and lipofectamine 2000 as the positive control.

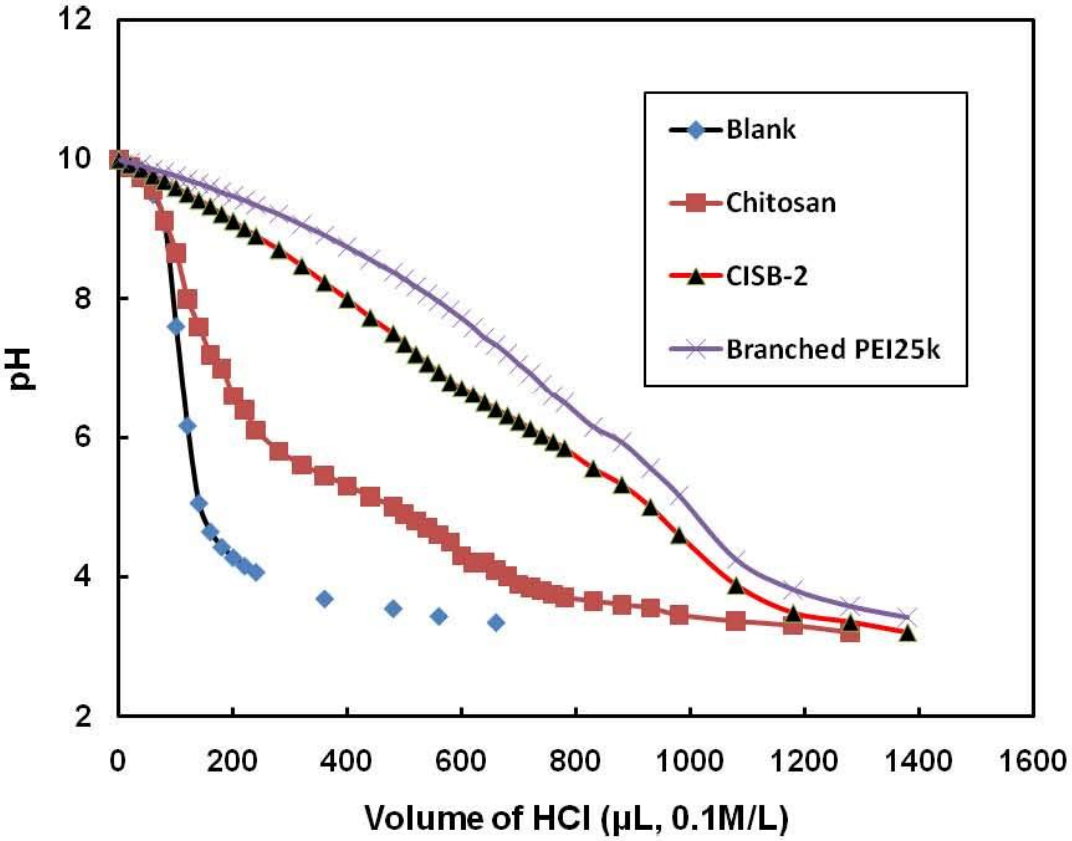

Figure S7. Comparison on the buffering capacity of various polymers.

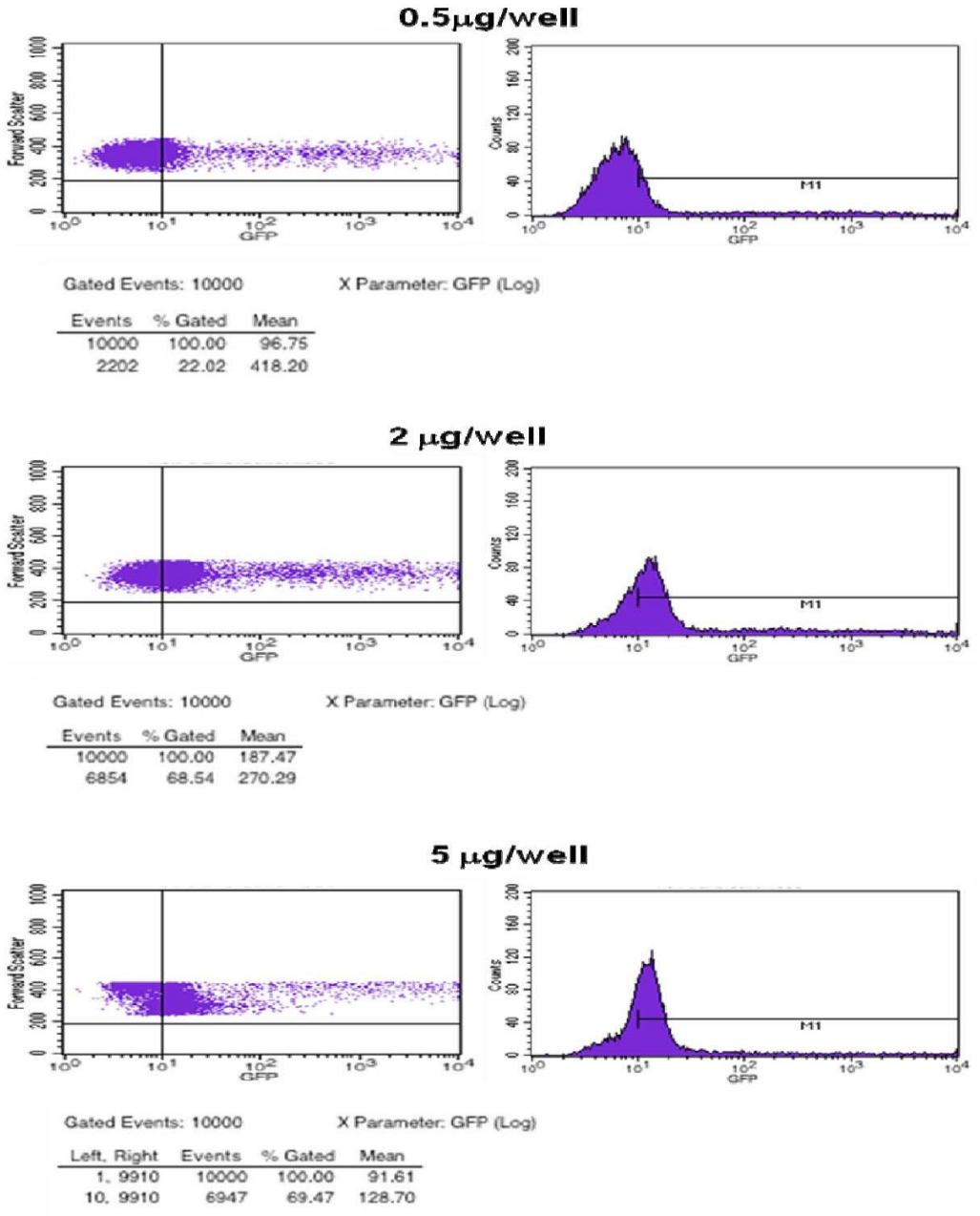

Figure S8. Gene transfection efficiency of the CISB-2 against the 293T cells measured by flow cytometer at the pDNA concentrations of 0.5, 2.0 and 5.0 μg/well in 24-well plates.